From the
Department of Veterinary Sciences
Faculty of Veterinary Medicine
Ludwig-Maximilians-University of Munich
Prof. Dr. Hermann Ammer

Performed under the supervision of
Prof. Dr. Thomas Simmet
Institute of Pharmacology of Natural Products & Clinical Pharmacology
Faculty of Medicine, Ulm University

Pharmacological Studies of a Novel Inhibitor of the Mammalian Target of Rapamycin (mTOR) Signaling Pathway

Inaugural Thesis
for the
Doctor Degree in Veterinary Medicine
Faculty of Veterinary Medicine
Ludwig Maximilians University of Munich

From
Samy Abd EL-Raouf Fahim Khalafalla Morad
from Qena, Egypt

Munich 2010

Printed with the permission of the Faculty of Veterinary Medicine
Ludwig Maximilians University of Munich

Dekan:	Univ.-Prof. Dr. Braun
Bericterstatter:	Univ.-Prof. Dr. Ammer
Korreferent/en:	Univ.-Prof. Dr. Gabius
	Univ.-Prof. Dr. Stangassinger
	Univ.-Prof. Dr. Hirschberger
	Univ.-Prof. Dr. Wanke

Defence date: July 24, 2010

This work is dedicated to
my parents, my wife, my son, my daughter,
and the spirit of Abd El Mageed Foud

Table of Contents

ABBREVIATIONS

4EBP1	Eukaryotic translation initiation factor 4E-binding protein 1
AKβBA	Acetyl-11-keto-β-boswellic acid
AKT/PKB	Protein kinase B
AKT inhibitor VIII	3-Dihydro-1-(1-((4-(6-phenyl-1H-imidazo[4.5-g]quinoxalin-7-yl)phenyl)methyl)-4-piperidinyl)-2Hbenzimidazol-2-one
AMPK	Adenosine monophosphate-activated protein kinase
APS	Ammonium persulfate
ATCC	American Tissue Culture Collection
ATM	Ataxia telangiectasia mutated
BME	β-Mercaptoethanol,
BSA	Bovine serum albumin
CAM	Chick embryo chorioallantoic membrane
CCI-779	mTOR inhibitor (temsirolimus)
C-KβBA	3-Cinnamoyl-11-keto-β-boswellic acid
DMSO	Dimethyl sulfoxide
DTT	Dithiothreitol
EDTA	Ethylene diamine tetra acetic acid
EIF4E	Eukaryotic translation initiation factor 4E
ERK (MAPK)	Extracellular signal-regulated kinase
MAPK	Mitogen-activated protein kinase
FACS	Fluorescence-Activated Cell Scan (Sorting)
FCS	Fetal calf serum
FITC	Fluorescein isothiocyanate
FKBP12	FK506-binding protein of 12 kDa
FRB	FKBP12-rapamycin binding
GAP	GTPase activating protein
GDP	Guanosine-diphosphate
GTP	Guanosine-triphosphate
HPLC	High-pressure liquid chromatography
HRP	Horseradish peroxidase
IGFs	Insulin-like growth factors
KβBA	11-Keto-β-boswellic acid
Ki-67	Cellular marker for proliferation
MEF	Mouse embryonic fibroblast
MnK	Mitogen-activated protein kinase interacting kinase
Mol	Mole
mSIN1	mammalian stress-activated protein kinase (SAPK)-interacting protein
mTOR	mammalian target of rapamycin
mTORC	mTOR complex
p70S6K	70-kDa S6 protein kinase
PAGE	Polyacrylamide gel electrophoresis
PBS	Phosphate-buffered saline

PDK1	Phosphoinositide-dependent protein kinase 1
pH	Potential of hydrogen
PI3K	Phosphatidylinositol-3-kinase
PIP3	Phosphatidylinositol 3-phosphate
PKC	Protein kinase C
PP2A	Protein phosphatase 2 A
PRAS40	Proline-rich AKT substrate 40 kDa
PRR5	Proline-rich protein 5 (Protor)
PS	Phosphatidylserine
PTEN	Phosphatase and tensin homolog
PVDF	Polyvinylidene difluoride
Raptor	Regulatory associated protein of TOR
Rheb	Ras homologue enriched in brain
Rictor	Rapamycin insensitive component of TOR
RIPA	Radioimmuno-precipitation assay buffer
RSK	Ribosomal S6 kinase
RSK1	Ribosomal protein S6 kinase alpha-1
SDS	Sodium dodecyl sulfate
Ser	Serine
SLB	Sample loading buffer
TBE	Trisborate-EDTA buffer
TBS	Tris-buffered saline
TBS-T	Tris-buffered saline and Tween 20
TEMED	Tetramethylethylendiamine
Thr	Threonine
Tricine	N-(2-hydroxy-1,1-bis(hydroxymethyl)ethyl)glycine
TSC1 (hamartin)	Tuberous sclerosis protein 1
TSC2 (tuberin)	Tuberous sclerosis protein 2
TUNEL	Terminal deoxynucleotidyl transferase dUTP nick end labeling
Tween 20	Polyoxyethylene-20-sorbitan monolaurate
Tyr	Tyrosine

1. INTRODUCTION

1.1 APOPTOSIS

For the maintenance of cellular homeostasis, an exact balance between cellular proliferation and cell death is of utmost importance. If mitosis would proceed without cell death, an 80 year old person would have 2 tons of bone marrow and lymph nodes and an intestinal tract 16 km long (Kerr et al. 1972).

The term “apoptosis” was first coined in 1972 by Kerr et al. and originates from the Greek words apo = from and ptosis = falling, symbolizing leaves falling from trees or petals falling from flowers, a natural process of death. The apoptotic mode of cell death is an active and defined process that plays an important role in the development of multicellular organisms and in the regulation and maintenance of the cell populations in tissues under physiologic and pathologic conditions. The disappearance of a cell by apoptosis creates “hardly a ripple” whereas necrosis is capable of producing inflammation. Programmed cell death is encoded in the genome. Each cell possesses the necessary molecular machinery required to undergo apoptosis, and the process can be initiated by specific cell signaling events. Numerous studies in recent years have revealed that apoptosis is a constitutive suicide program expressed in most, if not all cells, and can be triggered by a variety of extrinsic and intrinsic signals. Because the decision to live or to die critically contributes to the regulation of the immune response, the apoptotic pathways are kept under tight control (Elmore 2007; Hotchkiss et al. 2009).

1.1.1 Historical perspective

In 1858, Virchow characterized the changes occurring in cells shortly after death as either necrosis, where “the mortified cell is left in its external form” or “necrobiosis or shrinkage necrosis, where the cell vanishes and can no longer be seen in its previous form” (Virchow R et al. 1859). The term “necrobiosis” was succeeded by the term “chromatolysis” 26 years later, when Flemming described the morphological changes taking place during regression of the epithelium in mammalian lymphoid

follicles. In this study, the first drawings were produced, which illustrated what we now recognize as apoptosis (Flemming 1885). The theory of cell death as a mechanism involved in development, maintenance of homeostasis, control of organ size, and elimination of dysfunctional cells evolved over the following decades. In the late 1960s, apoptosis research was greatly facilitated by the use of electron microscopy. Now, the morphological changes occurring in apoptosis could be studied in much greater detail (Kerr 1969; Kerr 1971).

A scientific landmark in apoptosis research occurred in 1972, when Kerr and colleagues published a paper in which they coined the term “apoptosis” (derived from a Greek word for “dropping off”, as in falling leaves) and defined this phenomenon as a type of orderly, active process by which cells undergo a series of morphological changes, ultimately leading to recognition and engulfment by phagocytes. They provided evidence that this built-in death program was not only evident during development or during pathological conditions, but also in the normal mature organism, continuing throughout life. The authors defined an important role for apoptosis in homeostasis and suggested that deregulation of apoptosis could lead to pathological conditions such as cancer (Kerr et al. 1972).

At the beginning of the following decade, the interest for apoptosis was greatly increased with the discovery that glucocorticoids induce apoptosis and endonuclease activation in lymphocytes (Wyllie 1980). A few years later, the activation of endonucleases in apoptosis was demonstrated by gel electrophoresis, providing the first clear biochemical evidence for apoptosis (Duke et al. 1983). An understanding of the apoptosis process at the genetic and molecular level was initiated in 1986, when Horvitz, a Nobel Prize laureate of 2002, and Ellis discovered a set of genes in the nematode C. elegans that were involved in apoptosis (Ellis et al. 1986). These genes were later found to have homologues in a vast number of organisms, including humans. Since then, the list of apoptosis-related genes has expanded.

1.1.2 Natural occurrence of apoptosis

Apoptosis is a widespread phenomenon occurring throughout the animal kingdom and human being. It is becoming clear that many of the genes involved in apoptosis control in mammals also function in plants. Apoptosis is involved in plant gamete fertilization, embryogenesis and development (Yin et al. 2003). The process has been described as dynamic, well coordinated but complex and is important in both the development and maintenance of living organisms (Clarke et al. 1998).

Apoptotic processes begin as early as fertilization and are involved in a wide range of critical processes involved in homeostasis and development. Examples include development of the nervous system, whereby more nerve cells are produced than required (Oppenheim et al. 2001). Apoptosis adjusts the number of neuron, glial and neuroprogenitor cells to the number of target cells and it has been estimated that between 30-50% of all developed neurons die during development (Osborne 2004). Apoptosis is also involved in neural tube formation which in the developing embryo forms the brain, spinal cord, spinal nerves and spinal column.

Apoptosis also occurs during morphogenesis of various body structures including muscle, epithelial, intestinal, gonadal cells and the immune system (Hengartner et al. 1994). In non-aquatic vertebrates including humans, apoptosis of the inter-digital webs in the early embryo is important in the formation of fingers and toes (Hurle et al. 1996). In amphibians regression of the tail and gills of the tadpole, occurs as a result of substantial apoptosis (Fox 1973). In animals, which undergo metamorphosis, larval tissues that are no longer required are eliminated by apoptosis whilst the adult body parts emerge (Dyche 1979). Development of the reproductive tract requires regression of the male (wolffian) or female (müllerian) duct systems to produce a male or female embryo, and is another example of apoptosis.

Apoptosis is just as important to the organism during postnatal development into adulthood. It is a mechanism whereby cells, which have served their purpose or become nonfunctional, can be eliminated safely without causing harm to the host. Follicular atresia of the post-ovulatory follicle and involution of the mammary gland

post-weaning are two examples of normal tissue regression achieved by apoptosis (Elmore 2007). Regulation of the immune system also requires apoptosis (Hotchkiss et al. 2009). The separation of the digits during limb development is classical example of the effect of apoptosis during apoptosis. Defective lymphocytes, lymphocytes that threaten an autoimmune attack or those, which have performed their duties, can all be eliminated safely via apoptosis (Gercel-Taylor et al. 2002; Osborne 2004).

Furthermore, apoptotic cell death helps to shape the future inner ear structure, which starts from incubation day 5 in the chick inner ear. In cardiac morphogenesis, cell death is essential in generating the overall four-chambered architecture of the heart. In rat skeletal muscle, cell death persists during the first three postnatal weeks, suggesting an indispensable role for cell death in the development of skeletal muscle (Osborne 2004).

1.1.3 Morphological features of apoptosis

During the early process of apoptosis, cell shrinkage and pyknosis are visible by light microscopy (Kerr et al. 1972). With cell shrinkage, the cells are smaller in size, the cytoplasm is dense and the organelles are more tightly packed. Pyknosis is the result of chromatin condensation and this is the most characteristic morphological feature of apoptosis (Osborne 2004) (Figure 1).

Extensive plasma membrane blebbing followed by karyorrhexis and separation of cell fragments into apoptotic bodies during a process called "budding." Apoptotic bodies consist of cytoplasm with tightly packed organelles with or without a nuclear fragment. The organelle integrity is still maintained and all of this is enclosed within an intact plasma membrane. These bodies are subsequently phagocytosed by macrophages, parenchymal cells, or neoplastic cells and degraded within phagolysosomes (Wyllie 1980; Ucker et al. 1992; Mills et al. 1998; Kawabata et al. 1999). Macrophages that engulf and digest apoptotic cells are called "tingible body macrophages" and are frequently found within the reactive germinal centers of lymphoid follicles or occasionally within the thymic cortex. The tingible bodies are the

bits of nuclear debris from the apoptotic cells. There is essentially no inflammatory reaction associated with the process of apoptosis nor with the removal of apoptotic cells because: (1) apoptotic cells do not release their cellular constituents into the surrounding interstitial tissue; (2) they are quickly phagocytosed by surrounding cells thus likely preventing secondary necrosis; and, (3) the engulfing cells do not produce inflammatory cytokines (Savill et al. 2000; Kurosaka et al. 2003).

1.1.4 Apoptosis versus necrosis

The alternative to apoptotic cell death is necrosis, which is considered to be a toxic process, where the cell is a passive victim and follows an energy-independent mode of death. But since necrosis refers to the degradative processes that occur after cell death, it is considered by some to be an inappropriate term to describe a mechanism of cell death. Oncosis is therefore used to describe a process that leads to necrosis with karyolysis and cell swelling, whereas apoptosis leads to cell death with cell shrinkage, pyknosis, and karyorrhexis. Therefore the terms "oncotic cell death" and "oncotic necrosis" have been proposed as alternatives to describe cell death that is accompanied by cell swelling. However, these terms are not widely used at this time (Majno et al. 1995; Levin et al. 1999).

Some of the major morphological changes that occur with necrosis include cell swelling, formation of cytoplasmic vacuoles, distended endoplasmic reticulum, formation of cytoplasmic blebs, condensed, swollen or ruptured mitochondria, disaggregation and detachment of ribosomes, disrupted organelle membranes, swollen and ruptured lysosomes, and eventually disruption of the cell membrane (Kerr et al. 1972; Majno et al. 1995; Trump et al. 1997). This loss of cell membrane integrity results in the release of the cytoplasmic contents into the surrounding tissue sending chemotactic signals with eventual recruitment of inflammatory cells. By contrast, apoptotic cells do not release their cellular constituents into the surrounding interstitial tissue and are quickly phagocytosed by macrophages or adjacent normal cells, there is essentially no inflammatory reaction (Savill et al. 2000; Kurosaka et al. 2003) (Figure 1 and Table 1).

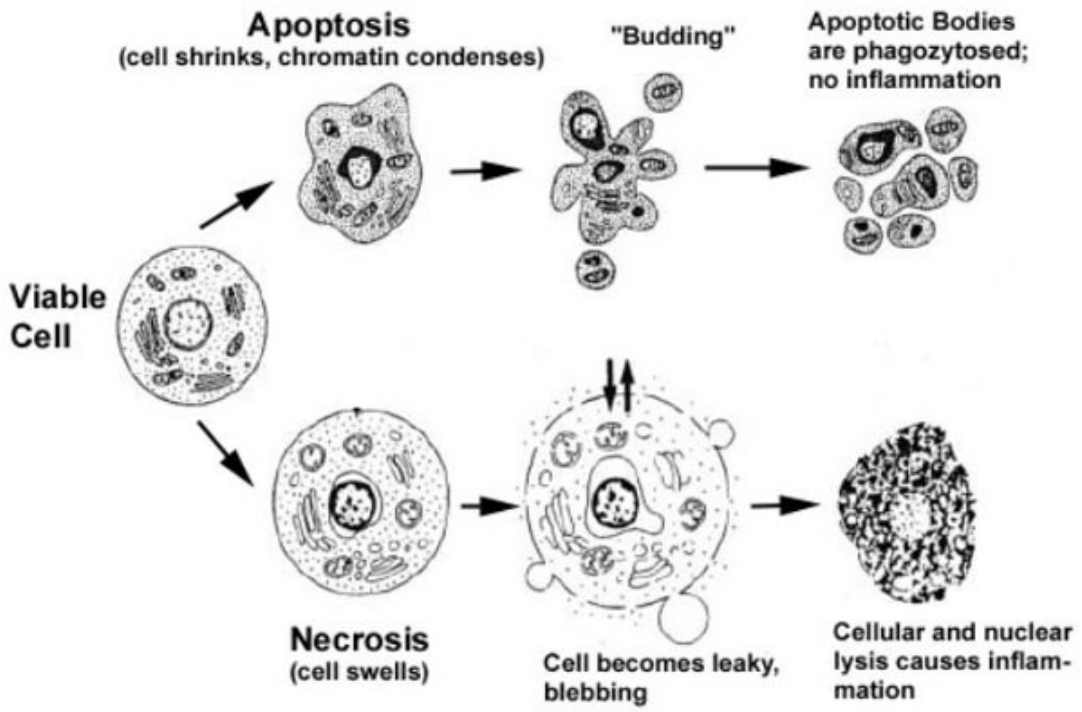

Figure 1. Hallmarks of the apoptotic and necrotic cell death process
Apoptosis includes cellular shrinking, chromatin condensation and margination at the nuclear periphery with the eventual formation of membrane-bound apoptotic bodies that contain organelles, cytosol and nuclear fragments and are phagocytosed without triggering inflammatory processes. The necrotic cell swells, becomes leaky and finally is disrupted and releases its contents into the surrounding tissue resulting in inflammation. Modified from (Van Cruchten et al. 2002)

Table 1. Comparison of morphological features of apoptosis and necrosis (Elmore 2007)

Apoptosis	Necrosis
Single cells or small clusters of cells	Often contiguous cells
Cell shrinkage and convolution	Cell swelling
Pyknosis and karyorrhexis	Karyolysis, pyknosis, and karyorrhexis
Intact cell membrane	Disrupted cell membrane
Cytoplasm retained in apoptotic bodies	Cytoplasm is released
No inflammation	Inflammation is usually present

1.1.5 Biochemical features of apoptosis

Apoptotic cells exhibit several biochemical modifications such as protein cleavage, protein cross-linking, DNA breakdown, and phagocytic recognition that together result in the distinctive structural pathology described previously (Hengartner et al. 1994).

Caspases belong to the family of cysteine proteases, which play essential roles in apoptosis and inflammation. They are expressed as inactive proenzyme forms in most cells and once activated, can often activate other procaspases, allowing the initiation of a protease cascade. Some procaspases can also aggregate and autoactivate. This proteolytic cascade, in which one caspase can activate other caspases, amplifies the apoptotic signaling pathway and, thus, leads to rapid cell death.

DNA breakdown by Ca^{++} and Mg^{++} dependent endonucleases also occurs, resulting in DNA fragments of 180 to 200 base pairs (Bortner et al. 1995). A characteristic "DNA ladder" can be visualized by agarose gel electrophoresis with ethidium bromide staining and ultraviolet illumination.

Another biochemical feature is the expression of cell surface markers that results in the early phagocytic recognition of apoptotic cells by adjacent cells, permitting quick phagocytosis with minimal compromise to the surrounding tissue. This is achieved by the movement of the normally inward-facing phosphatidylserine of the cell's lipid bilayer to the outer layer of the plasma membrane resulting in the surface expression of phosphatidylserine (Bratton et al. 1997).

1.1.6 Apoptosis pathways (induction of apoptosis)

There are three alternative pathways, through which apoptosis can be initiated, 1-Death receptor (extrinsic) pathway, 2- Mitochonderial (Intrinsic) pathway, 3-Perforin/granzyme pathway (Figure 2).

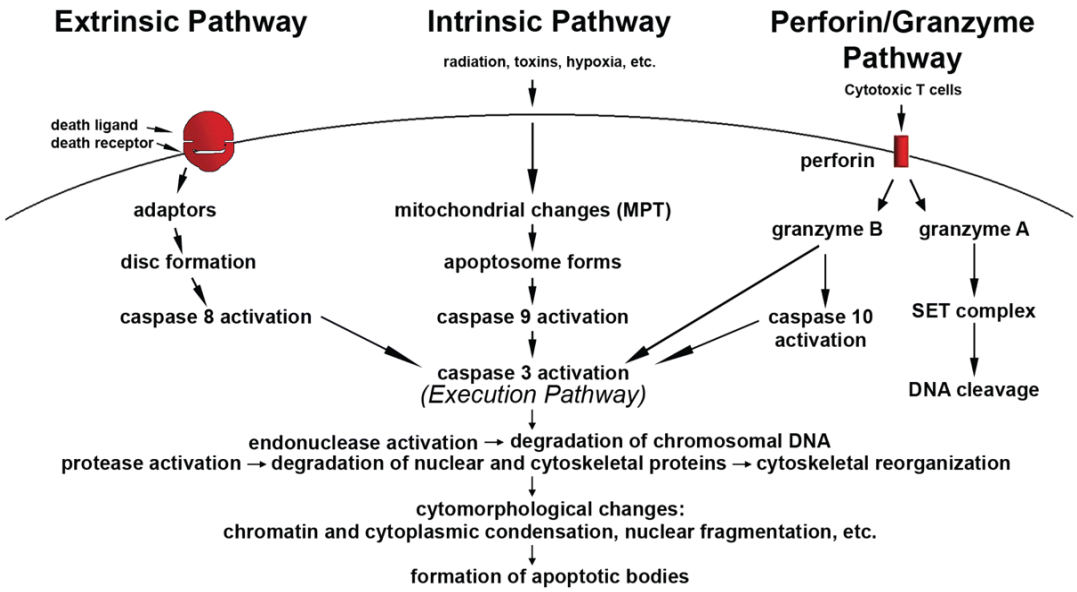

Figure 2. Schematic representation of apoptosis pathways

The two main pathways of apoptosis are extrinsic and intrinsic, as well as, a perforin/granzyme pathway. Each requires specific trigger signals to initiate an energy-dependent cascade of molecular events. Each pathway activates its own initiator caspase (8, 9, and 10) which, in turn, will activate the executioner caspase 3. However, granzyme A works in a caspase-independent fashion. The execution pathway results in characteristic cytomorphological features including cell shrinkage, chromatin condensation, formation of cytoplasmic blebs and apoptotic bodies and finally phagocytosis of the apoptotic bodies by adjacent parenchymal cells, neoplastic cells or macrophages (Elmore 2007).

1.1.6.1 Extrinisic (death receptor) pathway

The extrinsic pathway is mediated by the death receptor CD95 (APO-1/Fas). Triggering of CD95 by its natural ligand or agonistic antibodies induces the formation of DISC that consists of the adapter protein FADD and FLICE/caspase 8. Complex formation is initiated through homophilic interaction of the death domains present in the intracellular part of both CD95 and FADD. FADD, in addition, contains a second interaction region called the DED, which couples to caspase 8 as the most proximal element in the caspase cascade. Further downstream, caspase 8 presumably triggers the proteolytic activation of other caspases and cleavage of cellular substrates (Schulze-Osthoff et al. 1998; Krammer 1999)

1.1.6.2 Intrinsic (mitochondrial) pathway

The mitochondrial pathway of apoptosis is activated by DNA damage, cell cycle deregulation, hypoxia, and growth factor withdrawal. Signals induced by these stimuli lead to permeabilization of the outer membrane of the mitochondria, promoting the release of cytochrome c. When cytochrome c is released, it associates with apoptotic protease activating factor 1 (Apaf-1), allowing for the recruitment of an inactive initiator caspase, procaspase 9. The resulting protein complex, the apoptosome, enables the activation of procaspase 9 into caspase 9. Caspase 9 then activates executioner caspases such as caspase 3 (Li et al. 1997; Stennicke et al. 1999).

1.1.6.3 Perforin/granzyme pathway

T-cell mediated cytotoxicity is a variant of type IV hypersensitivity, where sensitized $CD8^+$ cells kill antigen-bearing cells. These cytotoxic T lymphocytes (CTLs) are able to kill target cells via the extrinsic pathway and the FasL/FasR interaction is the predominant method of CTL-induced apoptosis (Brunner et al. 2003). However, they are also able to exert their cytotoxic effects on tumor cells and virus-infected cells via a novel pathway that involves secretion of the transmembrane pore-forming molecule perforin with a subsequent exophytic release of cytoplasmic granules through the pore and into the target cell (Trapani et al. 2002). The serine proteases granzyme A and granzyme B are the most important component within the granules.

Granzyme B will cleave proteins at aspartate residues and will therefore activate procaspase 10 and can cleave factors like ICAD (inhibitor of caspase activated DNAse) (Sakahira et al. 1998). Reports have also shown that granzyme B can utilize the mitochondrial pathway for amplification of the death signal by specific cleavage of Bid and induction of cytochrome c release (Barry et al. 2002; Russell et al. 2002). However, granzyme B can also directly activate caspase 3. In this way, the upstream signaling pathways are bypassed and there is direct induction of the execution phase of apoptosis.

1.2 Mammalian target of rapamycin (mTOR) signaling

1.2.1 The mTOR proteins

The TOR proteins are a family of serine/threonine protein kinases that include ataxia–telangiectasia mutated (ATM), Rad3-related (ATR), DNA-dependent protein kinase (DNA-PK), and suppressor of morphogenesis in genitalia-1 (SMG-1) protein kinase. These kinases are characterized by large size (>2,500 amino acid) and a C-terminally located kinase domain (Abraham 2004). The C-terminal kinase domains are similar to the kinase domain of phosphoinositide-3-kinase (PI3K), and from here they get the name PI3K-related kinases (PIKKs). The N-terminus possesses 20 tandem HEAT domains, which are named based on their presence in Huntingtin protein, Elongation factor 3, the A subunit of PP2A and TOR1.

The mammalian target of rapamycin (mTOR) is an atypical serine/threonine protein kinase with a molecular weight of 290 kDa. Structurally, the N-terminus of mTOR consists of 20 tandemly repeated motifs (HEAT motifs).

The C-terminus consists of mutated FRAP-ataxia-teleangiectasia (FAT, FRAP) domain, a transformation/transcription domain-associated protein domain, an FKPB12-rapamycin-binding (FRB) domain, a catalytic kinase domain, and a FAT carboxy-terminal domain (FAT C-terminus, FATC). It is speculated that the HEAT repeats serve to mediate protein-protein interactions, the FRB domain as suggested by its name provides a docking site for the FKBP12/rapamycin complex, and the FAT and FATC domains modulate mTOR kinase activity via unknown mechanisms (Yang et al. 2007) (Figure 3).

Figure 3. The primary structure of the mTOR protein
Starting from the N terminus to the C terminus, mTOR protein consists of HEAT (huntingtin, EF3, A subunit of PP2A, TOR) repeat domains, FRAP-ataxia-teleangiectasia (FAT) domain. FRB domain (FKBP12-rapamycin binding), is a small protein domain able to bind FKBP12-rapamycin complex. The C-terminal FATC domain has been proposed to interact with the FAT domain to yield a configuration that exposes the catalytic domain (after (Bai et al. 2009)).

The mTOR pathway is a key regulator of cell growth and proliferation and increasing evidence suggests that its deregulation is associated with human diseases, including cancer and diabetes (Sarbassov et al. 2005). The mTOR signaling pathway is considered to be the central regulator of ribosome biogenesis, protein synthesis, and cell growth.

mTOR is found in two structurally and functionally distinct complexes to regulate growth and metabolism. In mammals, the mTOR complex 1 (mTORC1) contains mTOR, mLST8 (G protein beta protein subunit-like, GβL), PRAS40 (a proline-rich Akt substrate of 40 kDa, a raptor-interacting protein), raptor (regulatory associated protein of mTOR), and deptor (mTOR-interacting protein, inhibitory protein). mTORC1 is sensitive to the immunosuppressive and anticancer drug rapamycin. mTORC2 contains mTOR, mLST8, rictor (rapamycin-insensitive companion of mTOR, also known as the mammalian homolog of AVO3P, mAVO3), mSIN1 (mammalian stress-activated protein kinase interacting protein 1, MIP1, mAVO1, the mammalian homolog of Avo1p, necessary for mTORC2 assembly and Akt/PKB phosphorylation), PRR5 (proline-rich protein 5, belongs to the small family of pseudo-response regulators (PRRs)) and deptor. The mTORC2 complex is insensitive to rapamycin (Bai et al. 2009; Peterson et al. 2009) (Figure 4).

The two complexes signal via different effectors pathways to control distinct cellular processes. The mTORC1 protein kinase complex is the central component of a pathway that promotes growth in response to insulin, energy levels, and amino acids and is deregulated in common cancers. The mTORC2 complex phosphorylates Akt at Serine 473 (Ser473) and regulates the actin cytoskeleton (Jacinto et al. 2004; Sarbassov et al. 2005; Sancak et al. 2008).

Figure 4. Schematic representation of the mTOR complex components
The mTORC1 complex consists of mTOR, mLST8, PRAS40 and raptor and the mTORC2 complex consists of mTOR, mLST8, rictor, mSIN1, and PRR5 (after (Bai et al. 2009; Peterson et al. 2009)).

1.2.2 Regulation of mTOR Activity

1.2.2.1 Activation of mTOR by the PI3K signaling pathway

The phosphoinositide 3-kinase (PI3K) pathway has a critical role in aggressive tumorigenesis. PI3K signaling is activated by various extracellular signals including peptide growth factors such as insulin and insulin-like growth factors (IGFs). The PI3K activity that results in PIP3 production is tightly controlled and negatively regulated by several phosphatases. The PTEN (phosphatase and tensin homolog on chromosome 10) lipid phosphatase dephosphorylates PIP3 at the 3' position, whereas SHIP-1 phosphatase dephosphorylates it at the 5' position, in both cases limiting the production of PIP3. Genetic inactivation of PTEN, e.g. by mutation, leads to constitutive activation of the PI3K/AKT/TSC2/mTORC1 cascade (Hay et al. 2004).

AKT is a serine/threonine kinase, also known as protein kinase B, a critical downstream effector of PI3K. Mammalian cells express three Akt proteins encoded by different genes. Full activation of AKT requires AKT phosphorylation at Ser473 and Threonine (Thr308) by PI3K and PDK1 (the phosphoinositide-dependent protein kinase), respectively. AKT phosphorylates TSC2, destabilizes it and disrupts its interaction with TSC1 leading to activation of mTOR (Bai et al. 2009) (Figure 5, Figure 6).

1.2.2.2 Inhibition of mTOR by the LKB1/AMPK/TSC2 signaling pathway

The serine/threonine kinase LKB1 is a tumor suppressor gene. LKB1 is a central regulator of cell polarity and energy metabolism through its capacity to activate adenine monophosphate-activated protein kinase (AMPK). AMPK is activated in response to ATP depletion or increased AMP levels. Activation of AMPK phosphorylates and activates TSC2 inducing mTOR downregulation (Bai et al. 2009; Meric-Bernstam et al. 2009) (Figure 5, Figure 6).

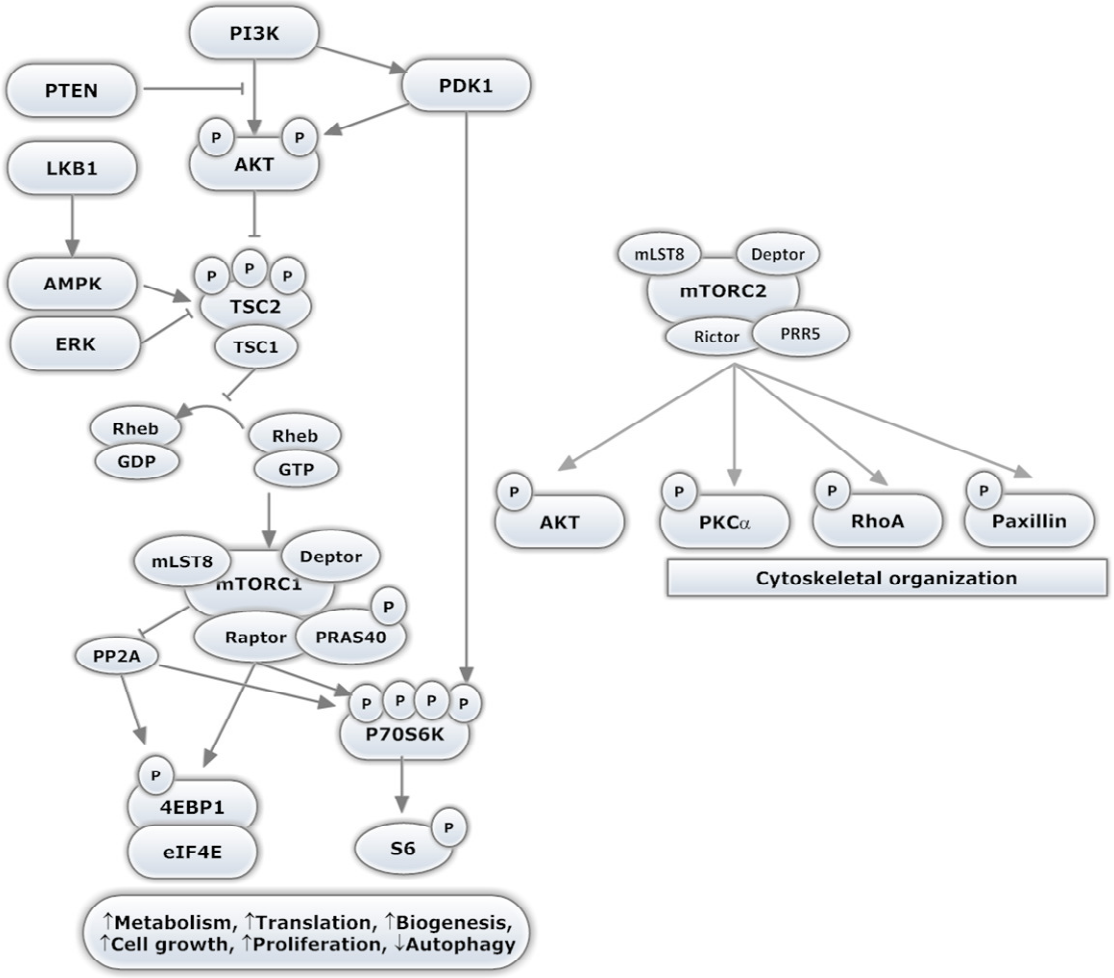

Figure 5. The mammalian target of rapamycin (mTOR) signaling
Arrows represent activation, bars represent inhibition. mTOR signaling regulates critical cellular processes (after (Meric-Bernstam et al. 2009)).

1.2.2.3 Inhibition of mTOR by the tuberous sclerosis complex (TSC1/TSC2)

Tuberous Sclerosis Complex (TSC) is a genetic disorder that occurs upon mutation of either the TSC1 or TSC2 gene, which encodes Hamartin or Tuberin, respectively. The TSC1/TSC2 (TSC1/2) has been known as the major upstream inhibitory regulator of mTOR. TSC2 protein contains a GAP homology domain at its C-terminus. In vitro, TSC2 stimulates GTP hydrolysis of Rheb. TSC1 does not have any GAP activity and is not required for TSC2 GAP activity towards Rheb in vitro. Rheb (Ras homolog enriched in brain) is a member of the Ras family proteins. Rheb, a small GTPase that belongs to a unique family within the Ras superfamily of GTPases. The small GTPase Rheb is a positive upstream regulator of the target of mTORC1. TSC2 regulates Rheb-GTP levels. TSC2 acts as a GTPase-activating protein (GAP) for Rheb. Therefore, TSC2 inhibits Rheb activity. Rheb in its active GTP-bound state (Rheb-GTP) binds to and activates mTORC1. TSC1/2 inhibits mTORC1 activity by limiting the amount of GTP-bound Rheb available to stimulate mTORC1 (Hay et al. 2004; Bai et al. 2009).

Multiple signaling cascades converge on TSC2, leading to its phosphorylation and inactivation. TSC2 is phosphorylated by multiple kinases, including Akt, RSK1, ERK, and AMPK (Bai et al. 2009) (Figure 6).

Active Akt phosphorylates TSC2 directly on multiple sites (Ser939, Ser981, and Thr1462). Phosphorylation of TSC2 inactivates the GTPase activator domain function of TSC2, disrupts the TSC1/2 complex and stimulates activity of Rheb and mTOR (Tee et al. 2003).

Under energy starvation conditions, the AMP-activated protein kinase (AMPK) phosphorylates TSC2 at Thr1227 or Ser1345. The phosphorylation of TSC2 at these sites by AMPK improves the ability of TSC2 to inhibit mTOR activity by activating GAP activity of TSC2 (Inoki et al. 2003).

ERK, and RSK directly phosphorylate TSC2 at Ser664 and Ser1798 resulting in inhibition of TSC2 function (Bai et al. 2009).

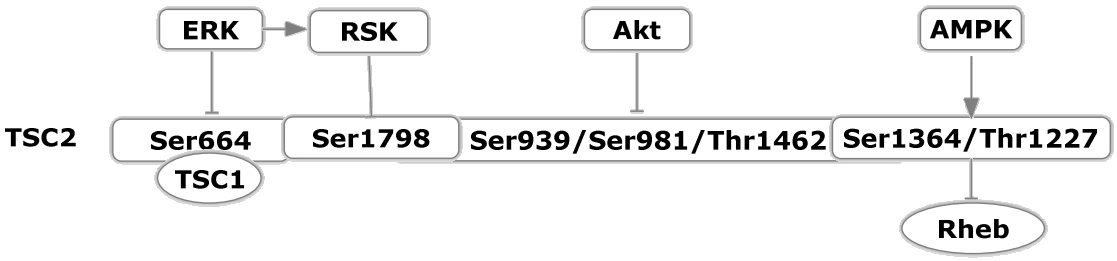

Figure 6. Schematic representation of TSC2/TSC1 complex regulation.
(after (Bai et al. 2009)).

1.2.2.4 Regulation of pathways downstream of mTOR

The downstream signals of mTOR are characterized by two independent targets, p70S6K and 4EBP1/eIF4E complex.

1.2.2.5 Regulation of p70S6K activation

The p70S6K is a major downstream effector of the mammalian target of rapamycin. The p70S6K is a mitogen-activated serine/threonine kinase, which plays a crucial role in the control of the cell cycle (during progression through the G1 phase), of growth and survival. The p70S6K phosphorylates the 40S ribosomal protein S6, leading to upregulation of translation and protein synthesis. The p70S6K is regulated by diverse extracellular signals. The activity of p70S6K is controlled by multiple phosphorylation events located within the catalytic, linker and pseudosubstrate domains. Activation of p70S6K depends on the level of its phosphorylation state at eight sites: Thr229, Ser371, Thr389, Ser404, Ser411, Ser418, Thr421, and Ser424. Phosphorylation of Thr229 in the catalytic domain and Thr389 in the linker domain are most critical for the kinase function. The mTORC1 complex phosphorylates p70S6K at Thr389 and Ser371. PDK1 binds to and phosphorylates p70S6K at Thr229 (Pearson et al. 1995; Pullen et al. 1997; Dufner et al. 1999). The carboxyl terminus of p70S6K has a set of Ser and Thr residues (Ser411, Ser418, Ser424, and Thr421), which might be phosphorylated by the MAP kinases ERK1/2 and p38 (Mukhopadhyay et al. 1992).

1.2.2.6 Regulation of the 4E-BP1/eIF4E complex

The 4E-BP1 is a downstream component of the mTOR pathway. 4E-BP1 is a protein identified as a repressor of the cap-binding protein (eIF4E). 4EBP1 binds to eIF4E, which prevents the formation of the active eIF4F complex (eIF4A-eIF4G-eIF4E complex). Hyperphosphorylation of 4EBP1 by mTOR results in the release of eIF4E, thus, allowing the translation complex to assemble (Hay et al. 2004). Downregulation of mTOR induces hypophosphorylation of 4E-BP1 leading to 4E-BP1 binding to eIF4E, and inhibition of cap-dependent translation.

Eukaryotic translation initiation factor 4E (eIF4E), the mRNA 5'-cap-binding protein, is a central component in the initiation and regulation of translation in eukaryotic cells. EIF4E binds to the mRNA cap structure to mediate the initiation of translation. EIF4E is implicated as important regulator of translation, which plays a crucial role in the malignant transformation, progression, and chemoresistance of many cancers Elevated eIF4E levels correlate with poor prognosis in many cancers including prostate cancer (De Benedetti et al. 2004). The level of free eIF4E might be raised due to increased eIF4E expression or increased phosphorylation and expression of 4EBP1 (De Benedetti et al. 2004).

Mnk1 phosphorylates eIF4E on its physiological site Ser209 only when eIF4E binds to eIF4F complex (Ross et al. 2006). The relation between the phosphorylation of eIF4E and protein translation is controversial. Thus, it has been reported that phosphorylation of eIF4E has either stimulatory (Waskiewicz et al. 1999) or inhibitory (Knauf et al. 2001), or has no effect at all (Morley et al. 2002) on protein translation. In addition, biophysical studies elucidated that phosphorylation of eIE4E decreases its cap-binding affinity, increasing the rate of eIF4E-m^7GTP cap complex dissociation (Scheper et al. 2002). However, this could depend on the cell type and the experimental condition used. This controversial situation somehow seem sto indicate that phosphorylation of eIF4E may not be necessary for the assembly of the eIF4E complex or the general protein translation. However, it has been clearly shown that inhibition of mTOR by rapamycin or other compounds in vitro and vivo increases the phosphorylation status of eIF4E (Tee et al. 2000; Sun et al. 2005; Wang et al. 2007;

Chen et al. 2009; Zhu et al. 2009). Combination of rapamycin and inhibitors against MnK, ERK, p38 MAPK or PI3K revealed that upregulation of eIF4E phosphorylation depends on PI3K signaling and is independent of the MnK signaling pathway (Sun et al. 2005). Knockdown of the MnK1 expression decreased the basal level of p-eIF4E but could not prevent its phosphorylation being increased by rapamycin. Knockdown of mTOR (mTOR siRNA) or raptor (raptor siRNA), yet not rictor (rictor siRNA) hindered the phosphorylation of eIF4E by rapamycin (Wang et al. 2007). This indicates that rapamycin induced eIF4E phosphorylation depends on the presence of mTOR.

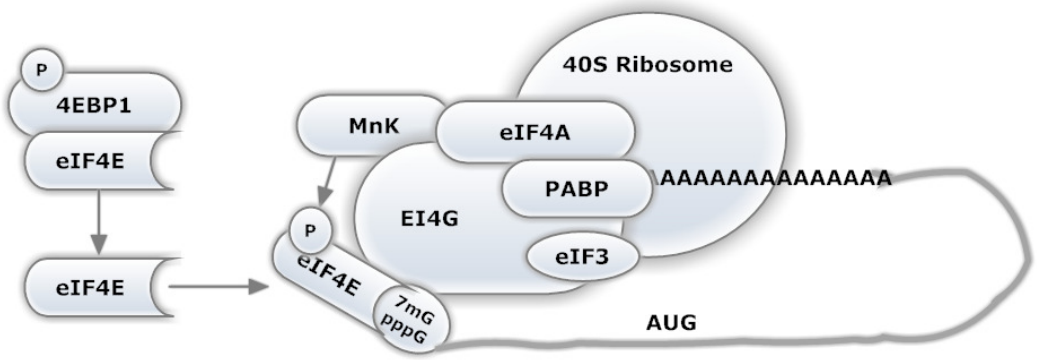

Figure 7. Mechanism of translation intiation

Hypophosphorylated 4EBP1 sequesters EIF4E. Hyperphosphorylation of 4EBP1 results in the dissociation of 4EBP1 from eIF4E and the subsequent association of eIF4E with eIF4G. EIF4G functions as a scaffolding protein that assembles translation factors required for efficient translation initiation. These include the RNA helicase eIF4A, the poly (A)-binding protein (PABP), and eIF3, which recruits the 40S ribosome to the 5" end of the mRNA. 4EBP1 and eIF4G have overlapping binding sites in eIF4E and, therefore, compete for binding to eIF4E (after (Wang et al. 2008)).

Cyclin D1 is considered to be the prime downstream target protein for eIF4E-dependent protein translation. Expression of eIF4E significantly correlates with increased cyclin D1 protein translation. eIF4E enhances nuclear export of cyclin D1 mRNAs (Mamane et al. 2004; Culjkovic et al. 2005). Targeting eIF4E with antisense oligodeoxynucleotides (ASO) or ribavirin diminished the expression of eIF4E-dependent proteins such as cyclin D1. Additionally, it has been shown that inhibition of mTOR signaling was associated with reduction of cyclin D1 expression (Dong et al. 2005; Averous et al. 2008; Yu et al. 2008).

Cyclin D1 has been shown to be implicated in several cancer types. Cyclin D1 is a key regulator of the G1 phase of the cell cycle, which drives cells through the G_1/S phase transition (Stacey 2003). Downregulation of cyclin D1 function results in cell cycle arrest in G_0/G_1 cell cycle phase.

1.2.2.7 Regulation of protein serine/threonine phosphatase

mTOR directly phosphorylates p70S6K and 4EBP1, and also indirectly increases their phosphorylation by inhibition of protein serine/threonine phosphatase (Dufner et al. 1999).

The two main classes of serine/threonine protein kinases, PP1 and PP2A, are extensively involved in many signaling pathways. Treatment of cells with phosphatase inhibitors calyculin A prevents 4EBP1 dephosphorylation. At the same time, inhibition of p70S6K activity by rapamycin, curcumin or amino acid deprivation requires phosphatase activity (Peterson et al. 1999; Yu et al. 2008). The serine/threonine phosphatase PP2A is a prime candidate for such a mTOR-dependent phosphatase. PP2A dephosphorylates p70S6K in vitro and associates with full-length p70S6K, rather than the rapamycin-resistant N- and C-terminal truncated p70S6K mutant (Peterson et al. 1999).

The role of phosphatase in mTOR signaling has been previously identified. Tap42, a protein phosphatase 2A (PP2A) regulatory subunit, is essential for mTOR-mediated signaling in yeast. Tap42 interacts with the catalytic subunits of type 2A phosphatase (PP2Ac), including Pph21 and Pph22, and several 2A-like phosphatases, such as Sit4, Pph3 and Ppg1. In cells under poor nutrient conditions, Tap42 is dissociated from the phosphatases. However, even under optimal growth conditions, Tap42 associates only with a small portion of the phosphatases. For instance, only 5–10% of Sit4 and PP2Ac is found to associate with Tap42 in actively growing cells. Tap42 acts as a phosphatase inhibitor, which binds and inhibits phosphatases in response to mTOR signaling activity (Di Como et al. 1996; Yan et al. 2006).

In more details, mTOR in the presence of sufficient nutrients directly phosphorylates TIP41, which causes release of TAP42. TAP42 can now bind to the catalytic subunit

of PP2A type phosphatases (Sit4, PPh21/22). Association of TAP42 with PP2A prevents its binding to the regulatory subunits A and B, and, thus, leads to inhibition of PP2A downstream phosphorylation. In the absence of nutrients or in the presence of rapamycin, mTOR does not phosphorylate TIP41. TIP41 can now bind to TAP42 and this binding prevents the association of TAP42, leading to binding of PP2A with subunits A and B and dephosphorylation of downstream targets. This results in inhibition of translation and transcription (Rohde et al. 2001)(Figure 8).

Mammalian cells also contain a homolog of Tap42, the α4 protein, which associates with PP2A phosphatases and modifies the substrate specificity of PP2A (Murata et al. 1997). The regulation of this complex may differ from that in yeast, as a recent study has suggested that PP2A is the target of mTOR. The p70S6K was found in a complex with a fraction of PP2A, and a model has been proposed, by which mTOR phosphorylation of PP2A results in phosphatase inactivation that prevents p70S6K dephosphorylation (Peterson et al. 1999; Rohde et al. 2001). In addition, TAP42 and α4 protein interfere with PP2A in vitro inducing dephosphorylation of 4EBP1 (Nanahoshi et al. 1998). On another hand, rapamycin treatment neither induced restoration of the phosphatase activity of PP2A nor did it cause dissociation of alpha4 and Tap42 from PP2A (Nanahoshi et al. 1998).

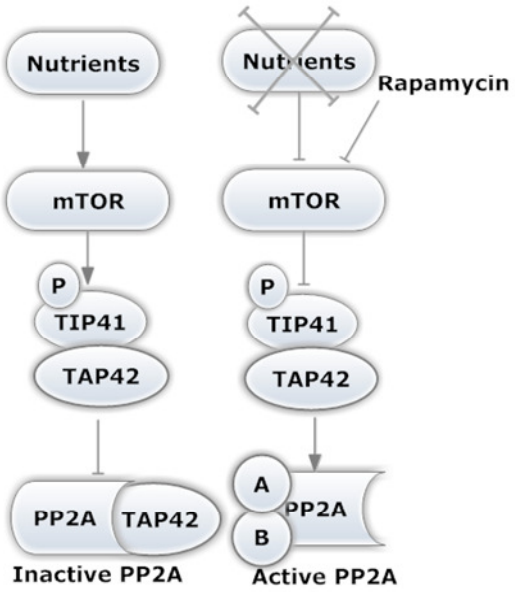

Figure 8. Model for mTOR regulation of PP2A activity

In the presence of sufficient nutrients mTOR directly phosphorylates TIP41, which causes release of TAP42. TAP42 can now bind to the catalytic subunit of PP2A type phosphatases (Sit4, PPh21/22). Association of TAP42 with PP2A prevents its binding to the regulatory subunits A and B, thus, leading to inhibition of PP2A downstream phosphorylation. In the absence of nutrients or in the presence of rapamycin, mTOR does not phosphorylate TIP41. TIP41 can now bind to TAP42 and this binding prevents the association of TAP42 leading to binding of PP2A with subunits A and B and dephosphorylation of downstream targets resulting in inhibition of translation and transcription (after (Rohde et al. 2001)).

1.2.3 mTOR related diseases and the challenges associated with targeting mTOR

Recent studies confirmed that the mTOR signaling pathway involved in various pathological disorders. The importance of the mTOR pathway in different human diseases including cancer is due to its elevated activity and the biological effects of its downstream target proteins, many of which promote cell survival, proliferation and growth. Therefore, the development of small molecules, which modulate the mTOR pathway, has translational potential into therapy.

Typically, mTOR hyperactivation is caused by inactivating mutations of certain suppressors genes in the mTOR signaling pathway like the TSC1/TSC2 complex, LKB1 or PTEN, resulting in mTOR-dependent cell growth.

The macrolide rapamycin is the classical inhibitor of the mTOR signaling pathway. The compound possesses immunosuppressive, antifungal and antitumor properties.

1.2.3.1 Tuberous sclerosis complex (Hamartomas)

Tuberous sclerosis complex (TSC) is an autosomal dominant multisystem disorder characterized by widespread hamartomas in several organs, including the brain, heart, skin, kidney, lung, and liver. TSC is caused by heterozygous mutations in the TSC1 or TSC2 gene (Kwiatkowski et al. 2005).

Hamartomas are benign focal tumour-like malformations. Hamartomas are defined as lesions that are (1) commonly present at birth, but can also be acquired (2) and are composed of aberrant mature or nearly mature structures. Unlike neoplasms, hamartomas lack the ability to grow continuously, resulting in a self-limiting proliferation. Hamartomas tend to originate from the lung, liver, spleen, kidney, and intestine, but uncommon examples have been noted in various other organs. Cell lacking TSC1/TSC2 exhibit activation of the mTOR signaling pathway (Chan et al. 2004; Kwiatkowski et al. 2005), which is thought to contribute to the clinical syndromes in TSC (Chan et al. 2004) . Preclinical data and phase I/II clinical trials

suggest that the use of mTOR inhibitors is beneficial in TSC patient (Lee et al. 2005; Sampson 2009).

1.2.3.2 Hamartoma related syndromes

Cowden disease, Bannayan-Riley-Ruvalcab syndrome (BRRS), proteus syndrome and Lhermitte-Duclos disease are hamartoma syndromes that share similarity to TSC, although they result from inactivating mutation in the tumor suppressor PTEN. PTEN-deficiency results in TSC1/TSC2 inhibition and subsequence hyperactivation of mTORC1. Recent studies indicated that mTOR inhibition with rapamycin may represent a suitable therapeutic option for the chemoprevention and treatment of Cowden disease patients and other tumor syndromes that involve defective PTEN function (Inoki et al. 2005; Squarize et al. 2008).

Peutz-Jeghers syndrome (PJS) is associated with hamartomas in the gastrointestinal tract. Recently, PJS was linked to the TSC-mTOR pathway. The gene mutated in this syndrome, STK11, encodes a protein kinase that phosphorylates and activates LKB1- AMPK signaling, an essential positive regulator of the TSC1/TSC2 complex. Recently it has been shown that rapamycin effectively suppresses Peutz-Jeghers polyposis in a mouse model, suggesting that rapamycin or its analogues may represent a new targeted therapy for the treatment of PJS (Inoki et al. 2005; Wei et al. 2008).

1.2.3.3 Polycystic kidney disease

Polycystic kidney disease (PKD) is generally a late-onset multisystem disorder characterized by large cysts in one or both kidneys and a gradual loss of normal kidney tissue, which can lead to chronic renal failure. The most common form is autosomal dominant polycystic kidney disease (ADPKD). ADPKD is caused by mutations in the PKD1 and PKD2 gene, which encode polycystin-1 (PC-1) and -2 (PC-2), respectively. TSC2 gene and PDK1 gene genes are located in close vicinity on the human chromosome 16 in a tail-to-tail orientation. Genetic molecular analysis has revealed that, in the majority of cases of severe polycystic kidney disease in

TSC revealed large deletions of chromosome 16 affecting both the TSC2 and the PKD1 gene. Indeed, TSC1 inactivation in the kidney results in massive renal cystogenesis (Boletta 2009).

In animal models for ADPKD, hyperactivation of mTOR was observed and mTOR inhibition could indeed retard cyst formation and progression of renal failure, which suggests that mTOR activity is the molecular mechanism underlying renal cyst formation (Tao et al. 2005). Recently, hyperactivated mTOR was found in cyst-lining epithelial cells in human ADPK patients and it was shown that treatment of human ADPKD transplant-recipient patients with rapamycin results in a significant reduction in native polycystic kidney size (Shillingford et al. 2006). It has also been recently demonstrated that rapamycin might be an effective therapeutic option for ADPKD patients that are prone to progress to end-stage renal disease (Serra et al. 2007).

1.2.3.4 Neurodegenerative disorders

It has been shown that the mTOR signaling pathway is associated with many neurological disorders (mental retardation syndromes, autism, Alzheimer's, Huntington's and Parkinson`s diseases) (Swiech et al. 2008; Hoeffer et al. 2010)

Autophagy is an intracellular bulk degradation process through which a portion of the cytoplasm is delivered to lysosomes for degradation. Thus, autophagy is the protective mechanism by which our body can fight against these neurodegenerative diseases, because these diseases develop from intracellular protein aggregations associated with mutant proteins (Mizushima 2005; Hara et al. 2006).

Interestingly, induction of autophagy by inhibition of the mTOR signaling pathway enhances the autophagic clearance of protein aggregates (Hara et al. 2006).

In a mouse model of Huntington disease, rapamycin attenuates huntingtin accumulation and cell death, Furthermore, rapamycin protects against neurodegeneration in a fly model of Huntington disease, and the rapamycin analog CCI-779 improved the performance on four different behavioral tasks and decreased

the aggregate formation in a mouse model of Huntington's disease (Ravikumar et al. 2004).

Moreover, treatment of a mouse model for Parkinson's disease with rapamycin prevents the development of dyskiesia (L-DOPA-motor side effect). Thus, mTOR inhibitors represent a promising target for the design of anti-parkinsonian therapies (Santini et al. 2009).

1.2.3.5 Cancer

The term cancer designates diseases with uncontrolled cell division resulting in local tumor or neoplasia formation. Cancer cells can also spread to other parts of the body through the blood or lymphatic systems.

Tumor suppressor genes are normal genes that slow down cell division, repair DNA, and eventually induce cells to die (a process known as apoptosis or programmed cell death). When tumor suppressor genes do not work properly, cells may grow out of control, leading to cancer. Many different tumor suppressor genes have been identified, including PTEN, p53, BRCA1, BRCA2, APC, and RB1.

Increased mTOR signaling pathway activity can occur by a number of mechanisms. A common mechanism is the loss of function of the tumor suppressor gene PTEN by mutation, deletion or silencing. The signaling pathways that regulate mTOR activity are frequently activated in human cancers (Sawyers 2003; Wan et al. 2007) (Table 2). The main mechanism by which mTOR can contribute to cancer development is through its effects on cell cycle progression and its anti-apoptotic activity. mTOR is required for cell cycle progression, and inhibition of mTOR activity by rapamycin arrests cells in the G_1 phase of the cell cycle. Expression of a rapamycin-resistant mutant of mTOR reduces the effect of rapamycin on the cell cycle progression. There is evidence that the effect of rapamycin on the cell cycle progression occurs by the inhibition of the downstream effectors of mTOR, p70S6K, and eIF4E. Moreover, inhibition of mTOR drives the cell into apoptosis. Many proteins in mTOR signaling pathway have already been implicated in cancer (Sawyers 2003; Wan et al. 2007). Therefore, the development of anti-cancer drugs related to the mTOR

pathway is consered to be very promising. Thus, clinical trials have already been started or conducted using mTOR inhibitors such as rapamycin, RAD001, CCI-799 and AP23579, for cancer treatment.

In clinical trials, rapamycin and three rapamycin analogues, CCI-779 (Temsirolimus), RAD001 (Everolimus), and AP23573 (Deforolimus) have been assessed for their efficacy as anticancer agents (Wan et al. 2007). Rapmycin tested in recent clinical studies for treatment of patients with recurrent PTEN-deficient glioblastoma, phase 1 clinical trial (Cloughesy et al. 2008). Rapamycin analogues were used in clinical trials for treatment of different cancers type (Table 3). Rapamycin and RAD001 can be administered orally. Yet, pharmacokinetic studies showed that both drug have low bioavailability. Therefore, the use of rapamycin as anticancer might be impractical, because of its poor water solubility and stability in solution. On the other hand, CCI-779 and AP23573 can be administered intravenously. CCI-779 was recently approved by U.S Food and Drug Administration (FDA) for treatment of renal cell carcinoma (Ballou et al. 2008; Morgan et al. 2009).

Table 2. Proteins in the mTOR signaling pathway already implicated in cancer (Sawyers 2003; Wang et al. 2007)

Protein	Dysfunction	Type of cancer
Upstream of mTOR		
PTEN	Mutation, deletion, or promoter methylation	Brain, bladder, breast, prostate, endometrial cancer, and glioplastoma
Akt	Gene amplification	Gastric adenocarcinoma, overian, breast, and pancreatic cancers
TSC1/TSC2	Gene mutation	TSC syndrome
Downstream of mTOR		
eIF4E	Gene amplification; protein over expression	Many human cancer types
p70S6K	Gene amplification	Breast, ovarian cancers
Cyclin D1	Gene amplification	Mantle cell lymphoma and breast cancer
Myc	Gene amplification	Burkitt´s lymphoma Other Myc-driven cancer
HIF	Gene amplification	Kidney cancer

Table 3. Clinical trials with mTOR inhibitors as anticancer agents (Wan et al. 2007; Cloughesy et al. 2008)

Compound	cancer	Trial phase
Rapamycin	Recurrent PTEN-deficient glioblastoma	Phase I
CCI-779	Refractory renal cancer, advanced breast cancer, mantle cell lymphoma, recurrent glioblastoma, advanced renal cancer	Phase II
RAD001	Advanced solid cancer and metastatic renal cancer	Phase I
AP23574	Advanced sarcomas and relapsed hematologic cancer	Phase II

1.2.3.6 Other disorders and drug resistances

The mammalian target of rapamycin (mTOR) acts as a central regulator of ribosome biogenesis, protein synthesis, cell growth, cell survival, cytoskeletal organization and most cell activities.

Dysregulation of mTOR signaling has been reported to be involved in cardiac hypertrophy (Inoki et al. 2005). It also plays an important role in metabolic disorders like obesity, type 2 diabetes, non-alcoholic fatty liver disease and Niemann-Pick type C (NPC) disease (Pacheco et al. 2008; Laplante et al. 2009).

A recent animal study revealed that the mTOR signaling pathway links diet-induced obesity with vascular senescence and cardiovascular diseases (Wang et al. 2009). Moreover, it has been shown that inhibition of the mTOR signaling pathway extended the lifespan in inverteberates (yeast, nematodes and fruits) and also in mammalians species (mice) (Harrison et al. 2009). Thus,the mTOR signaling pathway appears to be a key target to control many diseases.

Previous studies showed that the mTOR signaling pathway is implicated in the resistance to many anticancer drugs such as retinoic acid, vincristine and trastuzumab (Jiang et al. 2008)

1.3 Apoptosis and mTOR signaling

Apoptosis is the balance between pro- and antiapoptotic proteins. Defects in the apoptotic machinery are mainly due to either overexpression of antiapoptotic proteins (i.e. Bcl-2, Bcl-xL and survivin) or decrease of proapoptotic proteins (i.e. BAX and BAK, NBK/Bik, BAD, Par-4, Bim, cytochrome c, apoptosis-inducing factor (AIF)) resulting in uncontrolled growth and proliferation.

Many studies showed that activation of the mTOR signaling pathway is implicated in a decreased expression of proapoptotic proteins. Consistently, mTOR inhibitors induced apoptosis in different cell lines through upregulation of proapoptotic proteins and at the same time downregulation of antiapoptotic proteins. (Shinjyo et al. 2001; Tirado et al. 2005; Freilinger et al. 2006; Yan et al. 2006; Zhang et al. 2007; Wangpaichitr et al. 2008; Hayun et al. 2009).

Eukaryotic initiation factor 4E (eIF4E), downstream of mTOR, is responsible for cap-dependent translation and exhibits anti-apoptotic activity (Mamane et al. 2007). Consistently, it has been shown that eIF4E mediates resistance to apoptosis via increases cap-dependent translation (Herbert et al. 2000; Larsson et al. 2006). Additionally, it has been shown that targeting eIF4E with specific RNAi or eIF4E-binding peptides is able to induce apoptosis (Herbert et al. 2000; Dong et al. 2009).

The main biochemical hallmark of apoptosis is activation of caspase-3. Interestingly, caspase-dependent apoptosis is an important mechanism of cell death when the rapamycin derivative RAD001 is combined with 3 Gy radiations (Albert et al. 2006), Additionally, rapamycin can induce caspase-3 activation and induce apoptosis dependent on caspase-3 activation (Zhang et al. 2006).

All these findings indicate that the mTOR signaling pathway is an important target for the development of novel drugs for diseases-associated with apoptosis defect.

1.4 Aims of the study

We have previously shown that the pentacyclic triterpenoid acetyl-11-keto-ß-boswellic acid (AKβBA) induces apoptosis in vitro and in vivo (Syrovets et al. 2005). In comparison to AKβBA, the deacetylated derivative 11-keto-ß-boswellic acid (KBA) showed a decreased activity, pointing to the importance of the acetyl group at carbon number 3 of ring A.

The aim of present study was to,

i) synthesize a new ester derivative of KBA with enhanced proapoptotic activity,

ii) Clarify the putative antiproliferative effect of the new compound,

iii) Shed light on the type of cell death induced, and to

iv) Elucidate the mechanism behind this cell death.

2. MATERIALS and METHODS

2.1 Synthesis of 3-cinnamoyl-11-keto-β-boswellic acid (C-KβBA)

Materials

The synthesis of the corresponding new substance followed a common published method for esterification (Steglich reaction) (Neises et al. 1978), whereas the starting compound 11-keto-β-boswellic acid was extracted from a commercial oleogum resin of *Boswellia carterii* (Caesar & Lorentz GmbH; Hilden, Germany; batch number 72598287, tested corresponding to EB6) according to the method of Winterstein and Stein (Winterstein et al. 1932). The identity of the isolated 11-keto-β-boswellic acid was verified by MS and NMR analysis as described (Büchele et al. 2003). Cinnamic acid (19 mg, 84 µmol), 11-keto-β-boswellic acid (20 mg, 42 µmol), dicyclohexylcarbodiimide (17 mg, 84 µM) and dimethyl amino pyridine (4 mg, 21 µmol) were dissolved in 5 ml dry dichloromethane. This solution was stirred for 17 h at room temperature. The end of the reaction was controlled by a specific thin layer chromatography separation system. The precipitate was separated by filtration and the filtrate was evaporated with argon to dryness. After the residue was redissolved in methanol, 3-cinnamoyl-11-keto-β-boswellic acid was precipitated by addition of water. The precipitate was washed with water and purified by semipreparative reversed phase HPLC to chemical homogeneity (Belsner et al. 2003). The yield of the reaction was 70%. Mass spectra were recorded with a Finnigan SSQ 7000 single-stage-quadrupol mass spectrometer in negative chemical ionization (CI) mode. The scanned mass range was 10u to 2000u. 1-D-NMR and 2D-NMR spectra were recorded on a Bruker AVANCE 400 with a 5 mm QNB $^{1}H/^{13}C/^{31}P/^{13}F$ NMR probe and 5 mm BBI ^{1}H-BB z-GRD NMR probe, respectively.

2.2 Cell culture

Materials

Androgen-independent PC-3	ATCC (Teddington, UK)
Androgen-independent PC-3 PTEN	Professor Derek LeRoith, Professor of Medicine, Endocrinology Diabetes and Bone Disease Director of Metabolism Mount Sinai School of Medicine, New York City
Androgen-dependent LNCaP	ATCC (Teddington, UK)
Androgen-independent DU 145	ATCC (Teddington, UK)
Epithelial cell from normal prostate (RWPE-1)	ATCC (Teddington, UK)
Breast cancer cell line MDA-MB-231	ATCC (Teddington, UK)
Mouse embryonic fibroblasts MEFs ($TSC^{-/-}$) MEFs ($TSC^{+/+}$)	Professor David J. Kwiatkowski, Professor of Medicine, Brigham and Women's Hospital, Harvard Medical School
F-12K medium	Invitrogen, Karlsruhe, Germany
RPMI 1640 medium	PAA Laboratories GmbH, Austria
MEM medium	Invitrogen, Karlsruhe, Germany
Keratinocyte-SFM medium	Invitrogen, Karlsruhe, Germany
DMEM medium	Invitrogen, Karlsruhe, Germany
DMEM/F-12 medium	Invitrogen, Karlsruhe, Germany
EDTA (Titriplex III)	Merk KG, Darmstadt, Germany
Penicillin/streptomycin	Invitrogen, Karlsruhe, Germany
FCS “fetal calf serum”	Seromed, Berlin, Germany

Protocol

Cultivation

Cell lines	Medium
PC-3	F-12K, 10% FCS, 1X penicillin streptomycin
PC-3 PTEN	F-12K, 10% FCS, 500 µg/ ml geneticin
LNCaP	RPMI-1640, 10% FCS, 1X penicillin streptomycin, 1 mM sodium pyruvate, 2 mM L glutamate and 4.5 g/L glucose
DU 145	MEM,10% FCS, 1X penicillin streptomycin, 1 mM sodium pyruvate, 2 mM L glutamate and 1X non-essential amino acids (NEAA)
RWPE-1	Keratinocyte-SFM, 0.05 mg/ml bovine pituitary extract (BPE), 5 ng/ml human recombinant epidermal growth factor (EGF).
MDA-MB-231	Leibovitz's L-15 Medium, 10% FCS.
MEFs (TSC-/-) MEFs (TSC+/+)	DMEM, 10% FCS, 1X penicillin streptomycin. and DMEM/F-12, 10% FCS, 1X penicillin streptomycin, 1 mM sodium pyruvate, 4 mM L glutamate and 4.5 g/L glucose (for XTT assay)

Each cell line was cultivated according to data sheet from the cell bank.

Subculturing

The splitting ratio was 1:3 to 1:6 with medium renewal 2 to 3 times per week.

Freezing and thawing

Cells (3 x 10^6)/cryovial in 1.5 ml freezing medium (medium containing 10% DMSO) were frozen in an isopropanol box at -80^{o}C for 24 h, then stored in the vapor phase of liquid nitrogen.

The contents of a cryovial was thawed and suspended in 30 ml prewarmed complete medium. The culture was allowed to grow for at least 2 weeks before any experiments.

2.3 Antiproliferative effect of C-KβBA in vitro

2.3.1 Cell proliferation assay (XTT assay)

The assay is based on the measurement of the metabolization of tetrazolium salts (XTT, Roche Diagnostics) to water-soluble formazan salt by viable cells (mitochondrial reduction of tetrazolium salt).

Materials

C-KβBA, KBA, Methyl-KBA, AKβBA, cinnamic acid	B. Büchele Institute of Pharmacology of Natural Products & Clinical Pharmacology, Ulm University, Germany
Akt inhibitor VIII	Calbiochem, San Diego, USA
Temsirolimus (CCI-779)	LC laboratories, Woburn, USA
Rapamycin	Sigma-Aldrich, Steinheim, Germany
Cell proliferation Kit (XTT)	Roche Diagnostics, Mannheim, Germany
Microtiter plate	BD, Falcon, San Jose, USA
ELISA reader	Dynatech MR 7000, Germany

XTT labeling mixture

125 µM sodium XTT
25 µM phenazine methosulfate

Protocol

The indicated cell lines (in 200 µl of culture medium/ well) were seeded in a 96-well plate (flat bottom), treated with or without compounds, and incubated for various time periods at 37°C in a 5% CO_2 atmosphere. Before the end of the experiment, 50 µl of XTT labeling mixture was added per well and the plates were incubated for another 4 h at 37°C in 5% CO_2. The spectrophotometric absorbance of the sample was measured using a microtiter plate (ELISA) reader at 450 nm and a reference filter 630 nm.

2.3.2 Clonogenic survival assay

The clonogenic assay is based on the ability of a single cell to grow into a colony. It is also the method of choice to determine the effectiveness of the cytotoxic agents over a long period of time.

Materials

Methanol	Sigma-Aldrich, Steinheim, Germany
Acetic acid	VMR International S.A.S, France
Crystal violet	Sigma-Aldrich, Steinheim, Germany
PBS	Gibco, Karlsruhe, Germany
Spectrophotometer	Dynatech MR 7000, Germany

Fixation solution	Staining solution
10% Methanol	0.4% Crystal violet
10% Acetic acid	20% Methanol

Protocol

PC-3 cells were harvested from cultures growing in the log-phase and were plated at a density of 3000 cells/well in a 6-well plate. After 24 h, the cells were treated with C-KβBA or 0.5% DMSO (as control) in 1% FCS. On the third day, the medium was removed and new medium (10% FCS) was added. After 6 days, the wells were washed twice with ice-cold PBS and fixed for 10 min in 1 ml fixation solution. Colonies were stained with 1 ml staining solution for 10 min. The staining solution was removed and the wells were washed with water to remove excess dye, and dried at room temperature overnight. Photos of the plates were taken, and the colonies were subsequently solubilized in 33% acetic acid followed by spectrophotometric analysis at 540 nm.

2.3.3 Antiproliferative effect of C-KβBA in vivo

We used the chick embryo chorioallantoic membrane as a bioassay to investigate the cytotoxicity and apoptotic parameters of C-KβBA in vivo.

Materials

Anti Ki-67 antibody	DAKO, Glostrup, Denmark
TUNEL Kit	Roche Diagnostics, Mannheim, Germany
Anti p-p70S6K antibody	Epitomics, Hamburg, Germany

Protocol

For the application of the compound in the xenograft model, PC-3 cells were grafted into silicone rings placed onto the chorioallantoic membrane (CAM) of chicken eggs. The fertilized chicken eggs were incubated at 37°C at constant humidity (Syrovets et al. 2005). On day six, 0.7×10^6 PC-3 cells in the log growth phase were seeded in 20 µl medium/Matrigel (1: 1, v/v) in 6 mm silicone ring were placed onto the CAM. Starting from day 2 after seeding, the cells were topically treated once daily either

with 20 µl compound or 0.5% DMSO alone (control). On day 12, the xenografts were histologically analyzed.

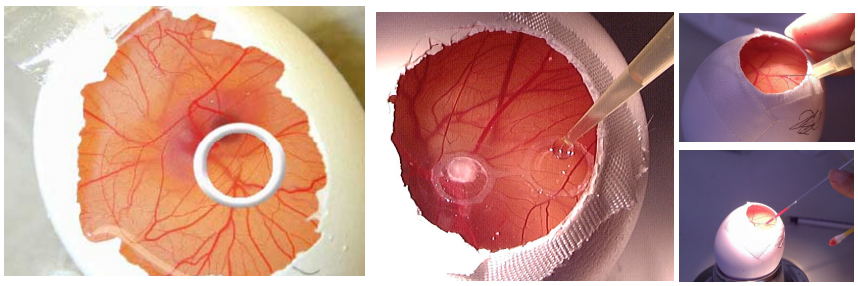

Figure 9. Application of compounds onto the chorioallantoic membrane (CAM) of a fertilized chicken egg.

2.4 Analysis of apoptosis parameters

2.4.1 Expression of phosphatidylserine on the cell surface

Apoptosis is characterized by a variety of morphological features such as loss of membrane asymmetry and attachment, condensation of the cytoplasm and nucleus, and internucleosomal cleavage of DNA. One of the earliest indications of apoptosis is the translocation of the membrane phospholipids' phosphatidylserine (PS) from the inner to the outer leaflet of the plasma membrane. Once, it exposed to the extracellular environment, binding sites on PS become available for annexin V, a 35-36 kDa, Ca^{+}-dependent, phospholipid-binding protein with a high affinity for PS.

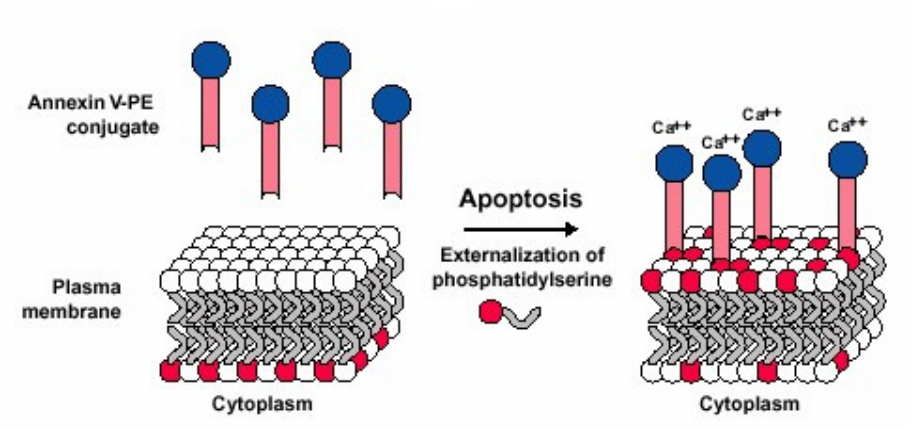

Figure 10. Schematic representation of phosphatidylserine (PS) phospholipid flipping to the outer membrane leaflet during apoptosis and subsequent binding of exogenously added annexin V to the cell surface
(http://www.bdbiosciences.ca/canada/pharmingen/product_pages/annexinv/)

Materials

Annexin V-FITC	Roche Diagnostics, Mannheim, Germany
PBS (with 2 mM $CaCl_2$)	Gibco, Karlsruhe, Germany
Propidium iodide	Sigma-Adlrich, Steinheim, Germany
FACScan	Becton Dickinson, Franklin Lakes, USA

Citric acid solution

1.35 M potassium chloride

0.15 M sodium citrate

Binding buffer

500 ml Sterofundin (B. Braun Avitum AG, Melsungen, Germany)

5 ml 1 M HEPES

Protocol

PC-3 cells were exposed to the desired concentrations of C-KβBA for 24 h. Subsequently both, floating and adherent cells, were collected. The floating cells were collected by centrifugation at 400 x *g* for 5 min, whereas adherent cells were harvested by citric acid solution and collected by centrifugation at 400 x *g* for 5 min. The pooled cells were resuspended in F-12K medium (10% FCS) and incubated for 20 min at 37°C. Then the cells were collected by centrifugation at 400 x *g*, resuspended in 100 µl of binding buffer, and mixed with annexin V-FITC and propidium iodide according to the manufacturer's instructions. In cells undergoing apoptosis annexin V binds to PS, which is translocated from the inner to the outer leaflet of the cytoplasmic membrane. Double staining is used to distinguish between viable, early apoptotic and necrotic or late apoptotic cells. Untreated control cells were also included in the analysis. Annexin V-FITC signals were recorded in FL1-H and propidium iodide in FL2-H. Cells in the bottom left quadrant (annexin V-negative, propidium iodide-negative) are viable, whereas cells in the right lower quadrant (annexin V-positive, propidium iodide-negative) are in the early stages of apoptosis, and the cells in the top right quadrant (annexin V-positive, propidium iodide-positive) are in later stages of apoptosis and necrosis.

2.4.2 Measurement of caspase activity

Caspases (cysteine-aspartic acid proteases) are a family of cysteine proteases, which play essential roles in apoptosis. A member of this family, caspase 3 (CPP32, apopain, YAMA) has been identified as a key effector caspase of apoptosis of mammalian cells. Capase 3 activity was determined by proteolytic cleavage of the fluorogenic substrate (Z-DEVD–R110), which leads to formation of a fluorescent product that can be measured fluorimetrically.

Materials

Fluorogenic substrate Z-DEVD–R110 substrate	Molecular Probes/Invitrogen, Karlsruhe, Germany
QuantaMaster™ UV VIS spectrofluorometer	Photon Technology International, Birmingham, NJ, USA

20x Cell lysis buffer

200 mM Tris-HCl, pH 7.5

2 M NaCl, 20 mM EDTA

0.2% TRITON X-100

5x Reaction buffer

50 mM PIPES, pH 7.4

10 mM EDTA

0.5% CHAPS

1 M DTT

Protocol

PC-3 cells (1 x 10^6) cultivated in F-12K medium for 24 h were treated with or without different concentrations of C-KβBA for 24 h, collected, and caspase activity was analyzed according to the manufacturer's protocol. Briefly, PC-3 cells were resuspended in 50 µL 1x cell lysis buffer on ice. After 30 min, 50 µL 2x reaction buffer (containing 10 mM DTT and 50 µM caspase substrate) was added and incubated for 30 min at room temperature. The samples were measured with a fluorescence spectrophotometer (496 nm/520 nm).

2.4.3 Measurement of DNA fragmentation

DNA fragmentation is a key feature of programmed cell death. Apoptosis is characterized by the activation of endogenous endonucleases with subsequent cleavage of chromatin DNA into internucleosomal fragments of 180-200 BP and multiples thereof.

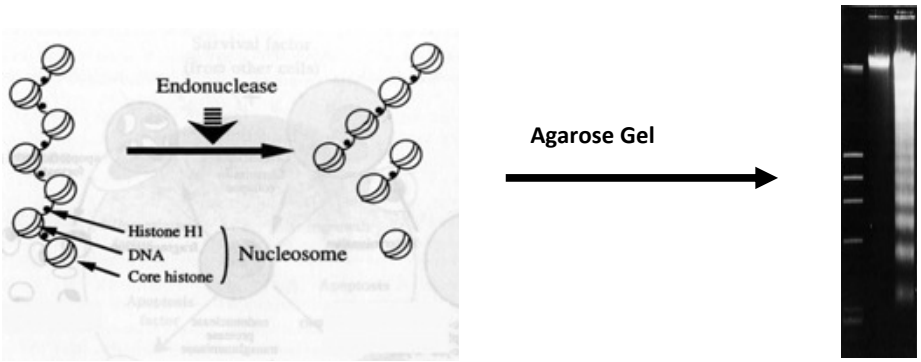

Figure 11. Scheme of the DNA fragmentation process and its analysis

Materials

PBS	Gibco, Karlsruhe, Germany
RNase A	Sigma-Aldrich, Steinheim, Germany
Proteinase K	Sigma-Aldrich, Steinheim, Germany
Agarose	Invitrogen, Karlsruhe, Germany
Photo apparatus easy 429	Herolab, Wiesloch, Germany
UV-Photometer	Herolab, Wiesloch, Germany
Electrophoresis apparatus	Biometra, Göttingen, Germany

Genomic DNA extraction buffer

5 mM Tris-HCl, pH 8.0
20 mM EDTA
0.8% (w/v) SDS

Electrophoresis buffer

TBE (Tris/borate/EDTA) buffer, 5x
445 mM Tris base
445 mM boric acid
10 mM EDTA, pH 8.0

6x Loading buffer

3 ml glycerol (30%)
25 mg bromophenol blue (0.25%)
dH_2O to 10 ml

Protocol

PC-3 cells were cultured for 24 h in F-12K medium, 10% FCS, and then treated with or without C-KβBA in medium/1% FCS for 96 h with daily medium changes. Floating cells were collected by centrifugation, washed with PBS, and lysed with 20 µl genomic DNA extraction buffer with 2 µl RNAse (50 mg/ml)) at 37^{o}C for 30 min with shaking, then 10 µl proteinase K (20 mg/ml) were added, and incubated at 50^{o}C for 90 min with shaking. Then genomic DNA extractions were analyzed by electrophoresis on a 1.5% agarose gel run at 50 V for 4 h. After staining with ethidium bromide (1 µg/ml), the presence of DNA ladders could be visualized under UV light.

2.5 Cell cycle analysis

The DNA contents of cells can provide information about the cell cycle and consequently the effect of added stimuli on the cell cycle, e.g. after drug treatment. The most commonly used DNA dye is propidium iodide, which intercalates in the DNA helix and fluoresces strongly red. Propidium iodide is excited at 488 nm, and can be analyzed on most common flow cytometers. Propidium iodide also stains double-stranded RNA. Therefore, the latter has to be removed with ribonucleases. The progression of cells through the cell cycle was examined using flow cytometry.

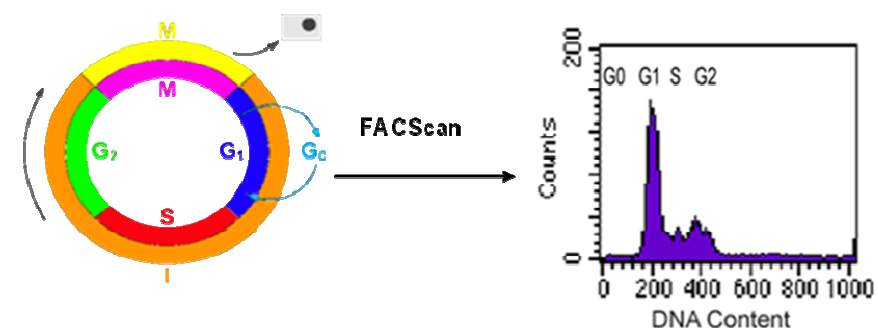

Figure 12. Scheme of flow cytometric cell cycle analysis
(Modified: http://upload.wikimedia.org/wikipedia/commons/2/22/Cell_Cycle_2.png)

Materials

Ethanol	Merck, Darmstadt, Germany
PBS	Gibco, Karlsruhe, Germany
Propidium iodide	Sigma-Aldrich, Steinheim, Germany
RNase A	Sigma-Aldrich, Steinheim, Germany
Flow cytometry	FACScan, Becton Dickinson, Franklin Lakes, NJ, USA
CellQuest software	Becton and Dickinson, Franklin Lakes, NJ, USA
Modfit software	Becton and Dickinson, Franklin Lakes, NJ, USA

<u>Propidium iodide staining buffer</u>

1x PBS
50 µg/ml propidium iodide
40 µg/ml DNase-free RNase A

Protocol

Cells were either left untreated or treated with C-KβBA for 24 h in 1% FCS medium, then harvested by trypsinization, collected by centrifugation 400 x *g* for 5 min, fixed in 70% ethanol (-20°C overnight) and washed once with PBS. After centrifugation, the cells were resuspended in 1 ml of propidium iodide solution. The cells were incubated at room temperature for 30 min in the dark, and the DNA contents were analyzed using the flow cytometer and CellQuest software. The data were analyzed with Modfit software.

2.6 Protein phosphatase assay

Serine/threonine phosphatase activity was determined using malachite green phosphatase assay. This assay is a non-radioactive serine/threonine phosphatase assay, which measures free inorganic phosphate (Pi) that is released from a phosphopeptide substrate. The free inorganic phosphate reacts with malachite green to form an ammonium molybdate-malachite green phosphate complex, which absorbs at or near 620 nm.

Materials

Protein phosphatase peptide substrate H-Arg-Arg-Ala-pThr-Val-Ala-OH, (RRApTVA, K-R-pT-I-R-R)	Enzo Life Sciences GmbH, Lörrach Germany
Protease inhibitor cocktail (P1860)	Sigma-Aldrich, Steinheim, Germany

Malachite green solution A

10 mM ammonium molybdate,
1 N HCl
3.4% ethanol
0.034% malachite green

Phosphatase lysis buffer

20 mM HEPES (pH 7.4)
0.1% NP-40
0.1 mM $MgCl_2$
1 mM EGTA
30 mM β-mercaptoethanol (BME)
1 mM phenylmethylsulfonyl fluoride (PMSF)
Protease inhibitor cocktail
Freshly added 5 µl PMSF, 10 µl protease inhibitor cocktail and 2.4 µl BME to 1 ml buffer

Malachite green additive (solution B)

1% Tween®-20

Phosphate assay buffer

50 mM Tris-HCl (pH 7.0) and 0.1 mM EDTA
200 µM phosphopeptide substrate

Malachite green detection solution

1 ml solution A
10 µl solution B

Protocol

PC-3 cells, 0.2 x 10^6, were cultivated in 6-well plates for 24 h in 10% FCS medium followed by overnight starvation in 0% FCS medium. The cells were pretreated with calyculin A for 20 min, then treated with C-KβBA in the presence or absence of calyculin A for 30 min. The cells were activated by 1% FCS for 30 min. After that the cells were washed with 0.9% NaCl, scraped into phosphate lysis buffer on ice, and sonicated for 8X with ultrasonicator. After centrifugation at 2000 *g* at 4^{o}C for 5 min, the supernatants were used for phosphatase assay. Cell lysates (5 µl) were diluted in 20 µl phosphatase assay buffer at room temperature for 5 min. The reaction was terminated by adding 100 µl malachite green detection solution and 15 min later the absorbance at 630 nm was measured and corrected by subtracting the reading of the bank without lysates.

2.7 Analysis of protein expression

Western blotting (immunoblotting) is a rapid and sensitive assay for the detection and characterization of proteins that works by exploiting the specificity inherent in antigen-antibody recognition. It involves the solubilization and electrophoretic separation of proteins, glycoproteins, or lipopolysaccharides by SDS PAGE or urea-PAGE, followed by quantitative transfer and irreversible binding to nitrocellulose, PVDF, or nylon. This technique has been useful in identifying specific antigens recognized by polyclonal or monoclonal antibodies, and is highly sensitive (1 ng of antigen can be detected).

Materials

Methanol	Sigma-Aldrich, Steinheim, Germany
Skim milk powder	Carl Roth, Karlsruhe, Germany
BSA endotoxin-free	Sigma-Aldrich, Steinheim, Germany
Calyculin A (CA)	Santa Cruz Biotechnology, Heidelberg, Germany
Okadaic acid (OA)	Santa Cruz Biotechnology, Heidelberg, Germany
Protease inhibitor cocktail (P1860)	Sigma-Aldrich, Steinheim, Germany
Compound C	Calbiochem/EMD Biosciences, San Diego, USA
BCA Protein Assay Kit	Pierce, Rockford, USA
Rainbow marker	Amersham Biosciences, Freiburg, Germany
PVDF membrane	Amersham Biosciences, Freiburg, Germany
Hyperfilm	Amersham Biosciences, Freiburg, Germany
ECL substrate reagent	Amersham Biosciences, Freiburg, Germany
Electrophoresis apparatus (Mini Protean II)	BioRad Laboratory, Munich, Germany
Power supply	BioRad Laboratory, Munich, Germany
Sonorex RK 100 SH	Bandelin, Berlin, Germany

2.7.1 Preparation of samples

Whole cell lysates

Cells were seeded in 9 cm plates (0.5 x 10^6) for 24 h, then the cells were starved using serum-free medium overnight, after that the cells were either left untreated or treated with C-KβBA for different time point, followed by activation of the cells by 1% FCS for 30 min. Cells were harvested by scraping in the medium on ice, collected by centrifugation, 400 x *g* at 4°C for 5 min. The pellet was washed in ice-cold PBS. After another centrifugation, the pellet was resuspended in lysis buffer (RIPA buffer) and stored on ice for 15 min, followed by 15 min sonication on ice. The solution was cleared by centrifugation (21,000 x *g* at 4°C for 5 min) and the protein solution transferred to fresh eppendorf tubes. The protein solution was diluted 1: 3 with 3x sample lyses buffer, boiled at 95°C for 5 min and stored at -20°C or used directly for electrophoresis.

RIPA buffer:

(Radio Immuno Precipitation Assay buffer):
150 mM Sodium chloride
1.0% NP-40 or Triton X-100
0.5% Sodium deoxycholate
0.1% Sodium dodecyl sulphate (SDS)
50 mM Tris-HCl, pH 8.0
Add 1:100 protease and phosphatase inhibitors

Sample lysis buffer (3X SLB):

150 mM Tris-HCl (pH 7.0)
12% SDS
6% β-mercaptoethanol
30% glycerol
0.05% Coomassie Brilliant Blue

Cytosolic (cytoplasmic) and nuclear extracts

Cells were seeded in 9 cm Petri dishes (1x 10^6) for 24 h, then the cells were starved using serum-free medium overnight, after that the cells were either left untreated or treated with C-KβBA for 30 min, followed by activation of the cells by 1% FCS for 30 min. Cells were harvested by scraping in the medium on ice, collected by centrifugation (400 x *g* at 4°C for 5 min) and resuspended in 150 µl of buffer A for 10 min. Samples were centrifuged at 3000 x *g* at 4°C for 5 min to collect the

supernatants containing cytosolic proteins for determination of IκB-α by Western blot analysis. The pelleted nuclei were resuspended in 50 µl of buffer B. After 20 min at 4°C, the samples were sonicated on ice for 10 min, then the lysates were centrifuged 25,000 x *g* at 4°C for 5, and supernatants containing the nuclear proteins were transferred to new vials. Subsequently, nuclear extractions were analyzed by Western blot against NFκB-p65 protein and topoisomerase (Topo) I as control for loading.

Buffer A	Buffer B
10 mM HEPES (PH 7.9)	10 mM HEPES (PH 7.9)
1.5 mM MgCl	1.5 mM MgCl
10 mM KCl	0.42 mM NaCl
0.1% Igepal CA630	0.5 mM DTT
0.5 mM DTT	25% glycerol
	0.2 mM EDTA

Add 1:100 protease and phosphatase inhibitors, and DTT freshly before using.

2.7.2 Protein determination

The method, developed by (Smith et al. 1985), is based on the bicinchoninic acid (BCA) reaction for the colorimetric detection and quantification of total protein. This method combines the well-known reduction of Cu^{++} to Cu^{+} by protein in an alkaline medium (the biuret reaction) with the highly sensitive and selective colorimetric detection of the cuprous cation (Cu^{+}) using a reagent containing bicinchoninic acid. The purple-colored reaction product of this assay is formed by the chelation of two molecules of BCA with one cuprous ion. This water-soluble complex exhibits a strong absorbance at 562 nm. The protein contents of the lysates can, thus, be quantified by comparing the absorption with a calibration curve prepared with increasing concentrations of BSA in H_2O. The measurements were performed in ELISA plates with an ELISA plate reader.

Protocol

Cell lysates were diluted 1: 10 in H_2O. 100 µl of BCA working solution was added to lysate solutions and 60 min were allotted for the color shift to develop. The plates were measured at 562 nm

2.7.3 SDS-PAGE

The protein samples described above were separated by denaturing SDS-polyacrylamide gel electrophoresis. Sodium dodecyl sulfate (SDS) is anionic detergent that binds to the hydrophobic parts of the proteins and solubilizes them. Thereby, proteins lose secondary and tertiary structures and only retain their primary structure. SDS confers a high negative charge to the proteins proportional to the length of the amino acid chain, thus, covering any charges the proteins displayed themselves. In an electric field, the negatively charged proteins are drawn towards the anode, and they are separated solely on the basis of their size by the pores of the polyacrylamide gel. Further unfolding of the proteins is achieved by adding the reducing agent, dithiothreitol (DTT) or β-mercaptoethanol (BME), by which disulfide bonds inside the proteins are cleaved.

The molecular weight is determined by comparison with molecular weight standard mixtures.

Protocol

All protein separations were carried out in discontinuous gel electrophoresis, where a stacking gel allows proteins to be concentrated in a line before they enter the separation gel (Table 4). The concentration of the separation gel was adjusted depending on the size of the protein to be detected (Table 5). Electrophoresis was carried out using a vertical apparatus Mini Protean II that allows two gels to be run in parallel.

Samples with equal amounts of protein and the molecular weight marker were loaded into the slots of the prepared polyacrylamide gels. Electrophoresis was run at 70 V for stacking and at 110 V for separation of the protein mixture.

Table 4. Composition of SDS-PAGE gels (16 ml end volume)

Ingredients	Stacking gel	Separating Gel		
	4%	10%	12%	15%
3XGB	2.66 ml	5.31 ml	5.31 ml	5.31 ml
AB 30%	1.06 ml	5.33 ml	6.40 ml	8.00 ml
Glycerol 50%	-------	3.36 ml	3.36 ml	2.24 ml
H_2O	4.23 ml	1.86 ml	0.77 ml	0.35 ml
1 % APS	50 µl	100 µl	100 µl	100 µl
TEMED	8 µl	10 µl	10 µl	10 µl

Table 5. Concentration of polyacrylamide used for the separation of proteins with different molecular weight

(Sambrook et al. 2001).

Acrylamide concentration (%)	Linear Range of Separation (kDa)
5	57-212
7.5	36-94
10	20-80
12	12-60
15	10-43

2.7.4 Western blotting and detection of proteins

For detection of the protein of interest, the protein bands were transferred after electrophoresis onto blotting membranes, incubated with specific antibodies and visualized by chemiluminescence reagents.

Protocol

Western blot was carried out by semi-dry blotting using a discontinuous buffer system. Polyvinylidene difluoride (PVDF) membranes were activated by soaking in methanol for 2 min followed by at least 15 min in blotting buffer with filter papers. The transfer stack consisted of 6 filter papers wetted in blotting buffer, followed by the membrane, the gel and finally 6 filter papers soaked in blotting buffer.

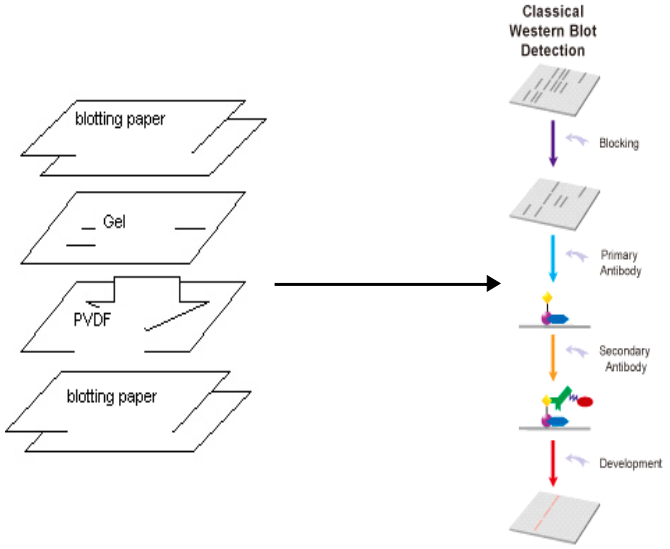

Figure 13. Western immunoblotting technique and detection of the proteins of interest

The transfer was performed on a Transblot SD semidry transfer cell. The transfer was performed at 1.5 mA /cm^2 for 40-60 min depending on the size of the protein to be detected. After transfer, the membranes were blocked in 5% non-fat dry milk in TBS-T for 1 h at room temperature. Subsequently; the membranes were immersed in the respective antibody solution (Table 4) diluted in 5% non-fat dry milk in TBS-T overnight at 4° C. After three wash steps in TBS-T for 10 min each, the adequate secondary horseradish peroxidase-labeled antibody was applied for 45 min at room temperature. Development of the blot was carried out after three more washings (TBS-T, 10 min each) with the ECL Plus substrate solution. Thereafter, the membranes were exposed to X-ray film for the appropriate time period. For all

Western blots, actin was used as control for the quantification of the amounts of loaded protein. Western blot results are representative of at least three independent experiments.

Table 6. Antibodies used for immunoblotting

Antibody	Company	Cat.No.	Species/Mol. Weight	Dilution
Actin	Chemicon	MAB1501	Mouse, 42 kDa	1:1000 in 5% milk
Akt1	Cell Signaling	2967	Mouse, 60 kDa	1:1000 in 5% milk
C-myc	Santa Cruz	sc-789	Rabbit, 67 kDa	1:500 in 5% BSA
Cyclin D1	Santa Cruz	sc-717	Rabbit, 36 kDa	1:1000 in 5% BSA
eIF4E	Santa Cruz	P-2 (sc 9976)	Mouse, 28 kDa	1:1000 in 5% BSA
ERK1/2	Cell Signaling	9102	Rabbit, 42, 44 kDa	1:1000 5% BSA
IκB-α	Cell Signaling	9242	Rabbit, 39 kDa	1:1000 in 5% milk
NF-κB p65	Epitomics	1546-1	Rabbit, 65 kDa	1:1000 in 5% milk
p-70S6K	Santa Cruz	sc-8418	Mouse, 70 kDa	1:1000 in 5% BSA
p-Akt^{Ser473}	Upstate	5756	Rabbit, 60 kDa	1:1000 in 5% milk
P-eIF4E^{Ser209}	Santa Cruz	sc 12885	Mouse, 28 kDa	1:1000 5% BSA
p-ERK	Cell Signaling	9106	Mouse, 42, 44 kDa	1:2000 5% milk
p-p70S6K	Epitomics	CO4159	Rabbit, 70 kDa	1:5000 in 5% BSA
p-PDK ^{Ser241}	Cell Signaling	3061	Rabbit, 58, 68 kDa	1:1000 in 5% milk
Topo I	Santa Cruz	sc-789	Rabbit, 100 kDa	1:1000 in 5% BSA
α-tubulin	Oncogene Research	CP06	Mouse, 60 KDa	1:5000 in 5% milk

Solutions and Buffers for Immunoblotting

30% Acrylamide solution (AB)

30% acrylamide
0.8% N-N´-methylenebisacrylamide
100 ml H_2O

TBS (Tris-buffered saline)

200 mM Tris-HCl
1.37 M NaCl (PH 7.6)

TBS-T

TBS + 0.1% Tween

Phosphatase inhibitors (100X)

125 mM NaF
250 mM β-glycerophosphate
25 mM Na_3VO_4 (sodium orthovanadate)

Blocking buffer

5% milk in TBS-T
or
5% BSA in TBS-T

3x Gel buffer (GB)

3 M Tris HCl (pH 8.45)
0.3% SDS
18.16 g Tris
10 ml 5 N HCl
50 ml H_2O

Blotting buffer

192 mM glycine
25 mM Tris (pH 8.3)
10% or 20% methanol

Cathode buffer

100 mM Tris (pH 8.25)
100 mM Tricine
0.1% SDS

Anode buffer

100 Tris-HCl (pH 8.9)

2.8 FKHR (FOXO1) ELISA

Enzyme-linked immunosorbent assay (ELISA) was used to investigate the effect of C-KβBA on the activity of Forkhead box O1 (FOXO1). Forkhead box (FOX) consensus DNA sequence has been immobilized on 96-well plates. FKHR contained in nuclear extracts binds specifically to this DNA molecule, and is detected through the use of an antibody directed against FKHR. Addition of a secondary antibody conjugated to horseradish peroxidase (HRP) provides a sensitive colorimetric readout that is easily quantified by spectrophotometry.

Materials

TransAM^{TM} FKHR (FOXO1) activity assay kit	Active Motif, Rixensart, Belgium
ELISA reader	Dynatech MR 7000, Germany

Protocol

PC-3 cell (3 x 10^6) cultivated in F-12K medium for 24 h were treated with C-KβBA, KBA and AKT VIII inhibitor (positive control) for 3 h. FKHR (FOXO1) transcriptional activation was analyzed in isolated nuclear extracts from PC-3 using a commercially available transcription factor assay kit (TransAM^{TM} FKHR (FOXO1)) according to the manufacturer's instructions.

2.9 Statistical analysis

The results are expressed as the mean ± SEM. The significance was analyzed using the Newman-Keuls test for multigroup comparisons; $p < 0.05$ was considered significant. * $p < 0.05$, ** $p < 0.01$.

3. RESULTS

3.1 Synthesis of C-KβBA

Starting from pure 11-keto-β-boswellic acid, we synthesized by means of a Steglich esterification reaction (Neises et al. 1978) a novel compound, which we identified by MS and NMR as 3-cinnamoyl-11-keto-β-boswellic acid (Figure 14). The compound was obtained as white small crystals upon precipitation with water from methanol. Upon control of sample purity by TLC, HPLC, MS and one and two dimensional NMR no contamination was detected. UV λ_{max} = 266 nm (methanol); CI-MS: m/z = 601 M^+-H (calcd. for M^+-H Peak $C_{39}H_{53}O_5$: 601.38). Fragmentation of the novel compound showed characteristic fragments, m/z = 481 (loss of part from cinnamic acid), m/z = 453 (loss of carbonmonoxid), m/z = 409 (loss of carbondioxid) and two typical fragments for 11-keto-β-boswellic acid (m/z = 232 and 273 Da) (Pardhy et al. 1978). The NMR analyses showed an intact connectivity of the triterpenoid and also the cinnamic acid fragment. The comparison with the educt (11-keto-β-boswellic acid) correlation indicated remarkable shifts in the A-ring, distinctive at position 3. The HMBC experiment revealed a long-range coupling between the proton at position 3 (δ = 5.46 ppm) and the carboxylic group (position 31, δ = 166.09 ppm) of the cinnamic acid ester. The MS results and the NMR A-ring shift suggested the shown structural connections, the HMBC long-range coupling verified the connection of the cinnamic acid compound with the triterpene at position 3 with a high yield. Based on the known conformational data (Belsner et al. 2003), the known dd multiplet (2,6 Hz) of the proton in position 3 (equatorial), and the pattern of proton coupling (positions 3, 2, 1), the conformation of the cinnamoyl derivative was established.

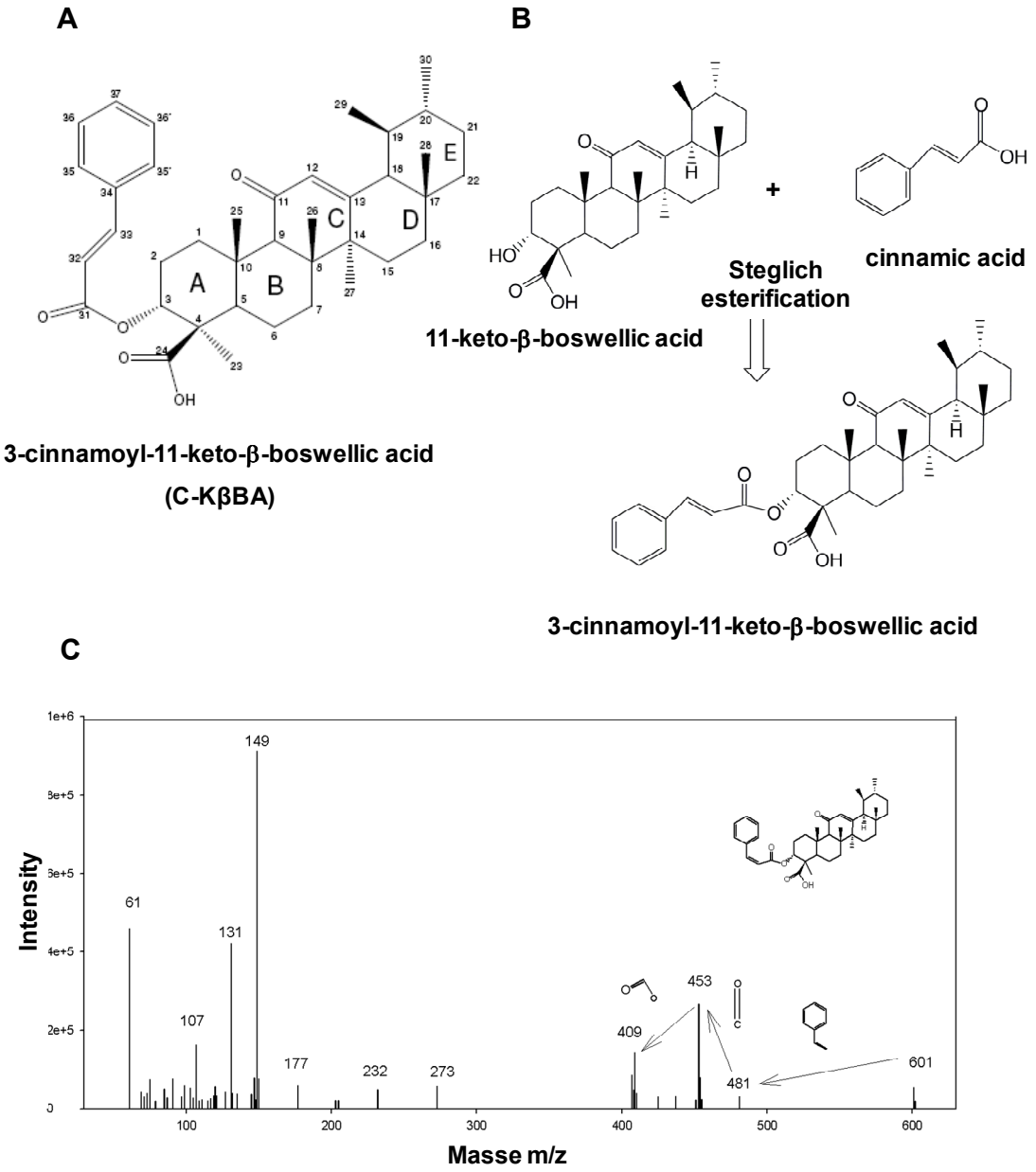

Figure 14. Structure, synthesis and mass-spectroscopy of C-KβBA

A) Structure and numbering scheme with the determining HMBC correlation of C-KβBA. B) Scheme for C-KβBA synthesis. C) Mass-spectroscopy was performed using a Finnigan MAT electrospray ionisation mode.

Table 7. NMR of C-KβBA

^{1}H-NMR and ^{13}C-NMR assignments (δ in ppm) for 3-cinnamoyl-11-keto-β-boswellic acid. (100 MHz ^{13}C NMR, 400 MHz ^{1}H NMR, $CDCL_3$).

	δ^{13}C (ppm)	M.	δ^{1}H (ppm)	M.
1	34.76	CH_2	1.35	m
			2.60	m
2	23.66	CH_2	1.72	m
			2.31	
3	73.17	CH	5.46	d
4	46.76	C		
5	50.66	CH	1.51	m
6	18.80	CH_2	1.74	m
			1.89	m
7	32.95	CH_2	1.74	m
			1.51	m
8	45.1	C		
9	60.43	CH	2.47	s
10	37.46	C		
11	199.17	C		
12	130.55	CH	5.57	s
13	164.82	C		
14	43.78	C		
15	27.26	CH_2	1.24	m
			1.92	m
16	27.56	CH_2	1.04	m
			2.11	m
17	33.98	C		
18	59.05	CH	1.52	m
19	39.29	CH	1.49	m
20	39.34	CH	0.94	m
21	30.93	CH_2	1.45	m
			1.30	m
22	40.93	CH_2	1.49	m
			1.34	m
23	23.96	CH_2	1.30	s
24	181.7			s
25	13.25	CH_3	1.18	s
26	18.43	CH_3	1.22	s
27	20.53	CH_3	1.39	s
28	28.87	CH_3	0.83	s
29	17.44	CH_3	0.80	d
30	21.14	CH_3	0.94	s
31	166.09	C		
32	118.45	CH	6.48	d
33	144.9	CH	7.70	d
34	134.44	C		
35	128.09	CH	7.54	m
35’		CH	7.54	m
36	128.86	CH	7.39	m
36’		CH	7.39	m
37	130.27	CH	7.39	m

3.2 Antiproliferative effect of C-KβBA

The antiproliferative effect of C-KβBA on PC-3 cells was measured by using an XTT assay. The data revealed that treatment of PC-3 cells with C-KβBA for 24 and 48 h exerts a concentration- and time-dependent inhibition of the proliferation of PC-3 cells with an IC_{50} value of 4.2 and 3.8 µM, respectively (Figure 15). Our data showed that C-KβBA is more potent than the parent compounds (cinnamic acid and KBA), also more potent than other derivatives, such as cinnamic acid methyl ester and AKβBA.

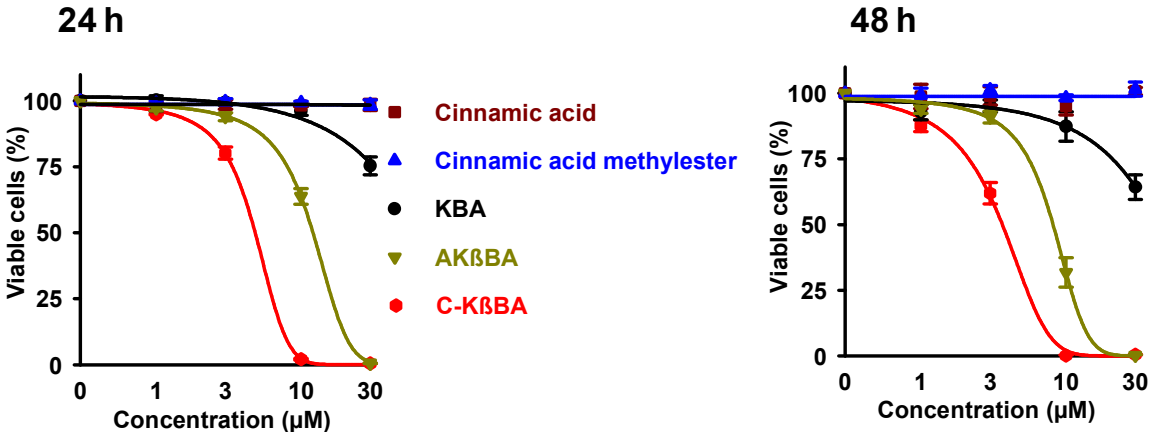

Figure 15. Antiproliferative effect of C-KβBA and the parent compounds on PC-3 cells
Antiproliferative effect of C-KβBA and the parent compounds on PC-3 cells were measured by an XTT assay. PC-3 cells were treated with above-mentioned compounds for 24 and 48 h. The amount of cells in control samples treated with DMSO solvent (0.5%) was set to 100%. Data are mean ± SEM from three independent experiments.

Furthermore, C-KβBA has a remarkable cytotoxic profile, not only on PC-3 cell line, but also on LNCaP and DU 145 prostate cancer cell lines (Figure 16).

Interestingly, C-KβBA showed a relatively selective efficacy against prostate cancer cells (PC-3 cell line) compared to normal prostate epithelial cell (RWPE-1 cell line) with IC_{50} values of 3.6 µM and 10.8 µM, respectively (Figure 17).

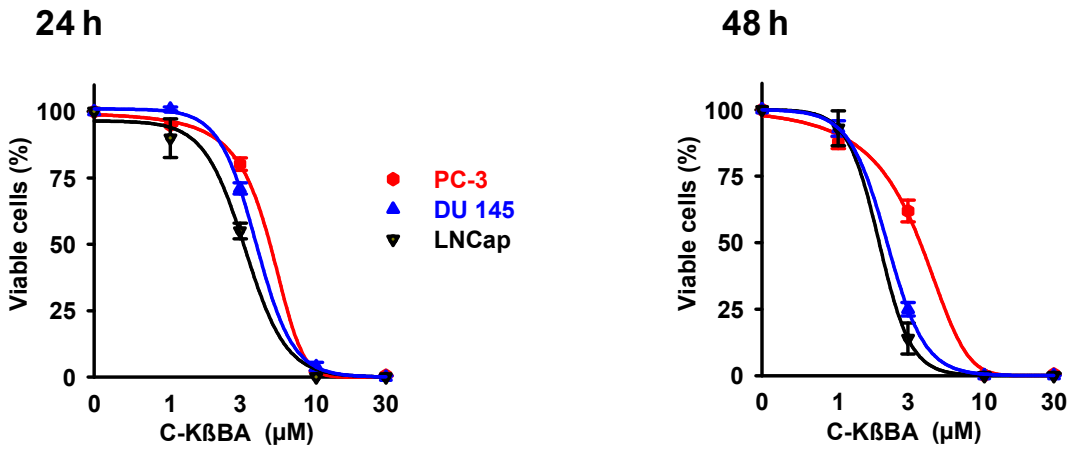

Figure 16. Antiproliferative effect of C-KβBA on different cell lines
Antiproliferative effect of C-KβBA on different prostate cancer cell lines was measured by an XTT assay. The indicated cell lines were treated with C-KβBA for 24 and 48 h. The amount of cells in control samples treated with DMSO solvent (0.5%) was set to 100%. Data are mean ± SEM from three independent experiments.

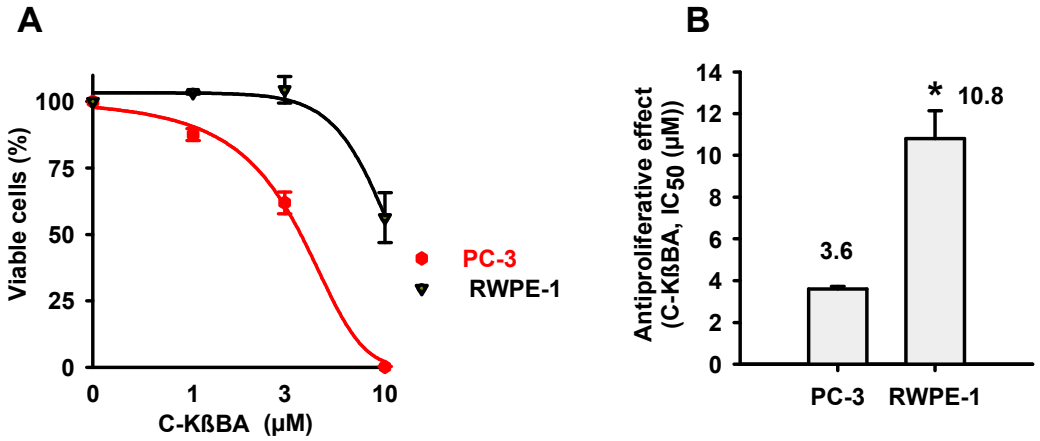

Figure 17. C-KβBA shows relatively selective antiproliferative effects against tumor cells
Antiproliferative effect of C-KβBA on the PC-3 cell line (prostate cancer) and the RWPE-1 cell line (normal prostate epithelial cells) was measured by an XTT assay. A) Indicated cell lines were treated with C-KβBA for 48 h. The amount of cells in control samples treated with DMSO solvent (0.5%) was set to 100%. B) The results are expressed as IC_{50} value from both cell lines. Data are mean ± SEM from three independent experiments. Statistical analysis was performed using the Newman-Keuls test, *p < 0.05.

To determine whether the PC-3 cell line is able to recover from the antiproliferative effect of C-KβBA or not, we treated PC-3 cells with C-KβBA for 24 h, then we changed the medium to C-KβBA-free medium for 6 days. The cell viability was measured by a clonogenic survival assay. The results demonstrate that the PC-3

cells were not able to recover from a single treatment with C-KβBA at a concentration as low as 1 μM. At the same time, the long time treatment with C-KβBA induced a stronger anticlonogenic effect than CCI-779, an inhibitor of mTOR signaling that used in clinical trials (Figure 18).

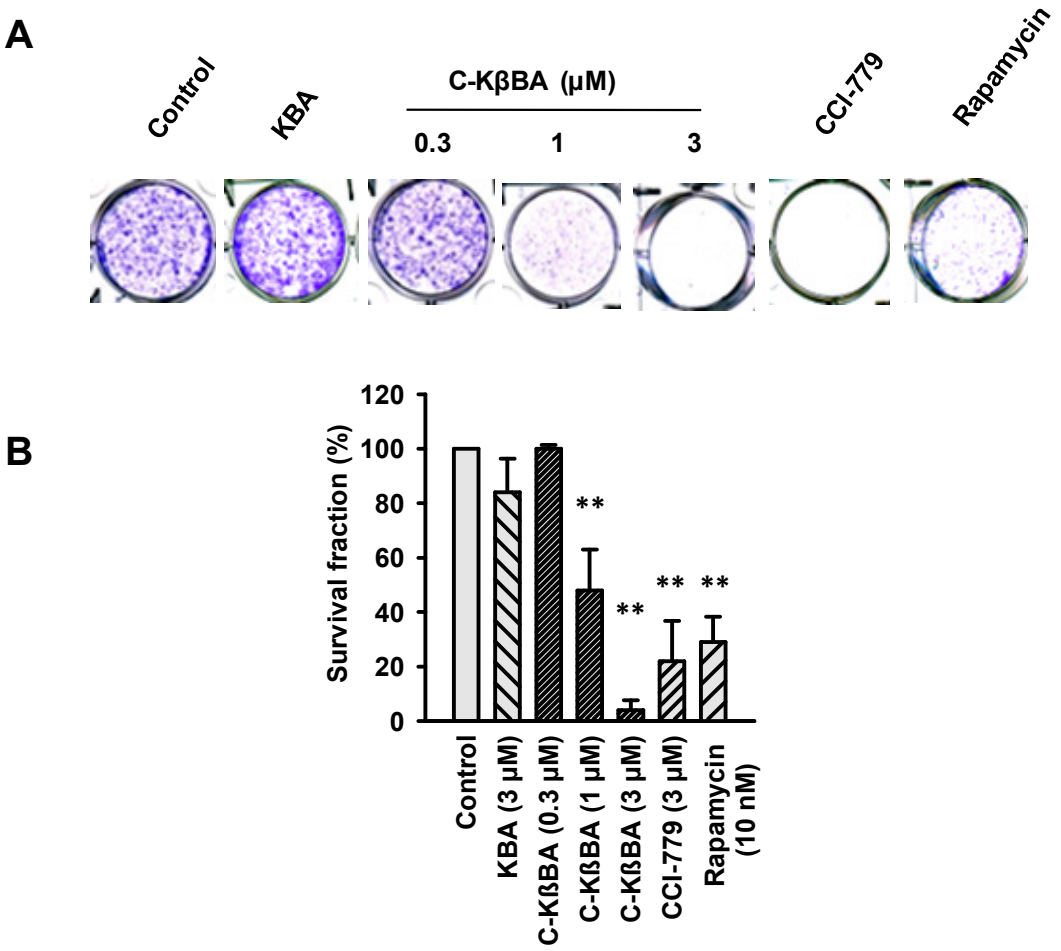

Figure 18. The antiproliferative effect of C-KβBA on PC-3 cells is irreversible

A) The antiproliferative effect of C-KβBA on the PC-3 cell line for longer time was measured by an XTT assay. PC-3 cells were treated with the indicated compounds for 24 h, then the cells were cultivated in compounds-free medium for 6 day. Photos had been taken of the plates, then the colonies were solubilized in 33% acetic acid, followed by spectrophotometric analysis (clonogenic survival assay). B) The results are expressed as mean ± SEM of three independent experiments. Statistical analysis was performed using the Newman-Keuls test, $^{**}p < 0.01$.

3.3 C-KβBA induces cell cycle arrest

Because cell proliferation and growth controlled by the progression of the cells through the well-defined stages of the cell cycle, we next determined the effects of C-KβBA on the cell cycle progression of PC-3 cells. We analyzed the cell cycle distribution by flow cytometry using propidium iodide DNA staining. The flow cytometric analyses of the DNA profile showed that the treatment of PC-3 cells with various concentrations of C-KβBA (1 and 3 μM) for 24 and 48 h effectively arrested PC-3 cells in the G_1 phase of the cell cycle (Figure 19).

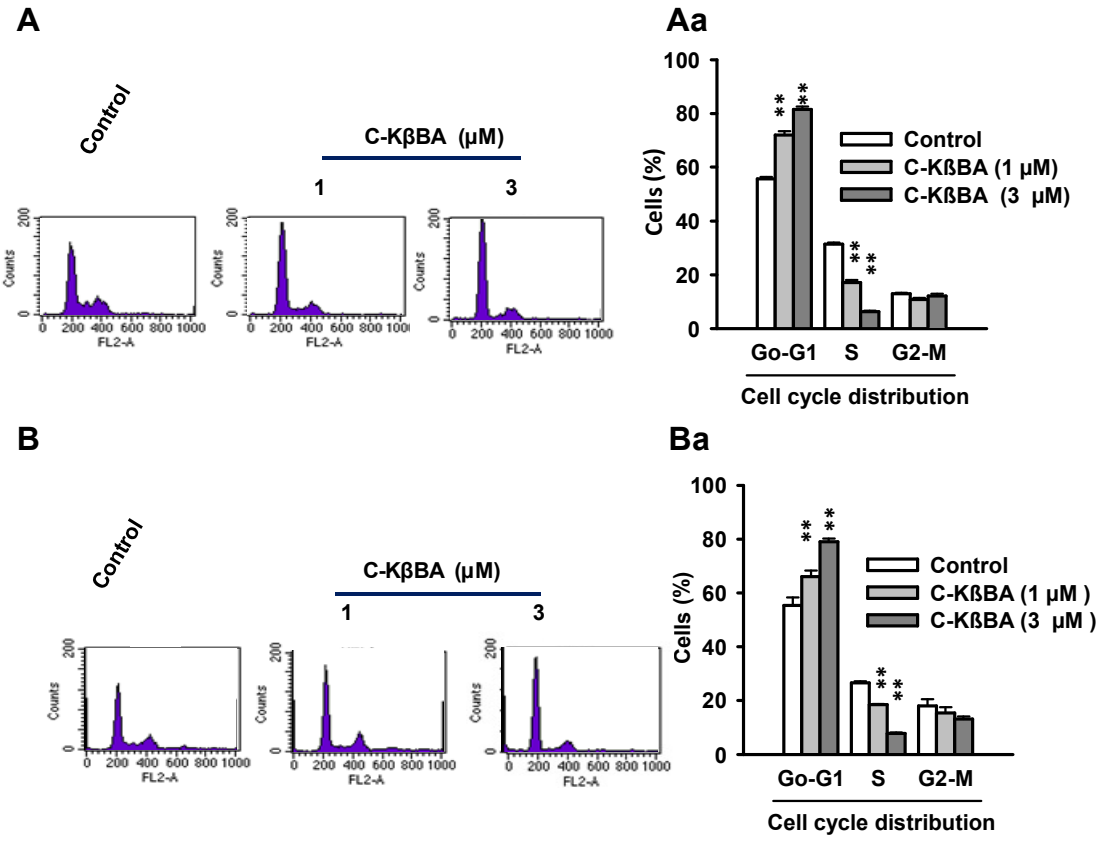

Figure 19. C-KβBA induces cell cycle arrest

The effects of C-KβBA on the cell cycle distribution was measured by flow cytometry (FACS). PC-3 cells were treated with various concentrations of C-KβBA for 24 h (A) and 48 h (B). The cells were fixed in ethanol, subsequently stained with propidium iodide and analyzed by FACS. Cell cycle analysis was performed and quantified by using ModFit software (Aa and Ba). The data represent three independent experiments. Statistical analysis was performed using Newman-Keuls test, $^{**}p < 0.01$.

C-KβBA treatment significantly increased the proportion of cells in the G_1 phase (Figure 19, Aa and Ba). This is an interesting finding because PC-3 cells express mutant p53 alleles, losing the function of p53. Therefore, it appears that C-KβBA is able to arrest cells in the G_0/G_1 phase and inhibit the proliferation of PC-3 cells in a p53-independent manner.

3.4 C-KβBA triggers apoptosis in vitro

The next step was performed to evaluate which type of cell death occurred in PC-3 cells upon C-KβBA exposure. We investigated the proapoptotic activity of C-KβBA by measuring several apoptotic parameters, such as the expression of phosphatidylserine on the cell surface, caspase activation and the definitive sign of apoptosis, DNA laddering.

3.4.1 C-KβBA induces phosphatidylserine expression on the cell surface

During apoptosis, phosphatidylserine physiologically located at the inner membrane leaflet is flipped to the cell surface, where it serves as an "engulfing" signal for neighboring cells (Vermes et al. 1995). Treatment of PC-3 cells with 3, 5 or 10 μM C-KβBA for 24 h triggered expression of phosphatidylserine on the outer membrane leaflet, as determined by FITC-labelled annexin V and propidium iodide staining, followed by flow cytometric analysis (Figure 20). The result revealed that C-KβBA exerts expression of phosphatidylserine in PC-3 cells in a concentration-dependent manner.

3.4.2 C-KβBA induces caspase-3 activation

Caspases are crucial mediators of the programmed cell death (apoptosis). Among them, caspase-3 is a crucial effector caspase, catalyzing the specific cleavage of many key cellular proteins. Caspase-3 is essentail for some typical hallmarks of apoptosis and is indispensable for apoptotic chromatin condensation and DNA fragmentation (Porter et al. 1999). We show here that treatment of PC-3 cells for 24

h with C-KβBA induces caspase-3 activation in a concentration-dependant manner (Figure 21).

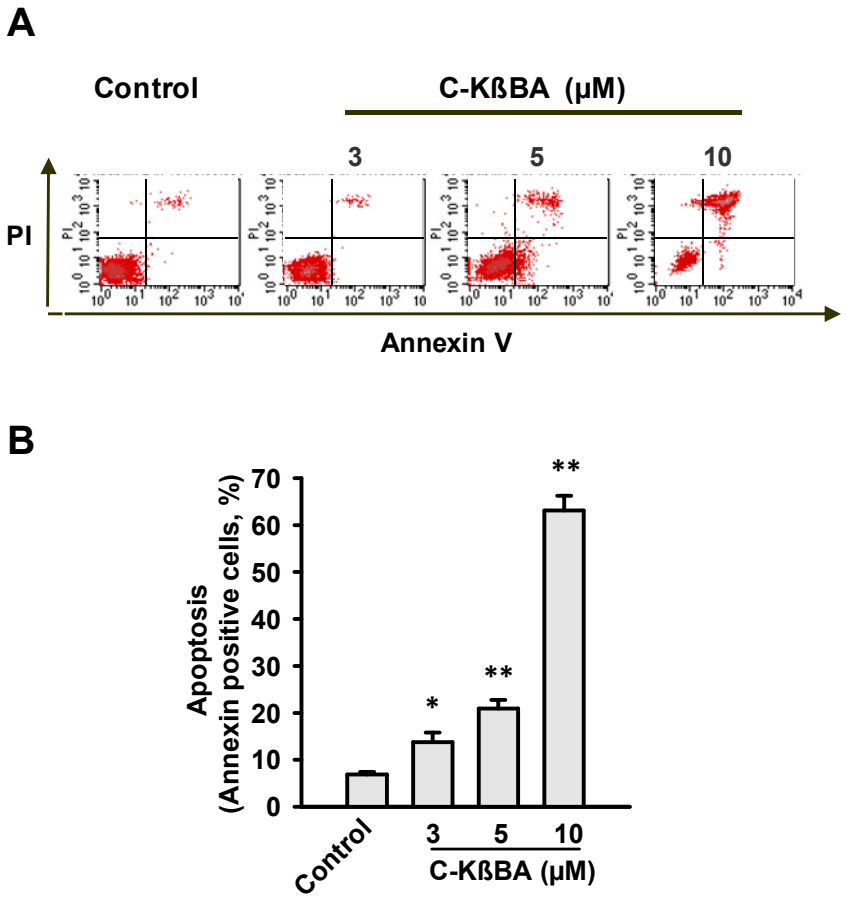

Figure 20. C-KβBA induces phosphatidylserine expression on the cell surface

A) PC-3 cells were treated C-KβBA (3, 5, and 10 µM) for 24 h, harvested, stained with annexin V/propidium iodide and analyzed by flow cytometry. Untreated control cells were also included in the analysis. Annexin V-FITC signals are recorded in FL1-H and propidium iodide in FL2-H. Cells in the bottom left quadrant (annexin V-negative, propidium iodide-negative) are viable, whereas cells in the lower right quadrant (annexin V-positive, propidium iodide-negative) are in the early stages of apoptosis, and the cells in the top right quadrant (annexin V-positive, propidium iodide-positive) are in later stages of apoptosis and necrosis. B) Apoptosis analysis was performed and quantified by using ModFit software. Data are mean ± SEM from three experiments. Statistical analysis was performed using the Newman-Keuls test, * $p < 0.05$, ** $p < 0.01$.

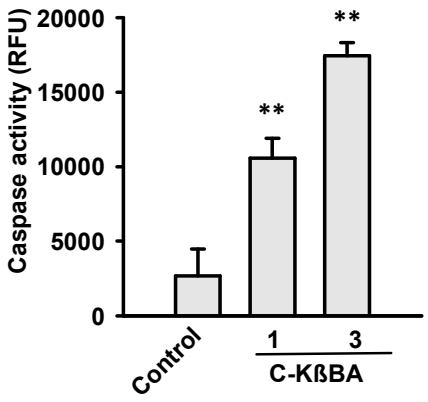

Figure 21. C-KβBA induces caspase-3 activation

Capase-3 activity was measured by proteolytic cleavage of the fluorogenic substrate Z-DEVD-R110. Cells were treated for 24 h with the corresponding concentrations of C-KβBA or vehicle as control. The caspase activity was measured fluorometrically with an excitation wavelength of 496 nm and an emission wavelength of 520 nm. Data are mean ± SEM from three experiments. Statistical analysis was performed using the Newman-Keuls test, $^{**}p < 0.01$.

3.4.3 C-KβBA induces DNA laddering

A biochemical hallmark of apoptosis is the cleavage of chromosomal DNA into oligonucleosome-sized fragments by endonuclease activation triggered by caspase 3, a process called DNA fragmentation or DNA laddering. Our result revealed that treatment of PC-3 cells with C-KβBA (5 μM) for 96 h led to a typical DNA laddering pattern (Figure 22).

.

Figure 22. C-KβBA induces DNA laddering
PC-3 cells treated with C-KβBA (5 μM) for 96 h. The cell lysates were analyzed for DNA fragmentation by agarose gel electrophoresis. The data shown are representative for three independent experiments.

3.5 C-KβBA inhibits growth, proliferation, and triggers apoptosis in vivo

To verify the proapoptotic and antiproliferative activity of C-KβBA in vivo, we next xenotransplanted PC-3 cells onto the chorioallantoic membranes (CAM) of fertilized chicken eggs. Immunohistochemical analysis of the tumor sections for human proliferation antigen Ki-67 (proliferation marker) revealed that C-KβBA had a concentration-dependent inhibitory effect on tumor proliferation.

By using the TUNEL technique for in situ detection of apoptosis, we showed that C-KβBA triggers apoptosis also in vivo (Figure 23). These data show that C-KβBA inhibits the growth of established PC-3 xenografts in vivo even more efficient than in vitro.

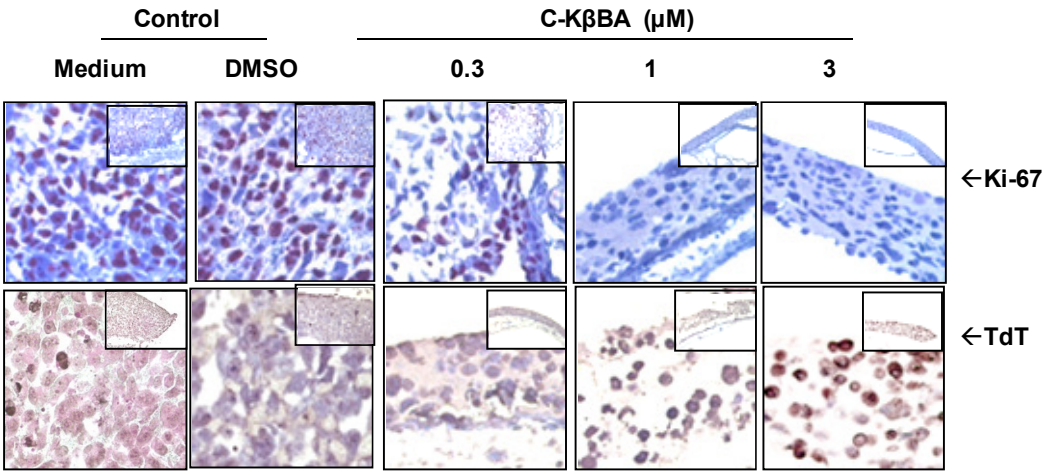

Figure 23. C-KβBA inhibits growth, proliferation, and triggers apoptosis in vivo
PC-3 cells (1×10^6) were grafted onto the chorioallantoic membranes of fertilized chicken eggs. After 2 days, the tumors were topically treated either with 20 μl of C-KβBA or DMSO alone (control) for 4 days before termination of the experiment. Tumor sections were stained against Ki-67 (proliferation marker, brown nuclear stain) and TUNEL (apoptosis marker, dark brown stain). Data shown are representative of 3 eggs each.

3.6 C-KβBA inhibits the mTOR signaling pathway

To better understand the mechanisms and pathways involved in the induction of apoptosis by C-KβBA, we have examined the effects of C-KβBA against several kinases known to be constitutively active in PC-3 cells. Previously we have shown that the acetylated form of KBA (AKβBA) induces apoptosis by downregulation of NF-κB signaling pathway (Syrovets et al. 2005). To figure out the relation between C-KβBA and NF-κB signaling pathway, overnight-starved PC-3 cells incubated with C-KβBA for 30 min followed by stimulation for 30 min with 1% FCS. Gel electrophoresis of cytosolic and nuclear extracts stained for IκB-α (NF-κB-inhibitory protein) and p65 (the major transcription activating NF-κB family member) revealed that C-KβBA did not altered the level of both proteins (IκB-α and p65). Also the Western immunoblot for IκB-α of the whole cell lysates from overnight starved PC-3 cells incubated with C-KβBA for 30 min followed by 30 min FCS 1% incubation indicated that C-KβBA did not altered the level of IκB-α protein (Figure 24). These results exclude the involvement of the NF-κB signaling pathway in the induction of apoptosis by C-KβBA.

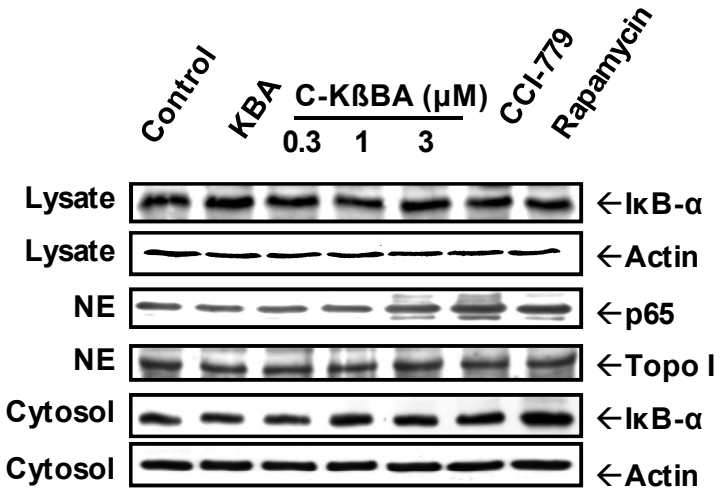

Figure 24. Effect of C-KβBA on the NF-κB signaling pathway

Whole cell lysates, cytosolic and nuclear fractions of PC-3 cells, starved overnight, treated with C-KβBA for 30 min and stimulated for 30 min with FCS, were used for Western blotting. Control cells were treated either with DMSO (0.5%) or CCI-779 or rapamycin used as positive controls. Data represent three independent experiments.

Further studies revealed that within 60 min, C-KβBA induced a rapid downregulation of the phosphorylation of p70S6K kinase in PC-3 cells (Figure 25). The p70S6 kinase 1 (p70S6K) is the best-characterized effector of mTOR (Ali et al. 2005). It has been shown that p70S6K and phospho-p70S6K are expressed at a higher level in prostate cancer cells compared to normal cells (Kremer et al. 2006). Inhibition of mTOR exerts hypophosphorylation of p70S6K in prostate cancer in vitro and vivo (Wu et al. 2005; Bianchini et al. 2008).

To determine the inhibitory effect of C-KβBA on mTOR signaling pathway, we examined the phosphorylation of p70S6K and eIF4E as prime candidates for mTOR downstream targets. PC-3 cells treated with C-KβBA (0.3, 1, 3 μM) for different time periods showed that C-KβBA inhibits the phosphorylation of p70S6K and eIF4E in concentration- and time-dependant manner without altering the total p70S6K protein (Figure 25).

The activity of mTORC1 and mTORC2 were further determined by monitoring the phosphorylation status of p70S6K at Thr389 and Akt at Ser473, respectively (Thoreen et al. 2009) (Figure 25).

Interestingly, C-KβBA also downregulated the phosphorylation of p70S6K in vivo, in the CAM assay. Moreover, C-KβBA was more effective in vivo than in vitro (Figure 26).

Hypophosphorylated 4E-BPs binds with high affinity to eIF4E, prevents association of eIF4E with EIF4G and formation of the eIF4E initiation complex, and, thereby, inhibits cap-dependent translation of mRNA. mTOR phosphorylates the eIF4E-binding protein (4E-BPs) and leads to dissociation of eIF4E (Hay et al. 2004). Inhibition of mTOR exerts upregulation of p-eIF4E in the prostate cancer cell line PC-3 (Bianchini et al. 2008) and in lung cancer cells (Chen et al. 2009). Here we show that C-KβBA upregulates eIF4E phosphorylation in the PC-3 cell line (Figure 25).

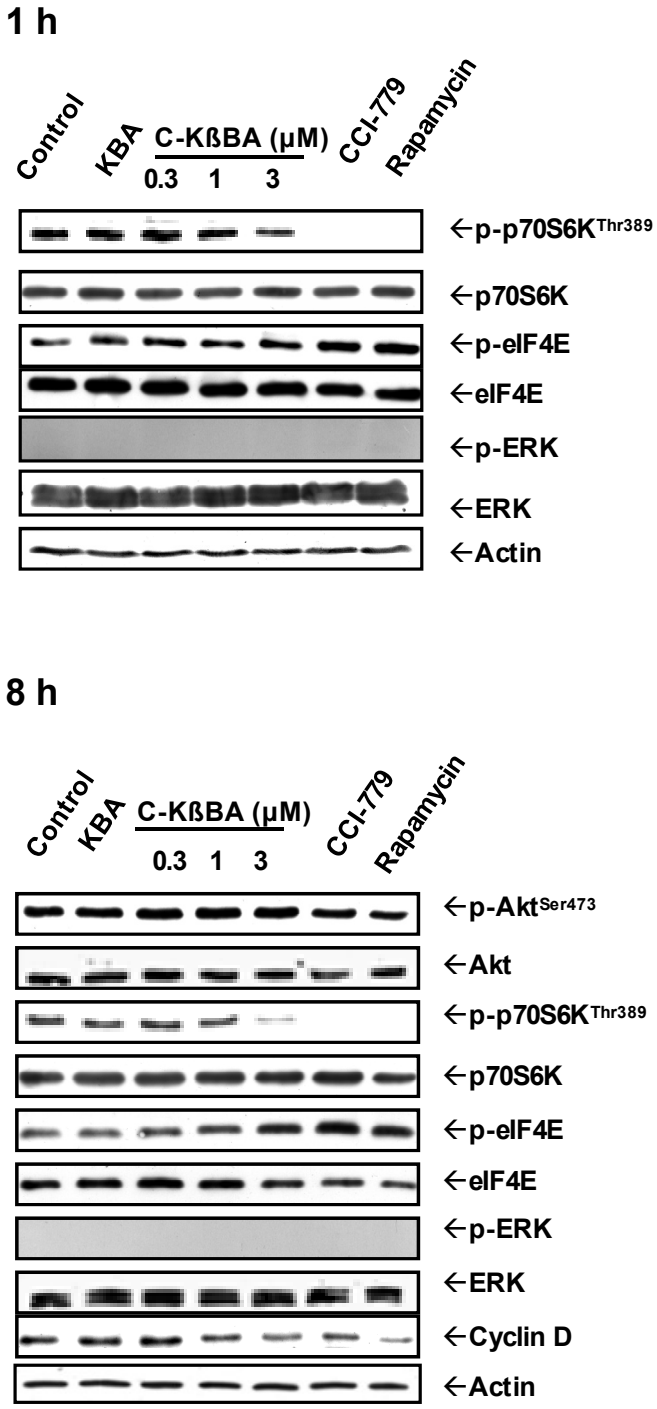

Figure 25. C-KβBA inhibits the mTOR signaling pathway in vitro

Whole cell lysates from PC-3 cells, starved overnight, treated with C-KβBA in the indicated concentration and stimulated for 30 min with 1% FCS, were used for Western blotting. Data shown are representative of three independent experiments.

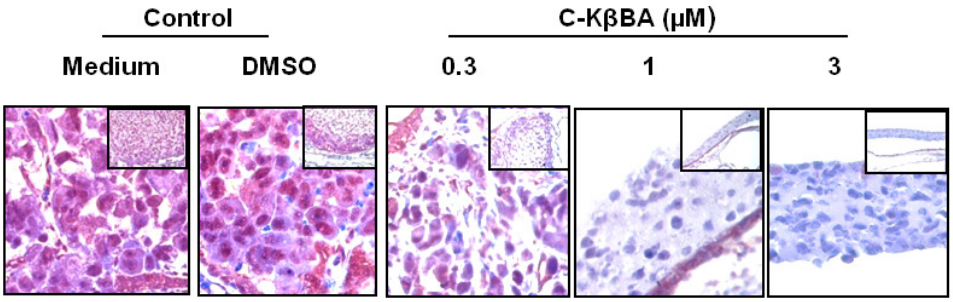

Figure 26. C-KβBA inhibits the mTOR signaling pathway in vivo

PC-3 cells (1 × 10^6) were grafted onto the chorioallantoic membranes of fertilized chicken eggs. After 2 days, the tumors were topically treated either with 20 μl of C-KβBA or DMSO alone (0.5%, control) for 4 days before termination of the experiment. The tumor sections were stained against p-p70S6K (AEC, red stain). Data shown are representative of 3 eggs each.

Activation of eIF4E is elevated significantly with progression of human and experimental prostate cancer, and significantly related to reduce patient survival. Reduction of eIF4E in prostate cancer cells elicits apoptosis in a cell cycle phase-independent manner (Graff et al. 2009). Here we show that C-KβBA, although it upregulated the eIF4E phosphorylation, concomitantly reduced eIF4E expression in prostate cancer cells (Figure 25).

The proto-oncogene cyclin D1 is an important regulator of G_1 to S-phase transition and an important cofactor for several transcription factors in numerous cell types (Alao et al. 2006). Inhibition of the mTOR signaling pathway induced down-regulation of cyclin D1 leading to cell cycle arrest at G_1 phase (Xu et al. 2006; Averous et al. 2008). Treatment of prostate cancer cell lines with C-KβBA for 8, 12 and 24 h downregulated cyclin D1 and mediated cell cycle arrest at G_1 phase as well (Figure 25).

PC-3 is a PTEN-null cell line. Loss of PTEN in this cell line is associated with a hyperactivated PI3K/Akt/TSC/mTORC1 pathway. To clarify that C-KβBA targets the mTOR signaling pathway, we measured the cytotoxicity by the XTT assay in PTEN positive PC-3 cells exposed to different concentrations of C-KβBA for 48 h. Compared to PTEN null PC-3 cells, we found that PTEN positive PC-3 cells are insensitive to C-KβBA. This confirmed our hypothesis that C-KβBA targets the mTOR signaling pathway (Figure 27).

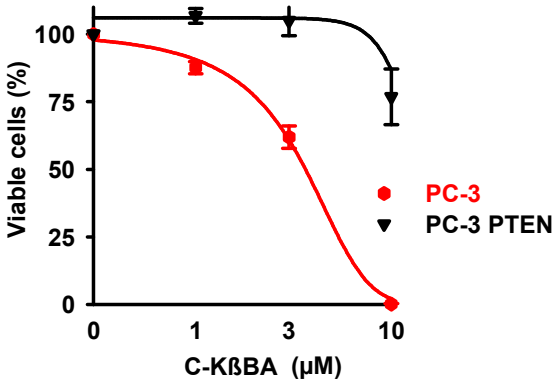

Figure 27. C-KβBA shows selective antiproliferative effects against the PTEN null cell line
Antiproliferative effect of C-KβBA on PC-3 cell line and PC-3 PTEN cell line was measured by the XTT assay. Indicated cells lines were treated with C-KβBA for 48 h. The amount of cells in control samples treated with DMSO solvent (0.5%) was set to 100%. Data are mean ± SEM from three independent experiments.

Taken together, inhibition of p70S6K phosphorylation, upregulation of eIF4E phosphorylation, downregulation of cyclin D1 and eIF4E expression, no alteration in AKT and ERK phosphorylation, and relative resistance of PTEN positive PC-3 to treatment with C-KβBA confirmed our hypothesis that C-KβBA inhibits the mTORC1 signaling pathway.

3.7 C-KβBA inhibits the mTOR signaling pathway independent from upstream kinases

The mTOR signaling is activated in response to growth factors and nutrients. Under such conditions, PI3K/Akt signaling will be activated and will regulate mTOR signaling. Activated Akt phosphorylates TSC2 inducing Rheb GTPase inactivation, which associates with and directly activates mTORC1. It is known that PDK1 phosphorylates and activates Akt at T309 and p70S6K at Thr229 (Meric-Bernstam and Gonzalez-Angulo 2009). Thus, C-KβBA could inhibit mTOR signaling by down-regulation of upstream kinases.

To determine whether C-KβBA would affect the activity of Akt and PDK1 or not, PC-3 cells were treated with and without C-KβBA for 30 min, then stimulated with 1% FCS for 30 min, followed by Western blot analysis of p-PDK1, p-Akt-Ser473, p-Akt-Thr308 and Akt. Our results revealed that treatment of PC-3 cells with C-KβBA did not affect the phosphorylation of both upstream kinases, PDK1 and Akt (Figure 28).

Moreover, we tested the effect of C-KβBA on the downstream targets of Akt (GSK-3β and FOXO) to ensure that there is no inhibition of Akt activity in cells treated with C-KβBA. Glycogen synthase kinase-3β (GSK-3β) is a serine threonine kinase involved in metabolism, neurodegeneration and cancer progression. It has been shown that GSK-3β regulates apoptosis in response to various stimuli. GSK-3β is phosphorylated by Akt at Ser9. Therefore, inhibition of Akt leads to downregulation of GSK-3β-Ser9 phosphorylation. Western blot analysis of GSK-3β-Ser9 showed that C-KβBA did not alter the phosphorylation status of GSK-3β on Ser9 (Figure 28).

Mammalian forkhead members of the class O (FOXO) are transcription factors including FOXO1, FOXO3a, and FOXO4. FOXO are key regulators of growth, metabolism, life span, and stress resistance. Akt phosphorylates FOXO leading to FOXO cytoplasmic retention and transcriptional inactivation. Inhibition of Akt activates FOXO transcription factors. ELISA assay for FOXO activity revealed that C-KβBA did not induce activation of FOXO transcription. The experiments showed that there is no relation between Akt and mTOR inhibition induced by C-KβBA (Figure 28).

This indicated that C-KβBA does not affect the activity of PDK1 or Akt, and induces inhibition of mTOR signaling independently of PDK1 and Akt signaling.

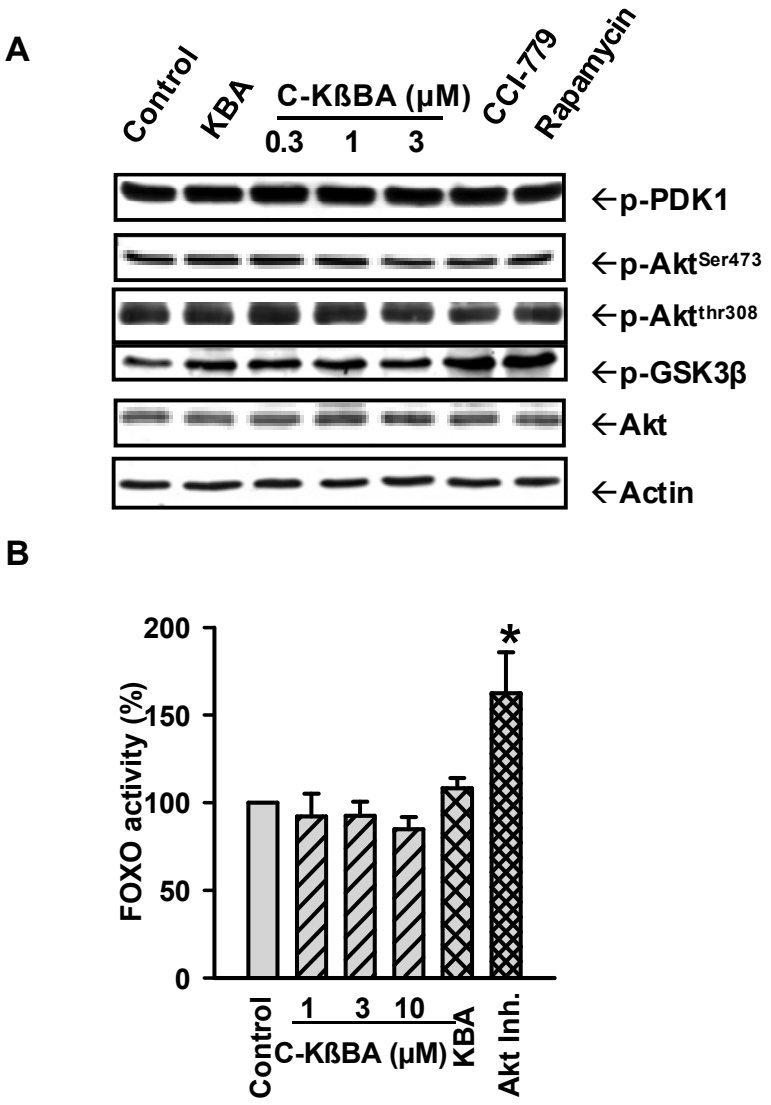

Figure 28. C-KβBA inhibits the mTOR signaling pathway independent from the upstream kinase Akt

A) Whole cell lysates from PC-3 cells, starved overnight, treated with C-KβBA for 30 min and activated for 30 min with 1% FCS, were used for Western immunoblotting. Data represent three independent experiments. B) The graphic presentation shows the effects of C-KβBA on FOXO1 activity. PC-3 cells were incubated with C-KβBA, KBA and the Akt inhibitor VIII (1 µM, positive control) for 3 h. FKHR (FOXO1) transcriptional activation was analyzed in isolated nuclear extracts from PC-3 cells using a commercially available transcription factor assay kit (TransAM™ FKHR (FOXO1)) according to the manufacturer's instructions.

3.8 C-KβBA inhibits the mTOR signaling pathway independent from the LKB1-AMPK signaling pathway

The AMPK-TSC network is negative upstream regulator of mTOR. In the response to low energy level or high AMP level, AMP kinase (AMPK) is phosphorylated by the liver Kinase B1 (LKB1) and activated; this leads to activation of TSC2 and inhibition of mTOR signaling (Meric-Bernstam et al. 2009). Therefore, we hypothesized that C-KβBA might inhibit mTOR signaling by direct activation of LKB1-AMPK signaling pathway.

To clarify, whether activation of LKB1 is involved in the C-KβBA-mediated inhibition of mTOR signaling, MDA-MB-231 cells, which do not express LKB1 mRNA or protein (Shen et al. 2002), were treated with C-KβBA at different concentration for 24 and 48 h, followed by XTT assay. The results showed that the lack of LKB1 did not rescue MDA-MB-231 cell line from C-KβBA-induced cytotoxicity (Figure 29).

In the next step, PC-3 cells treated with C-KβBA alone or with AMPK inhibitor (compound C) (Figure 29). The results reveal that pretreatment of the cells with compound C has no effect on C-KβBA-mediated inhibition of mTOR signaling (Figure 29).

Together, this data demonstrated that C-KβBA inhibits mTOR signaling independent of the LKB1-AMPK signaling pathway.

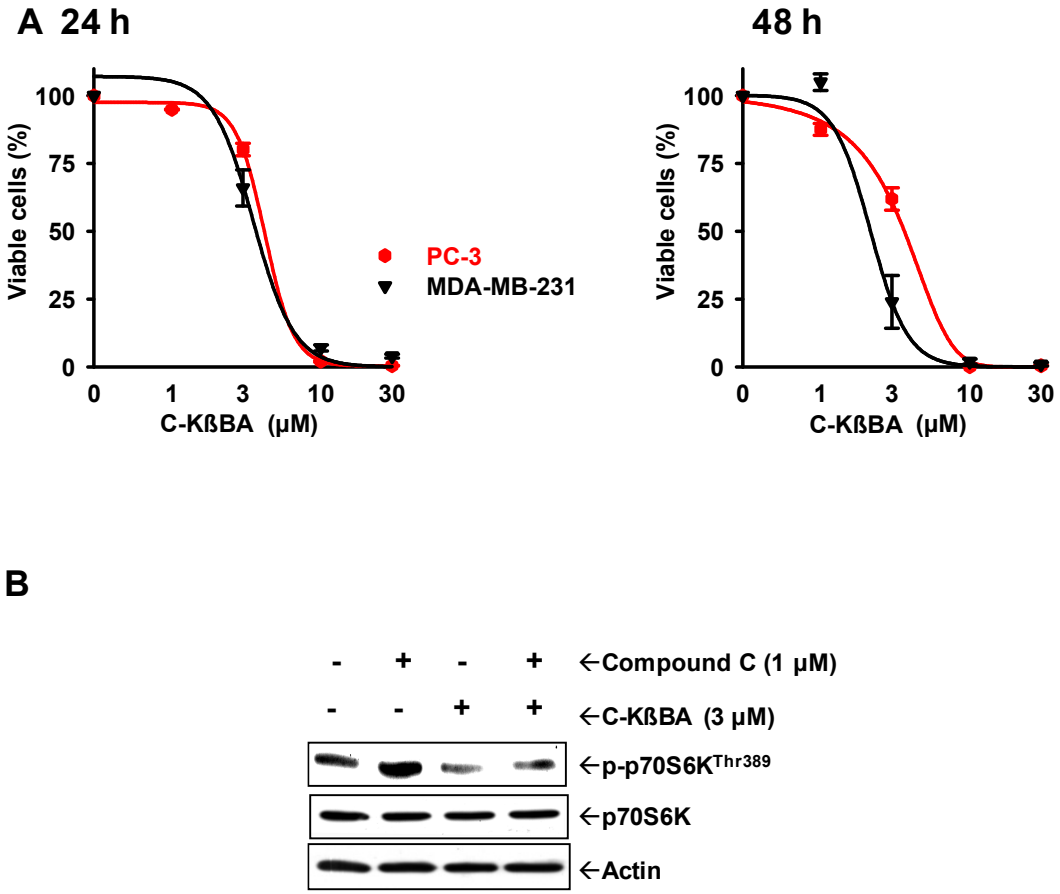

Figure 29. C-KβBA inhibits the mTOR signaling pathway independent from the LKB1-AMPK signaling pathway

A) PC-3 cells were treated for 24 h and 48 h with C-KβBA and the cytotoxicity was measured with XTT assay. B) Lysates from whole PC-3 cells, starved overnight, treated with 3 µM C-KβBA alone or with 1 µM AMPK inhibitor (compound C) for 30 min, followed by stimulation for 30 min with 1% FCS, were used for Western blotting. Data are mean ± SEM from three independent experiments.

3.9 C-KβBA inhibits the mTOR signaling pathway independent from the TSC complex

TSC2 is a negatively regulator for mTORC1. Multiple signaling cascades converge on TSC2, leading to its phosphorylation and inactivation. TSC2 is phosphorylated by multiple kinases, including Akt, ERK, RSK1 (a kinase downstream of ERK) and AMPK (Bai et al. 2009). In previous experiments, we showed that C-KβBA did not

affect the activity of Akt or AMPK signaling. At the same time, ERK phosphorylation was undetectable under the conditions tested (Figure 25). That indicates that C-KβBA could target the TSC complex to inhibit mTORC1 signaling.

To elucidate whether there is any relation between the mTOR inhibition and the TSC complex activation, we incubated C-KβBA with two mouse embryonic fibroblast cell lines, either expressing wild type TCS or deficient in TCS (MEFs $TSC^{+/+}$ and MEFs $TSC^{-/-}$) for 48 h (Figure 30). The results revealed that knockout of TSC did not rescue the cells from the C-KβBA-mediated apoptosis. This indicates that C-KβBA inhibits mTOR signaling pathway independent from the TSC complex.

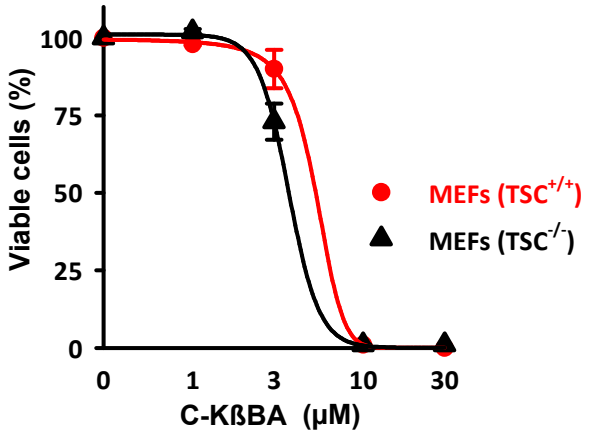

Figure 30. C-KβBA inhibits the mTOR signaling pathway independent from the TSC complex. Antiproliferative effect of C-KβBA on MEFs cell lines ($TSC^{-/-}$ and $TSC^{+/+}$) was measured by the XTT assay. The indicated cell lines were treated with C-KβBA for 48 h. The amount of cells in the control samples treated with DMSO solvent (0.5%) was set to 100%. Data are mean ± SEM from three independent experiments.

3.10 C-KβBA inhibits the mTOR signaling pathway independent from PP2A phosphatase activation

Protein phosphatase 2A (PP2A) is a trimeric complex consisting of a catalytic subunit (C), and the regulatory subunits A and B. PP2A controls the activity of p70S6K and 4E-BPs.

To explore the role of protein phosphatases in the C-KβBA-mediated inhibition of mTOR signaling, PC-3 cells were pretreated with the phosphatase inhibitors, calyculin A (a potent protein serine/threonine phosphatase inhibitor that inhibits both PP1 and PP2A) and okadaic acid (a potent PP2A inhibitor) for 20 min. Then the cells treated with or without C-KβBA, for 30 min followed by 30 min activation with 1% FCS. The cell lysates analyzed by Western immunoblotting (Figure 31). The results showed that calyculin A partially reversed the C-KβBA-mediated inhibitory effect on p70S6K phosphorylation, while okadaic acid had little effect on p70S6K phosphorylation in PC-3 cells.

Next, we evaluated the effect of C-KβBA on the PP2A activity. PC-3 cells pretreated with calyculin A for 20 min, and then treated with or without C-KβBA for 30 min, followed by 30 min activation with 1% FCS. The activity of the protein phosphatase in the cells treated with C-KβBA determined by malachite green phosphatase assay (Figure 31). This data showed that C-KβBA did not affect the activity of PP2A.

In these two experiments, treatment of PC-3 cells with C-KβBA had no effect on PP2A phosphatase activity. This revealed that C-KβBA inhibits the mTOR signaling pathway independent from PP2A activation.

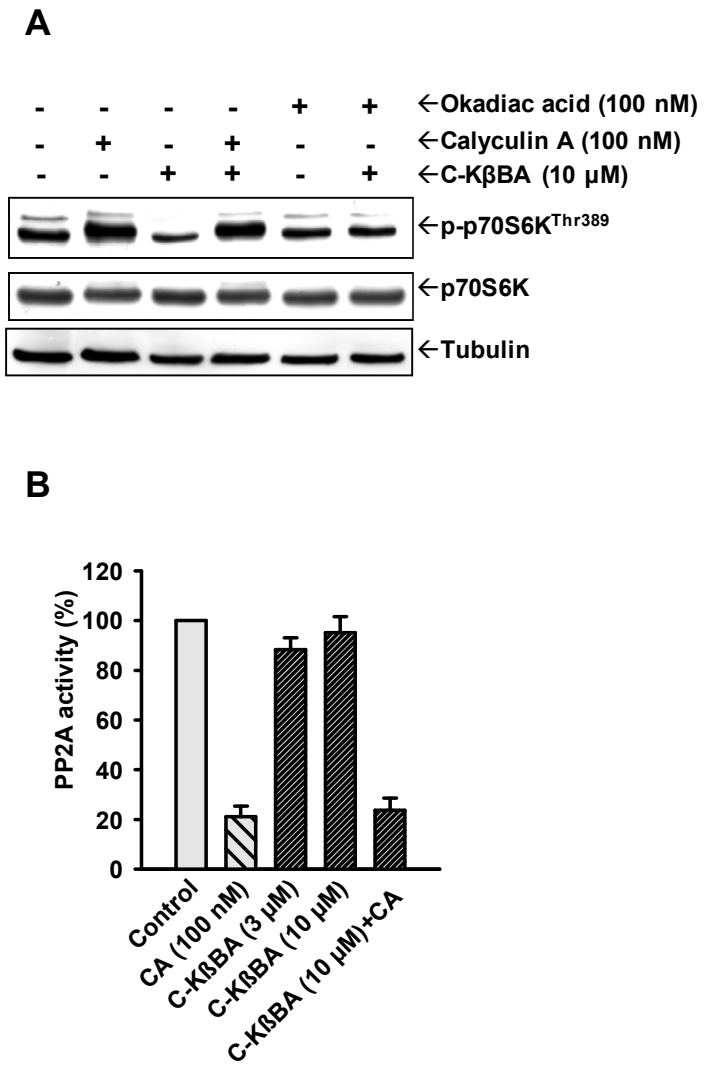

Figure 31. C-KβBA inhibits the mTOR signaling pathway independent from PP2A activation
A) Whole cell lysates from PC-3 cells, starved overnight, treated with 10 µM C-KβBA alone or with the indicated inhibitors for 30 min with stimulation for 30 min with 1% FCS, were used for Western immunoblotting using the indicated antibodies. D) The cells were pretreated with or without calyculin A (100 nM) for 20 min then incubated with different concentrations of C-KβBA for 30 min. The cells were harvested in phosphatase assay buffer and PP2A activities in lysates were determined as described in Material and Methods. Data are mean ± SEM from three independent experiments .

4. DISCUSSION

Programmed cell death (apoptosis) is a conserved pathway that is essential for development and tissue homoeostasis. Tissue homeostasis is the critical balance between cell proliferation and cell death (apoptosis). Disruption of this subtle equilibrium can lead to the onset of various pathological disorders including cancer. Defects in the apoptotic process have also been implicated in the pathogenesis of autoimmune diseases, such as type 1 diabetes (Sun et al. 2005; De Franco et al. 2007). Besides, it is involved in the pathogenesis of inflammatory bowel diseases, inflammatory allergic disorders (Druilhe et al. 2000; Duncan et al. 2003; Mudter et al. 2007; Tumes et al. 2008), and most ocular diseases (Tempestini et al. 2003). In addition, defective apoptosis has been implicated in the resistance to many chemotherapeutic drugs (Ikuta et al. 2005). In light of these findings, induction of apoptosis could be of great therapeutic interest for the treatment of a variety of diseases.

Our lab has previously shown that the pentacyclic triterpenoid acetyl-11-keto-β-boswellic acid (AKβBA) induces apoptosis in prostate cancer cell lines in vitro and in vivo (Syrovets et al. 2005). In comparison to AKβBA, its deacetylated derivative, 11-keto-β-boswellic acid (KBA), showed a decreased activity, pointing to the importance of the acetyl group at carbon number 3 of ring A. The aim of the present study was to modify this position in order to obtain a new derivative of KBA with enhanced proapoptotic activitiy. In our attempts to modify the substituent at carbon number 3, we have linked cinnamic acid to the hydroxyl group at carbon 3 of ring A of KBA, thereby creating the end product 3-cinnamoyl-11-keto-β-boswellic acid (C-KβBA).

Here we show that C-KβBA induced a concentration- and time-dependent inhibition of the proliferation of different cell lines including the prostate cancer cell lines PC-3, LNCaP, DU 145, and the mammary carcinoma cell line MDA-MB-231. Interestingly, C-KβBA was more potent than CCI-779, a mTOR inhibitor that is currently being evaluated in clinical trials.

Importantly, C-KβBA showed a preferential efficacy against prostate cancer cells, i.e. the PC-3 cell line harboring defects in the apoptosis pathway, compared to normal prostate epithelial cells, i.e. the RWPE-1 cell line, suggesting specificity of C-KβBA against the cells with defects in the apoptosis pathway. Since resistance to chemotherapy usually arises with time, we treated PC-3 cell line with C-KβBA only once, followed by incubation in medium free of C-KβBA for 6 day. These experiments revealed that already a single application of C-KβBA has a profound cytotoxic effect on PC-3 cells showing that PC-3 cells are not able to recover from the C-KβBA-mediated cytotoxicity, even when the cells kept in C-KβBA-free medium for 6 days.

It could further be demonstrated that C-KβBA induced apoptosis not only in vitro but also in vivo, suggesting that C-KβBA could be used for the treatment of diseases associated with defective apoptosis pathways. To elucidate the type of cell death triggered by C-KβBA, several apoptotic parameters, such as expression of phosphatidylserine on the cell surface, caspase activation, and DNA laddering were investigated.

Caspase activation is one of the best-known biochemical markers indicating the induction of apoptosis. Caspases belong to the family of cysteine-aspartic acid-directed proteases that play essential roles in the regulation of apoptosis. Caspases are widely expressed as inactive proenzymes, and once procaspases become activated, they trigger initiation of the protease cascade. Some procaspases can also aggregate and autoactivate. This proteolytic cascade, in which one caspase can activate other caspases, amplifies the apoptotic signaling pathway and thus leads to rapid cell death (Elmore 2007). Among them, caspase 3 is a frequently activated death protease, catalyzing the specific cleavage of many key cellular proteins. The effector caspase 3 is also required for some typical hallmarks of apoptosis such as apoptotic chromatin condensation and DNA fragmentation (Porter et al. 1999). Twenty-four h exposure of PC-3 cells to C-KβBA in concentrations as low as 1 μM C-KβBA induced already significant activation of caspase-3. This is consistent with the profound antiproliferative effect of C-KβBA on prostate cancer cells at this low concentration as verified for example by its anticlonogenic effect. Together, these

data unambiguously demonstrated that C-KβBA induced apoptotic cell death in prostate cancer cell lines.

The tumor suppressor gene PTEN (phosphatase and tensin homologue) is a plasma-membrane lipid phosphatase. PTEN is mutated in multiple advanced cancers and is also associated with cancer-susceptibility conditions such as Cowden syndrome (Inoki et al. 2005; Cully et al. 2006). PTEN mutation is frequently entangled with human prostate carcinoma progression (Huang et al. 2001) suggesting a crucial role of PTEN in the context of this disorder. Consistently, loss of PTEN expression is associated with tumorgenesis and metastasis. Indeed, the treatment-resistant PC-3 cells are a PTEN-null cell line. Loss of PTEN in this cell line is biochemically associated with a hyperactivated PI3K/Akt/TSC/mTORC1 pathway (Cantley et al. 1999) raising the interesting question whether this pathway might be targeted by C-KβBA.

The mammalian target of rapamycin (mTOR) acts as a central regulator of ribosome biogenesis, protein synthesis, cell growth, cell survival and cytoskeletal organization. The dysregulation of the mTOR signaling pathway is a hallmark for many diseases including cancer. It has been reported that the mTOR signaling pathway is associated with many neurological disorders (i.e. mental retardation syndromes, autism spectrum disorder, Alzheimer´s, Huntington's and Parkinson's disease) (Mizushima 2005; Santini et al. 2009; Hoeffer et al. 2010), and also with cardiac hypertrophy and polycystic kidney disease (Inoki et al. 2005; Boletta 2009). It also plays an important role in metabolic disorders including obesity, type 2 diabetes, and non-alcoholic fatty liver disease (Pacheco et al. 2008; Laplante et al. 2009). Mutations in LKB1, RasGAP (Ras GTPase-activating protein), TSC1, TSC2 and PTEN trigger development, e.g. of the Peutz-Jeghers syndrome, neurofibromatosis type I, and tuberous sclerosis syndrome, to name a few (Inoki et al. 2005).

Recent studies revealed that the mTOR signaling pathway links diet-induced obesity with vascular senescence and cardiovascular diseases (Wang et al. 2009). In addition, the mTOR signaling pathway has been implicated in the resistance of tumor cells to many anticancer drugs including retinoic acid, vincristine and trastuzumab

(Jiang et al. 2008). Moreover, it has been shown that inhibition of the mTOR signaling pathway extends the lifespan in invertebrates (i.e. yeast and nematodes) as well as in mammalians species (i.e. mice) (Harrison et al. 2009). Thus, the mTOR signaling pathway apparently represents a key element that controls many diseases. Therefore, many efforts have been devoted to the identification of new mTOR inhibitors for cancer therapy. The immunosuppressive macrolide rapamycin is considered as the classical mTOR inhibitor. Many mTOR inhibitors are now in clinical trials, such as CCI-779 and deforolimus (Witzig et al. 2005; Rizzieri et al. 2008).

To enlighten the molecular mechanism underlying the cell death induced by C-KβBA, we investigated a variety of kinase-related signaling pathways in PC-3 cells. Therefore, PC-3 cells were incubated with C-KβBA for various time periods. These investigations identified the downregulation of p70S6K phosphorylation as an event that occurred early after the treatment of PC-3 cells. In fact, the p70S6K is the best characterized effector downstream of mTORC1 (Ali et al. 2005) indicating that C-KβBA may target the PI3K/Akt/TSC/mTORC1 signaling pathway. Additionally, PDK1 has also been implicated in the regulation of the p70S6K phosphorylation (Meric-Bernstam et al. 2009). Therefore, the first step was to evaluate the relation between Akt (via TSC2), PDK1 and p70S6K phosphorylation. Western blot analysis of whole cell lysates from PC-3 cells exposed to C-KβBA and then stained for p-PDK1 and p-Akt showed that C-KβBA had no effect on either of both kinases. In this context, it should be notice that p-Akt-Ser473 is regulated by mTORC2. Therefore, the lack of effect of C-KβBA on p-Akt-Ser473 indicates that the compound has no effect on mTORC2 and this constellation supports our hypothesis that C-KβBA might target the mTORC1 signaling pathway.

Activation of LKB1 and AMPK inhibits p70S6K phosphorylation via TSC2 (Bai et al. 2009; Meric-Bernstam et al. 2009). TSC2 is also a negative regulator for mTORC1. Yet TSC2 is regulated not only by Akt and AMPK, but also by the ERK signaling pathway (Bai et al. 2009). However, in PC-3 prostate cancer cells, ERK is inactive because we failed to detect any phosphorylation of ERK. Additionally, treatment of

$TSC^{-/-}$ MEFs cells with C-KβBA did not rescue the cell from the cytotoxicity of C-KβBA. Thus, our data ruled out the effect of C-KβBA on the TSC2 signaling network.

Treatment of PTEN positive PC-3 cells (which blocks the mTOR signaling pathway), with C-KβBA revealed that PTEN positive PC-3 cells were more resistant to C-KβBA compared to regular PC-3 cells, which are PTEN negative. This finding confirmed our hypothesis that mTOR targets the mTORC1 signaling pathway.

Protein phosphatase 2A (PP2A) is a heterotrimeric enzyme. PP2A is one of the major cellular serine-threonine phosphatases and is involved in the regulation of cell homeostasis. Active mTOR phosphorylates p70S6K and 4EBP1 either directly or indirectly via inhibition of PP2A (Dufner et al. 1999). Therefore, C-KβBA could inhibit the phosphorylation of p70S6K by activation of PP2A. To clarify whether PP2A activation might be involved in the downregulation of p70S6K phosphorylation, PC-3 cells were pretreated with C-KβBA in the presence or absence of an PP2A inhibitor (okadaic acid) or an unspecific phosphatase inhibitor (calyculin A). This experiment showed that calyculin A partially reversed the inhibitory effect of C-KβBA on p70S6K, while okadaic acid had no effect on p70S6K phosphorylation in PC-3 cells indicating that PP2A does not play a role in the C-KβBA-mediated effect on the p70S6K phosphorylation. This was, further confirmed in an assay of PP2A phosphatase activity that clearly revealed that C-KβBA has no effect on the PP2A activity. Thus, C-KβBA inhibited the mTORC1 signaling pathway independent of PP2A activity. This is in agreement with previously reported data showing that inhibition of mTOR with rapamycin neither induced restoration of the phosphatase activity of PP2A nor did it cause dissociation of α4 and Tap42 from PP2A (Nanahoshi et al. 1998).

The eukaryotic initiation factor 4E (eIF4E) is a downstream target of mTORC1. The eIF4E is a mRNA 5´-cap-binding protein and is as such a central component in the initiation and regulation of translation in eukaryotic cells. EIF4E binding to the mRNA cap structure mediates the initiation of translation. Hypophosphorylation of 4EBP1 results in its high affinity binding to eIF4E. This binding prevents eIF4E association with eIF4G and thereby the formation of eIF4E initiation complex. As a consequence the cap-dependant translation of mRNA is inhibited. mTOR phosphorylates 4EBP1,

which leads to the dissociation of eIF4E and the subsequent initiation of translation (Hay et al. 2004). It is interesting to note that activation of eIF4E is significantly elevated with progression of human and experimental prostate cancer, and significantly correlates with a diminished patient survival. By contrast, experimental downregulation of the eIF4E expression in prostate cancer cells elicits apoptosis in a cell cycle phase-independent manner (Graff et al. 2009) suggesting an essential role of the mTOR-regulated eIF4E for the fate of prostate cancer patients.

The relation between the phosphorylation of eIF4E and protein translation is controversial. It has been reported that phosphorylation of eIF4E either enhanced (Waskiewicz et al. 1999), or inhibited (Knauf et al. 2001), or had no effect (Morley et al. 2002) on protein translation. Biophysical studies indicated that phosphorylation of eIE4E decreases its cap-binding affinity, thereby increasing the rate of eIF4E-m7GTP cap complex dissociation (Scheper et al. 2002). The seemingly contradictory findings concerning the relation between phosphorylation of eIF4E and the protein translation might possibly depend on the cell type and the experimental condition used. This controversial situation indicates that phosphorylated eIF4E may not necessarily be a part of the eIF4E complex required for general protein translation. However, it has been clearly shown that inhibition of mTOR by rapamycin or similar inhibitor compounds in vitro and vivo increase the phosphorylation status of eIF4E (Tee et al. 2000; Sun et al. 2005; Wang et al. 2007; Chen et al. 2009; Zhu et al. 2009). Combination of rapamycin and inhibitors against MnK, ERK, p38 MAPK or PI3K revealed that upregulation of the eIF4E phosphorylation depends on PI3K signaling but is independent on the MnK signaling pathway (Sun et al. 2005). Knock down of MnK1 expression decreased the basal level of p-eIF4E but could not prevent its phosphorylation increased by rapamycin. Knockdown of mTOR (mTOR siRNA) or raptor (raptor siRNA), but not of rictor (rictor siRNA), hinder the phosphorylation of eIF4E by rapamycin (Wang et al. 2007). This indicates that the rapamycin-induced eIF4E phosphorylation depends on the presence of mTOR. Here we show that C-KβBA upregulated the eIF4E phosphorylation in PC-3 cells and concomitantly downregulated the eIF4E expression.

To shed light on the role of eIF4E hyperphosphorylation and the translation process, we monitored the status of the cyclin D1 expression. Cyclin D1 is a key regulator of the G_1 phase of the cell cycle, and drives cells through the G_1/S phase transition (Stacey 2003). Cyclin D1 mRNA translation is complex, involving both cap-dependent and cap-independent mechanisms, and p70S6K has a central role in the regulation of the cyclin D1 expression (Koziczak et al. 2004). Cyclin D1 is considered the prime downstream target protein of eIF4E-mediated protein translation. Expression of eIF4E significantly correlates with the increase of cyclin D1 protein expression. eIF4E enhances the nuclear export of cyclin D1 mRNA (Mamane et al. 2004; Culjkovic et al. 2005). Activation of mTOR phosphorylates p70S6K and leads to the recruitment of the 40S ribosomal subunit into translating polysomes, which enhances the translation of mRNA with 5´ terminal oligopolypyrimidine (5´-TOP) (Jiang et al. 2008). PC-3 cells treated with C-KβBA exhibited a clear downregulation of the cyclin D1 expression. This implies that C-KβBA induces inhibition of the translation machinery by induction of eIF4E hyperphosphorylation as well as downregulation of the eIF4E protein expression.

The growth of an organ or a whole organism is mediated by increases in both cell size and cell number through the coordinated action of cell growth and cell cycle progression. Apoptosis is the physiological process by which the body removes unwanted cells, reforms and maintains the tissues and the organs. The disturbance between these two processes is the main reason for many diseases including cancer. This disturbance might be due to mutation of certain genes (e.g. PTEN) or activation of distinct signaling cascades (e.g. the mTOR signaling pathway). Under these conditions, the cells undergo continuous cell proliferation and growth, in the sense that they ‘forget’ how to die. Targeting the cell cycle at this point seems to be a prime opportunity to stop proliferation and growth of a tumor.

mTOR is widely known as a governor of cell cycle progression and proliferation (Peponi et al. 2006). It has been previously shown that the cell cycle arrest induced by rapamycin occurs via p70S6K. Consistently, expression of active p70S6K reversed the rapamycin-induced G_1 cell cycle arrest (Gao et al. 2004). Similarly, C-

KβBA induced cell cycle arrest in the G_1 phase providing further evidence that C-KβBA inhibits the mTORC1/ p70S6K signaling pathway.

Taken together, C-KβBA inhibits cell proliferation and induces apoptosis in vitro and vivo even at low concentrations and after a single, rather short exposure. C-KβBA elicits cell cycle arrest at G_1 with inhibition of the protein translation machinery that is associated with the downregulation of cyclin D1. These effects of C-KβBA are triggered by its inhibition of the mTOR signaling pathway that occurs independent from the upstream kinases Akt and PDK1, and independent from the negative regulators of the mTOR signaling, TSC2 and PP2A.

In conclusion, the capability of C-KβBA to inhibit the mTOR signaling pathway renders it an interesting lead compound for the development of novel pharmacotherapeutic approaches for the treatment of various diseases including cancer.

5. Summary

The apoptotic mode of cell death (programmed cell death) is an active and defined process that plays an important role in the development of multicellular organisms and in the regulation and maintenance of cell populations in tissues under physiologic and pathologic conditions. Since dysregulation of apoptosis is associated with the progress of many diseases, induction of apoptosis is an interesting pharmacological target for the therapy of many diseases. Our study shows that the novel semisynthetic pentacyclic triterpenoid C-KβBA has a profound antiproliferative effect on different tumor cell lines and that it induces apoptosis of tumor cells in vitro and vivo.

Previous studies have shown that the mammalian target of rapamycin (mTOR) is a key regulator for many cells activities, and that the perturbation of this signaling pathway is implicated in many diseases and metabolic disorders. Accordingly, targeting the mTOR signaling pathway seems to be a promising therapeutic approach for the treatment of various diseases and metabolic disorders.

We have shown in our study that C-KβBA downregulates the mTOR signaling pathway in vitro and vivo, which leads to the induction of cell cycle arrest in the G_0 cell cycle phase as well as downregulation of the protein translation machinery.

Together, the presented data strongly suggest that C-KβBA could serve as a lead compound for the development of novel treatment modalities for diseases and disorders associated with defects in the apoptosis machinery, or the mTOR signaling pathway, or both.

6. Zusammenfassung

Der programmierte Zelltod ist ein aktiver und wohldefinierter Prozess. Unter physiologischen und pathophysiologischen Bedingungen spielt er eine entscheidende Rolle sowohl bei der Entwicklung mehrzelliger Organismen als auch bei der Regulation und Erhaltung verschiedener Zellpopulationen. Da das Fortschreiten vieler Erkrankungen mit einer Fehlregulation der Apoptose einhergeht, wird der Apoptoseprozess heute als ein wichtiger Angriffspunkt pharmakologischer Therapieansätze betrachtet. Unsere Studien zeigen, dass das neuartige semisynthethische Triterpenoid C-KβBA einen starken antiproliferativen Effekt auf verschiedene Tumorzelllinien besitzt und dass es sowohl in vitro als auch in vivo zur Induktion von Apoptose führt.

In verschiedenen Studien konnte bereits früher gezeigt werden, dass dem „mammalian target of rapamycin“ (mTOR) eine Schlüsselrolle in der Regulation verschiedener Zellaktivitäten zukommt. Eine Störung dieses Signalweges kann mit vielerlei Erkrankungen und metabolischen Fehlfunktionen in Verbindung gebracht werden. Somit könnte der mTOR-Signalweg das Ziel eines vielversprechenden Therapieansatzes für die Behandlung diverser Erkrankungen und metabolischer Störungen sein.

In unseren Studien konnten wir zeigen, dass C-KβBA den mTOR Signalweg sowohl in vitro als auch in vivo hemmt. Diese Inhibition führt zu einem Zellzyklusarrests in der G0-Phase sowie zu einer Hemmung der Proteintranslation.

Zusammenfassend implizieren die hier präsentierten Daten, dass C-KβBA als eine prototypische Modellsubstanz für die Entwicklung neuer Therapieansätze für Erkrankungen mit aberranten Funktionen entweder der apoptotischen Maschinerie oder des mTOR-Signaltransduktionsweges dienen könnte.

7. Appendix

List of Figures

8. References

Abraham RT. PI 3-kinase related kinases: 'big' players in stress-induced signaling pathways. DNA Repair (Amst) 2004;3:883-887

Alao JP, Gamble SC, Stavropoulou AV, Pomeranz KM, Lam EW, Coombes RC and Vigushin DM. The cyclin D1 proto-oncogene is sequestered in the cytoplasm of mammalian cancer cell lines. Mol Cancer 2006;5:7

Albert JM, Kim KW, Cao C and Lu B. Targeting the Akt/mammalian target of rapamycin pathway for radiosensitization of breast cancer. Mol Cancer Ther 2006;5:1183-1189

Ali SM and Sabatini DM. Structure of S6 kinase 1 determines whether raptor-mTOR or rictor-mTOR phosphorylates its hydrophobic motif site. J Biol Chem 2005;280:19445-19448

Averous J, Fonseca BD and Proud CG. Regulation of cyclin D1 expression by mTORC1 signaling requires eukaryotic initiation factor 4E-binding protein 1. Oncogene 2008;27:1106-1113

Bai X and Jiang Y. Key factors in mTOR regulation. Cell Mol Life Sci 2009;

Ballou LM and Lin RZ. Rapamycin and mTOR kinase inhibitors. J Chem Biol 2008;1:27-36

Barry M and Bleackley RC. Cytotoxic T lymphocytes: all roads lead to death. Nat Rev Immunol 2002;2:401-409

Belsner k, Büchele B, Werz U, Syrovets T and Simmet T. Structural analysis of pentacyclic triterpenes from the gum resin of Boswellia serrata by NMR spectroscopy. Magn. Res. Chem. 2003;41:115-122

Bianchini A, Loiarro M, Bielli P, Busa R, Paronetto MP, Loreni F, Geremia R and Sette C. Phosphorylation of eIF4E by MNKs supports protein synthesis, cell cycle progression and proliferation in prostate cancer cells. Carcinogenesis 2008;29:2279-2288

Boletta A. Emerging evidence of a link between the polycystins and the mTOR pathways. Pathogenetics 2009;2:6

Bortner CD, Oldenburg NB and Cidlowski JA. The role of DNA fragmentation in apoptosis. Trends Cell Biol 1995;5:21-26

Bratton DL, Fadok VA, Richter DA, Kailey JM, Guthrie LA and Henson PM. Appearance of phosphatidylserine on apoptotic cells requires calcium-mediated nonspecific flip-flop and is enhanced by loss of the aminophospholipid translocase. J Biol Chem 1997;272:26159-26165

Brunner T, Wasem C, Torgler R, Cima I, Jakob S and Corazza N. Fas (CD95/Apo-1) ligand regulation in T cell homeostasis, cell-mediated cytotoxicity and immune pathology. Semin Immunol 2003;15:167-176

Büchele B, Zugmaier W and Simmet T. Analysis of pentacyclic triterpenic acids from frankincense gum resins and related phytopharmaceuticals by high-performance liquid chromatography. Identification of lupeolic acid, a novel pentacyclic triterpene. J Chromatogr B Analyt Technol Biomed Life Sci 2003;791:21-30

Cantley LC and Neel BG. New insights into tumor suppression: PTEN suppresses tumor formation by restraining the phosphoinositide 3-kinase/AKT pathway. Proc Natl Acad Sci U S A 1999;96:4240-4245

Chan JA, Zhang H, Roberts PS, Jozwiak S, Wieslawa G, Lewin-Kowalik J, Kotulska K and Kwiatkowski DJ. Pathogenesis of tuberous sclerosis subependymal giant cell astrocytomas: biallelic inactivation of TSC1 or TSC2 leads to mTOR activation. J Neuropathol Exp Neurol 2004;63:1236-1242

Chen L, Tian G, Shao C, Cobos E and Gao W. Curcumin modulates eukaryotic initiation factors in human lung adenocarcinoma epithelial cells. Mol Biol Rep 2009;

Clarke PG, Posada A, Primi MP and Castagne V. Neuronal death in the central nervous system during development. Biomed Pharmacother 1998;52:356-362

Cloughesy TF, Yoshimoto K, Nghiemphu P, Brown K, Dang J, Zhu S, Hsueh T, Chen Y, Wang W, Youngkin D, Liau L, Martin N, Becker D, Bergsneider M, Lai A, Green R, Oglesby T, Koleto M, Trent J, Horvath S, Mischel PS, Mellinghoff IK and Sawyers CL. Antitumor activity of rapamycin in a Phase I trial for patients with recurrent PTEN-deficient glioblastoma. PLoS Med 2008;5:e8

Culjkovic B, Topisirovic I, Skrabanek L, Ruiz-Gutierrez M and Borden KL. eIF4E promotes nuclear export of cyclin D1 mRNAs via an element in the 3'UTR. J Cell Biol 2005;169:245-256

Cully M, You H, Levine AJ and Mak TW. Beyond PTEN mutations: the PI3K pathway as an integrator of multiple inputs during tumorigenesis. Nat Rev Cancer 2006;6:184-192

De Benedetti A and Graff JR. eIF-4E expression and its role in malignancies and metastases. Oncogene 2004;23:3189-3199

De Franco S, Chiocchetti A, Ferretti M, Castelli L, Cadario F, Cerutti F, Rabbone I, Indelicato M, Mazzarino C, Chessa M, Bona G and Dianzani U. Defective function of the Fas apoptotic pathway in type 1 diabetes mellitus correlates with age at onset. Int J Immunopathol Pharmacol 2007;20:567-576

Di Como CJ and Arndt KT. Nutrients, via the Tor proteins, stimulate the association of Tap42 with type 2A phosphatases. Genes Dev 1996;10:1904-1916

Dong J, Peng J, Zhang H, Mondesire WH, Jian W, Mills GB, Hung MC and Meric-Bernstam F. Role of glycogen synthase kinase 3beta in rapamycin-mediated cell cycle regulation and chemosensitivity. Cancer Res 2005;65:1961-1972

Dong K, Wang R, Wang X, Lin F, Shen JJ, Gao P and Zhang HZ. Tumor-specific RNAi targeting eIF4E suppresses tumor growth, induces apoptosis and enhances cisplatin cytotoxicity in human breast carcinoma cells. Breast Cancer Res Treat 2009;113:443-456

Druilhe A, Letuve S and Pretolani M. [Eosinophil apoptosis in asthma]. Pathol Biol (Paris) 2000;48:566-573

Dufner A and Thomas G. Ribosomal S6 kinase signaling and the control of translation. Exp Cell Res 1999;253:100-109

Duke RC, Chervenak R and Cohen JJ. Endogenous endonuclease-induced DNA fragmentation: an early event in cell-mediated cytolysis. Proc Natl Acad Sci U S A 1983;80:6361-6365

Duncan CJ, Lawrie A, Blaylock MG, Douglas JG and Walsh GM. Reduced eosinophil apoptosis in induced sputum correlates with asthma severity. Eur Respir J 2003;22:484-490

Dyche WJ. A comparative study of the differentiation and involution of the Mullerian duct and Wolffian duct in the male and female fetal mouse. J Morphol 1979;162:175-209

Ellis HM and Horvitz HR. Genetic control of programmed cell death in the nematode C. elegans. Cell 1986;44:817-829

Elmore S. Apoptosis: a review of programmed cell death. Toxicol Pathol 2007;35:495-516

Flemming W. Uber die bildung von richtungsfiguren in saugethiereiern beim untergang graaf'scher follikel. Arch Anat Entwgesch 1885;461-501

Fox H. Ultrastructure of tail degeneration in Rana temporaria larvae. Folia Morphol (Praha) 1973;21:109-112

Freilinger A, Rosner M, Krupitza G, Nishino M, Lubec G, Korsmeyer SJ and Hengstschlager M. Tuberin activates the proapoptotic molecule BAD. Oncogene 2006;25:6467-6479

Gao N, Flynn DC, Zhang Z, Zhong XS, Walker V, Liu KJ, Shi X and Jiang BH. G1 cell cycle progression and the expression of G1 cyclins are regulated by PI3K/AKT/mTOR/p70S6K1 signaling in human ovarian cancer cells. Am J Physiol Cell Physiol 2004;287:C281-291

Gercel-Taylor C, O'Connor SM, Lam GK and Taylor DD. Shed membrane fragment modulation of CD3-zeta during pregnancy: link with induction of apoptosis. J Reprod Immunol 2002;56:29-44

Graff JR, Konicek BW, Lynch RL, Dumstorf CA, Dowless MS, McNulty AM, Parsons SH, Brail LH, Colligan BM, Koop JW, Hurst BM, Deddens JA, Neubauer BL, Stancato LF, Carter HW, Douglass LE and Carter JH. eIF4E activation is commonly elevated in advanced human prostate cancers and significantly related to reduced patient survival. Cancer Res 2009;69:3866-3873

Hara T, Nakamura K, Matsui M, Yamamoto A, Nakahara Y, Suzuki-Migishima R, Yokoyama M, Mishima K, Saito I, Okano H and Mizushima N. Suppression of basal autophagy in neural cells causes neurodegenerative disease in mice. Nature 2006;441:885-889

Harrison DE, Strong R, Sharp ZD, Nelson JF, Astle CM, Flurkey K, Nadon NL, Wilkinson JE, Frenkel K, Carter CS, Pahor M, Javors MA, Fernandez E and Miller RA. Rapamycin fed late in life extends lifespan in genetically heterogeneous mice. Nature 2009;460:392-395

Hay N and Sonenberg N. Upstream and downstream of mTOR. Genes Dev 2004;18:1926-1945

Hayun R, Okun E, Berrebi A, Shvidel L, Bassous L, Sredni B and Nir U. Rapamycin and curcumin induce apoptosis in primary resting B chronic lymphocytic leukemia cells. Leuk Lymphoma 2009;50:625-632

Hengartner MO and Horvitz HR. Programmed cell death in Caenorhabditis elegans. Curr Opin Genet Dev 1994;4:581-586

Herbert TP, Fahraeus R, Prescott A, Lane DP and Proud CG. Rapid induction of apoptosis mediated by peptides that bind initiation factor eIF4E. Curr Biol 2000;10:793-796

Hoeffer CA and Klann E. mTOR signaling: at the crossroads of plasticity, memory and disease. Trends Neurosci 2010;33:67-75

Hotchkiss RS, Strasser A, McDunn JE and Swanson PE. Cell death. N Engl J Med 2009;361:1570-1583

Huang H, Cheville JC, Pan Y, Roche PC, Schmidt LJ and Tindall DJ. PTEN induces chemosensitivity in PTEN-mutated prostate cancer cells by suppression of Bcl-2 expression. J Biol Chem 2001;276:38830-38836

Hurle JM, Ros MA, Climent V and Garcia-Martinez V. Morphology and significance of programmed cell death in the developing limb bud of the vertebrate embryo. Microsc Res Tech 1996;34:236-246

Ikuta K, Takemura K, Kihara M, Naito S, Lee E, Shimizu E and Yamauchi A. Defects in apoptotic signal transduction in cisplatin-resistant non-small cell lung cancer cells. Oncol Rep 2005;13:1229-1234

Inoki K, Corradetti MN and Guan KL. Dysregulation of the TSC-mTOR pathway in human disease. Nat Genet 2005;37:19-24

Inoki K, Zhu T and Guan KL. TSC2 mediates cellular energy response to control cell growth and survival. Cell 2003;115:577-590

Jacinto E, Loewith R, Schmidt A, Lin S, Ruegg MA, Hall A and Hall MN. Mammalian TOR complex 2 controls the actin cytoskeleton and is rapamycin insensitive. Nat Cell Biol 2004;6:1122-1128

Jiang BH and Liu LZ. Role of mTOR in anticancer drug resistance: perspectives for improved drug treatment. Drug Resist Updat 2008;11:63-76

Kawabata Y, Hirokawa M, Kitabayashi A, Horiuchi T, Kuroki J and Miura AB. Defective apoptotic signal transduction pathway downstream of caspase-3 in human B-lymphoma cells: A novel mechanism of nuclear apoptosis resistance. Blood 1999;94:3523-3530

Kerr JF. An electron-microscope study of liver cell necrosis due to heliotrine. J Pathol 1969;97:557-562

Kerr JF. Shrinkage necrosis: a distinct mode of cellular death. J Pathol 1971;105:13-20

Kerr JF, Wyllie AH and Currie AR. Apoptosis: a basic biological phenomenon with wide-ranging implications in tissue kinetics. Br J Cancer 1972;26:239-257

Knauf U, Tschopp C and Gram H. Negative regulation of protein translation by mitogen-activated protein kinase-interacting kinases 1 and 2. Mol Cell Biol 2001;21:5500-5511

Koziczak M and Hynes NE. Cooperation between fibroblast growth factor receptor-4 and ErbB2 in regulation of cyclin D1 translation. J Biol Chem 2004;279:50004-50011

Krammer PH. CD95(APO-1/Fas)-mediated apoptosis: live and let die. Adv Immunol 1999;71:163-210

Kremer CL, Klein RR, Mendelson J, Browne W, Samadzedeh LK, Vanpatten K, Highstrom L, Pestano GA and Nagle RB. Expression of mTOR signaling pathway markers in prostate cancer progression. Prostate 2006;66:1203-1212

Kurosaka K, Takahashi M, Watanabe N and Kobayashi Y. Silent cleanup of very early apoptotic cells by macrophages. J Immunol 2003;171:4672-4679

Kwiatkowski DJ and Manning BD. Tuberous sclerosis: a GAP at the crossroads of multiple signaling pathways. Hum Mol Genet 2005;14 Spec No. 2:R251-258

Laplante M and Sabatini DM. An emerging role of mTOR in lipid biosynthesis. Curr Biol 2009;19:R1046-1052

Larsson O, Perlman DM, Fan D, Reilly CS, Peterson M, Dahlgren C, Liang Z, Li S, Polunovsky VA, Wahlestedt C and Bitterman PB. Apoptosis resistance downstream of eIF4E: posttranscriptional activation of an anti-apoptotic transcript carrying a consensus hairpin structure. Nucleic Acids Res 2006;34:4375-4386

Lee L, Sudentas P, Donohue B, Asrican K, Worku A, Walker V, Sun Y, Schmidt K, Albert MS, El-Hashemite N, Lader AS, Onda H, Zhang H, Kwiatkowski DJ and Dabora SL. Efficacy of a rapamycin analog (CCI-779) and IFN-gamma in tuberous sclerosis mouse models. Genes Chromosomes Cancer 2005;42:213-227

Levin S, Bucci TJ, Cohen SM, Fix AS, Hardisty JF, LeGrand EK, Maronpot RR and Trump BF. The nomenclature of cell death: recommendations of an ad hoc Committee of the Society of Toxicologic Pathologists. Toxicol Pathol 1999;27:484-490

Li P, Nijhawan D, Budihardjo I, Srinivasula SM, Ahmad M, Alnemri ES and Wang X. Cytochrome c and dATP-dependent formation of Apaf-1/caspase-9 complex initiates an apoptotic protease cascade. Cell 1997;91:479-489

Majno G and Joris I. Apoptosis, oncosis, and necrosis. An overview of cell death. Am J Pathol 1995;146:3-15

Mamane Y, Petroulakis E, Martineau Y, Sato TA, Larsson O, Rajasekhar VK and Sonenberg N. Epigenetic activation of a subset of mRNAs by eIF4E explains its effects on cell proliferation. PLoS One 2007;2:e242

Mamane Y, Petroulakis E, Rong L, Yoshida K, Ler LW and Sonenberg N. eIF4E--from translation to transformation. Oncogene 2004;23:3172-3179

Meric-Bernstam F and Gonzalez-Angulo AM. Targeting the mTOR signaling network for cancer therapy. J Clin Oncol 2009;27:2278-2287

Mills JC, Stone NL, Erhardt J and Pittman RN. Apoptotic membrane blebbing is regulated by myosin light chain phosphorylation. J Cell Biol 1998;140:627-636

Mizushima N. The pleiotropic role of autophagy: from protein metabolism to bactericide. Cell Death Differ 2005;12 Suppl 2:1535-1541

Morgan TM, Koreckij TD and Corey E. Targeted therapy for advanced prostate cancer: inhibition of the PI3K/Akt/mTOR pathway. Curr Cancer Drug Targets 2009;9:237-249

Morley SJ and Naegele S. Phosphorylation of eukaryotic initiation factor (eIF) 4E is not required for de novo protein synthesis following recovery from hypertonic stress in human kidney cells. J Biol Chem 2002;277:32855-32859

Mudter J and Neurath MF. Apoptosis of T cells and the control of inflammatory bowel disease: therapeutic implications. Gut 2007;56:293-303

Mukhopadhyay NK, Price DJ, Kyriakis JM, Pelech S, Sanghera J and Avruch J. An array of insulin-activated, proline-directed serine/threonine protein kinases phosphorylate the p70 S6 kinase. J Biol Chem 1992;267:3325-3335

Murata K, Wu J and Brautigan DL. B cell receptor-associated protein alpha4 displays rapamycin-sensitive binding directly to the catalytic subunit of protein phosphatase 2A. Proc Natl Acad Sci U S A 1997;94:10624-10629

Nanahoshi M, Nishiuma T, Tsujishita Y, Hara K, Inui S, Sakaguchi N and Yonezawa K. Regulation of protein phosphatase 2A catalytic activity by alpha4 protein and its yeast homolog Tap42. Biochem Biophys Res Commun 1998;251:520-526

Neises B and Steglich W. Simple method for the esterification of carboxylic acids. Angew. Chem. Int. Ed. Engl 1978;17 522–524

Oppenheim RW, Flavell RA, Vinsant S, Prevette D, Kuan CY and Rakic P. Programmed cell death of developing mammalian neurons after genetic deletion of caspases. J Neurosci 2001;21:4752-4760

Osborne B (2004). When Cells Die II A comprehensive evaluation of apoptosis and programmed cell death. Apoptotic signaling in lymphocytes. Canada, John Wiley & Sons, Inc.

Pacheco CD and Lieberman AP. The pathogenesis of Niemann-Pick type C disease: a role for autophagy? Expert Rev Mol Med 2008;10:e26

Pardhy RS and Bhattacharyya SC. β-Boswellic acid, Acetyl- β -boswellic acid, Acetyl-II keto-β-boswellic acid & II-Keto- β -boswellic acid, Four pentacyclic Triterpene acids from the resin of Boswellia serrata Roxb Ind. J. Chem 1978;16B:176-178

Pearson RB, Dennis PB, Han JW, Williamson NA, Kozma SC, Wettenhall RE and Thomas G. The principal target of rapamycin-induced p70s6k inactivation is a novel phosphorylation site within a conserved hydrophobic domain. EMBO J 1995;14:5279-5287

Peponi E, Drakos E, Reyes G, Leventaki V, Rassidakis GZ and Medeiros LJ. Activation of mammalian target of rapamycin signaling promotes cell cycle progression and protects cells from apoptosis in mantle cell lymphoma. Am J Pathol 2006;169:2171-2180

Peterson RT, Desai BN, Hardwick JS and Schreiber SL. Protein phosphatase 2A interacts with the 70-kDa S6 kinase and is activated by inhibition of FKBP12-rapamycinassociated protein. Proc Natl Acad Sci U S A 1999;96:4438-4442

Peterson TR, Laplante M, Thoreen CC, Sancak Y, Kang SA, Kuehl WM, Gray NS and Sabatini DM. DEPTOR is an mTOR inhibitor frequently overexpressed in multiple myeloma cells and required for their survival. Cell 2009;137:873-886

Porter AG and Janicke RU. Emerging roles of caspase-3 in apoptosis. Cell Death Differ 1999;6:99-104

Pullen N and Thomas G. The modular phosphorylation and activation of p70s6k. FEBS Lett 1997;410:78-82

Ravikumar B, Vacher C, Berger Z, Davies JE, Luo S, Oroz LG, Scaravilli F, Easton DF, Duden R, O'Kane CJ and Rubinsztein DC. Inhibition of mTOR induces autophagy and reduces toxicity of polyglutamine expansions in fly and mouse models of Huntington disease. Nat Genet 2004;36:585-595

Rizzieri DA, Feldman E, Dipersio JF, Gabrail N, Stock W, Strair R, Rivera VM, Albitar M, Bedrosian CL and Giles FJ. A phase 2 clinical trial of deforolimus (AP23573, MK-8669), a novel mammalian target of rapamycin inhibitor, in patients with relapsed or refractory hematologic malignancies. Clin Cancer Res 2008;14:2756-2762

Rohde J, Heitman J and Cardenas ME. The TOR kinases link nutrient sensing to cell growth. J Biol Chem 2001;276:9583-9586

Ross G, Dyer JR, Castellucci VF and Sossin WS. Mnk is a negative regulator of cap-dependent translation in Aplysia neurons. J Neurochem 2006;97:79-91

Russell JH and Ley TJ. Lymphocyte-mediated cytotoxicity. Annu Rev Immunol 2002;20:323-370

Sakahira H, Enari M and Nagata S. Cleavage of CAD inhibitor in CAD activation and DNA degradation during apoptosis. Nature 1998;391:96-99

Sambrook J and Russell DW (2001). Molecular cloning : a laboratory manual. Cold Spring Harbor, N.Y., Cold Spring Harbor Laboratory Press.

Sampson JR. Therapeutic targeting of mTOR in tuberous sclerosis. Biochem Soc Trans 2009;37:259-264

Sancak Y, Peterson TR, Shaul YD, Lindquist RA, Thoreen CC, Bar-Peled L and Sabatini DM. The Rag GTPases bind raptor and mediate amino acid signaling to mTORC1. Science 2008;320:1496-1501

Santini E, Heiman M, Greengard P, Valjent E and Fisone G. Inhibition of mTOR signaling in Parkinson's disease prevents L-DOPA-induced dyskinesia. Sci Signal 2009;2:ra36

Sarbassov DD, Ali SM and Sabatini DM. Growing roles for the mTOR pathway. Curr Opin Cell Biol 2005;17:596-603

Sarbassov DD, Guertin DA, Ali SM and Sabatini DM. Phosphorylation and regulation of Akt/PKB by the rictor-mTOR complex. Science 2005;307:1098-1101

Savill J and Fadok V. Corpse clearance defines the meaning of cell death. Nature 2000;407:784-788

Sawyers CL. Will mTOR inhibitors make it as cancer drugs? Cancer Cell 2003;4:343-348

Scheper GC, van Kollenburg B, Hu J, Luo Y, Goss DJ and Proud CG. Phosphorylation of eukaryotic initiation factor 4E markedly reduces its affinity for capped mRNA. J Biol Chem 2002;277:3303-3309

Schulze-Osthoff K, Ferrari D, Los M, Wesselborg S and Peter ME. Apoptosis signaling by death receptors. Eur J Biochem 1998;254:439-459

Serra AL, Kistler AD, Poster D, Struker M, Wuthrich RP, Weishaupt D and Tschirch F. Clinical proof-of-concept trial to assess the therapeutic effect of sirolimus in patients with autosomal dominant polycystic kidney disease: SUISSE ADPKD study. BMC Nephrol 2007;8:13

Shen Z, Wen XF, Lan F, Shen ZZ and Shao ZM. The tumor suppressor gene LKB1 is associated with prognosis in human breast carcinoma. Clin Cancer Res 2002;8:2085-2090

Shillingford JM, Murcia NS, Larson CH, Low SH, Hedgepeth R, Brown N, Flask CA, Novick AC, Goldfarb DA, Kramer-Zucker A, Walz G, Piontek KB, Germino GG and Weimbs T. The mTOR pathway is regulated by polycystin-1, and its inhibition reverses renal cystogenesis in polycystic kidney disease. Proc Natl Acad Sci U S A 2006;103:5466-5471

Shinjyo T, Kuribara R, Inukai T, Hosoi H, Kinoshita T, Miyajima A, Houghton PJ, Look AT, Ozawa K and Inaba T. Downregulation of Bim, a proapoptotic relative of Bcl-2, is a pivotal step in cytokine-initiated survival signaling in murine hematopoietic progenitors. Mol Cell Biol 2001;21:854-864

Smith PK, Krohn RI, Hermanson GT, Mallia AK, Gartner FH, Provenzano MD, Fujimoto EK, Goeke NM, Olson BJ and Klenk DC. Measurement of protein using bicinchoninic acid. Anal Biochem 1985;150:76-85

Squarize CH, Castilho RM and Gutkind JS. Chemoprevention and treatment of experimental Cowden's disease by mTOR inhibition with rapamycin. Cancer Res 2008;68:7066-7072

Stacey DW. Cyclin D1 serves as a cell cycle regulatory switch in actively proliferating cells. Curr Opin Cell Biol 2003;15:158-163

Stennicke HR, Deveraux QL, Humke EW, Reed JC, Dixit VM and Salvesen GS. Caspase-9 can be activated without proteolytic processing. J Biol Chem 1999;274:8359-8362

Sun SY, Rosenberg LM, Wang X, Zhou Z, Yue P, Fu H and Khuri FR. Activation of Akt and eIF4E survival pathways by rapamycin-mediated mammalian target of rapamycin inhibition. Cancer Res 2005;65:7052-7058

Swiech L, Perycz M, Malik A and Jaworski J. Role of mTOR in physiology and pathology of the nervous system. Biochim Biophys Acta 2008;1784:116-132

Syrovets T, Gschwend JE, Buchele B, Laumonnier Y, Zugmaier W, Genze F and Simmet T. Inhibition of IkappaB kinase activity by acetyl-boswellic acids promotes apoptosis in androgen-independent PC-3 prostate cancer cells in vitro and in vivo. J Biol Chem 2005;280:6170-6180

Syrovets T, Gschwend JE, Büchele B, Laumonnier Y, Zugmaier W, Genze F and Simmet T. Inhibition of IκB kinase activity by acetyl-boswellic acids promotes apoptosis in androgen-independent PC-3 prostate cancer cells in vitro and in vivo. J Biol Chem 2005;280:6170-6180

Tao Y, Kim J, Schrier RW and Edelstein CL. Rapamycin markedly slows disease progression in a rat model of polycystic kidney disease. J Am Soc Nephrol 2005;16:46-51

Tee AR, Manning BD, Roux PP, Cantley LC and Blenis J. Tuberous sclerosis complex gene products, Tuberin and Hamartin, control mTOR signaling by acting as a GTPase-activating protein complex toward Rheb. Curr Biol 2003;13:1259-1268

Tee AR and Proud CG. DNA-damaging agents cause inactivation of translational regulators linked to mTOR signalling. Oncogene 2000;19:3021-3031

Tempestini A, Schiavone N, Papucci L, Witort E, Lapucci A, Cutri M, Donnini M and Capaccioli S. The mechanisms of apoptosis in biology and medicine: a new focus for ophthalmology. Eur J Ophthalmol 2003;13 Suppl 3:S11-18

Thoreen CC, Kang SA, Chang JW, Liu Q, Zhang J, Gao Y, Reichling LJ, Sim T, Sabatini DM and Gray NS. An ATP-competitive mammalian target of rapamycin inhibitor reveals rapamycin-resistant functions of mTORC1. J Biol Chem 2009;284:8023-8032

Tirado OM, Mateo-Lozano S and Notario V. Rapamycin induces apoptosis of JN-DSRCT-1 cells by increasing the Bax : Bcl-xL ratio through concurrent mechanisms dependent and independent of its mTOR inhibitory activity. Oncogene 2005;24:3348-3357

Trapani JA and Smyth MJ. Functional significance of the perforin/granzyme cell death pathway. Nat Rev Immunol 2002;2:735-747

Trump BF, Berezesky IK, Chang SH and Phelps PC. The pathways of cell death: oncosis, apoptosis, and necrosis. Toxicol Pathol 1997;25:82-88

Tumes DJ, Wong AC, Sewell WA, McColl SR, Connolly A and Dent LA. Differential rates of apoptosis and recruitment limit eosinophil accumulation in the lungs of asthma-resistant CBA/Ca mice. Mol Immunol 2008;45:3609-3617

Ucker DS, Obermiller PS, Eckhart W, Apgar JR, Berger NA and Meyers J. Genome digestion is a dispensable consequence of physiological cell death mediated by cytotoxic T lymphocytes. Mol Cell Biol 1992;12:3060-3069

Van Cruchten S and Van Den Broeck W. Morphological and biochemical aspects of apoptosis, oncosis and necrosis. Anat Histol Embryol 2002;31:214-223

Vermes I, Haanen C, Steffens-Nakken H and Reutelingsperger C. A novel assay for apoptosis. Flow cytometric detection of phosphatidylserine expression on early apoptotic cells using fluorescein labelled Annexin V. J Immunol Methods 1995;184:39-51

Virchow R and Chandler A (1859). Cellular pathology as based upon physiological and pathological histology. New York:, Dover Publications.

Wan X and Helman LJ. The biology behind mTOR inhibition in sarcoma. Oncologist 2007;12:1007-1018

Wang B, Yanez A and Novina CD. MicroRNA-repressed mRNAs contain 40S but not 60S components. Proc Natl Acad Sci U S A 2008;105:5343-5348

Wang CY, Kim HH, Hiroi Y, Sawada N, Salomone S, Benjamin LE, Walsh K, Moskowitz MA and Liao JK. Obesity increases vascular senescence and susceptibility to ischemic injury through chronic activation of Akt and mTOR. Sci Signal 2009;2:ra11

Wang X, Yue P, Chan CB, Ye K, Ueda T, Watanabe-Fukunaga R, Fukunaga R, Fu H, Khuri FR and Sun SY. Inhibition of mammalian target of rapamycin induces phosphatidylinositol 3-kinase-dependent and Mnk-mediated eukaryotic translation initiation factor 4E phosphorylation. Mol Cell Biol 2007;27:7405-7413

Wangpaichitr M, Wu C, You M, Kuo MT, Feun L, Lampidis T and Savaraj N. Inhibition of mTOR restores cisplatin sensitivity through down-regulation of growth and anti-apoptotic proteins. Eur J Pharmacol 2008;591:124-127

Waskiewicz AJ, Johnson JC, Penn B, Mahalingam M, Kimball SR and Cooper JA. Phosphorylation of the cap-binding protein eukaryotic translation initiation factor 4E by protein kinase Mnk1 in vivo. Mol Cell Biol 1999;19:1871-1880

Wei C, Amos CI, Zhang N, Wang X, Rashid A, Walker CL, Behringer RR and Frazier ML. Suppression of Peutz-Jeghers polyposis by targeting mammalian target of rapamycin signaling. Clin Cancer Res 2008;14:1167-1171

Winterstein A and Stein GZ. Untersuchungen in der Saponinreihe. Zur Kenntnis der Mono-oxy-triterpensäuren. Physiol. Chem. 1932;208:9-23

Witzig TE, Geyer SM, Ghobrial I, Inwards DJ, Fonseca R, Kurtin P, Ansell SM, Luyun R, Flynn PJ, Morton RF, Dakhil SR, Gross H and Kaufmann SH. Phase II trial of single-agent temsirolimus (CCI-779) for relapsed mantle cell lymphoma. J Clin Oncol 2005;23:5347-5356

Wu L, Birle DC and Tannock IF. Effects of the mammalian target of rapamycin inhibitor CCI-779 used alone or with chemotherapy on human prostate cancer cells and xenografts. Cancer Res 2005;65:2825-2831

Wyllie AH. Glucocorticoid-induced thymocyte apoptosis is associated with endogenous endonuclease activation. Nature 1980;284:555-556

Xu Y, Chen SY, Ross KN and Balk SP. Androgens induce prostate cancer cell proliferation through mammalian target of rapamycin activation and post-transcriptional increases in cyclin D proteins. Cancer Res 2006;66:7783-7792

Yan G, Shen X and Jiang Y. Rapamycin activates Tap42-associated phosphatases by abrogating their association with Tor complex 1. EMBO J 2006;25:3546-3555

Yan H, Frost P, Shi Y, Hoang B, Sharma S, Fisher M, Gera J and Lichtenstein A. Mechanism by which mammalian target of rapamycin inhibitors sensitize multiple myeloma cells to dexamethasone-induced apoptosis. Cancer Res 2006;66:2305-2313

Yang Q and Guan KL. Expanding mTOR signaling. Cell Res 2007;17:666-681

Yin X-M and Dong Z (2003). Essentials of apoptosis : a guide for basic and clinical research. Totowa, N.J., Humana Press.

Yu S, Shen G, Khor TO, Kim JH and Kong AN. Curcumin inhibits Akt/mammalian target of rapamycin signaling through protein phosphatase-dependent mechanism. Mol Cancer Ther 2008;7:2609-2620

Zhang JF, Liu JJ, Lu MQ, Cai CJ, Yang Y, Li H, Xu C and Chen GH. Rapamycin inhibits cell growth by induction of apoptosis on hepatocellular carcinoma cells in vitro. Transpl Immunol 2007;17:162-168

Zhang JF, Lu MQ, Cai CJ, Yang Y, Li H, Yi HM and Chen GH. The role of caspase-3 in rapamycin-induced apoptosis of hepatocellular carcinoma BEL-7402 cells. Ai Zheng 2006;25:1508-1511

Zhu W, Soonpaa MH, Chen H, Shen W, Payne RM, Liechty EA, Caldwell RL, Shou W and Field LJ. Acute doxorubicin cardiotoxicity is associated with p53-induced inhibition of the mammalian target of rapamycin pathway. Circulation 2009;119:99-106

9. Acknowledgement

I would like to say many thanks to my supervisor, Prof. Dr. med. Thomas Simmet, for his guidance and support over the past few years. During my time as a graduate student in his lab I have learned from him a great deal, not only technically, but also in terms of scientific thinking.

Special thanks to Prof. Dr. vet. med Hermann Ammer for his support and for giving me the possibility to defend my thesis under his auspices at the Faculty of Veterinary Medicine at Ludwig-Maximilians-University in Munich.

I will be always grateful to PD. Dr. Tatiana Syrovets for providing me with the tools necessary for pursuing a career in science. Also I will not forget that I learned from her a good deal in scientific writing, the critical evaluation of manuscripts and research proposals.

I also wish to thank Dr. Kai Pitterle, whose advice I followed in the lab aiming at standardization and optimization of any protocol I did.

I would like to thank our techicians, Karin Stölzle and Jenny Marinaci, and also Diana Gross, our secretary, for all their help and support during the course of my study. Many thanks to Berthold Büchele, our compounds source, for his sustained encouragement and advice. Thanks also to Felicitas Genze for her collaboration and CAM analysis.

Special thanks to my colleagues Oleg Lunov, Claudia Schmidt, and Dr. med. Magdalena Hagn, for their help and support and for making the lab fun and an enjoyable place to work.

Many thanks to the Egyptian Government, the Ministry of High Education and Culture Affairs and the Mission Sector for funding me during my PhD study.

I would like to thank my parents for their love and unending support over the course of my PhD and throughout my entire life. Finally, I would like to thank my wife, vet. med. Noha Foud, for her love and support and for always believing in me. Thank you for encouraging me when the times were tough, and for making the good time even better. You mean the world to me, and I could not have done this work without you. Thanks to Ahmed Samy who sustained me a lot during this period.

Curriculum Vitae

PERSONAL INFORMATION:

Name:	Samy Abd EL Raouf Fahim Khalafalla Morad
Birth Date:	January 01, 1979
Nationality:	Egyptian
Marital Status:	Married
Working address:	Department of Pharmacology, Faculty of Veterinary Medicine, South Valley University, Qena, Egypt
E-mail:	Samy_Morad@yahoo.com

EDUCATION:

2007 - 2010 **Ph.D. Student,** Pharmacology
Institute of Pharmacology of Natural Products and Clinical Pharmacology
Ulm University, Ulm, Germany

2002 - 2005 **Master Degree**, Pharmacology
(Pharmacokinetic Studies on one of Fluoroquinolones (Difloxacin) in Goats)
Faculty of Veterinary Medicine,
South Valley University, Qena, Egypt

1996 –2001 **Bachelor**, Veterinary Medicine,
Faculty of Veterinary Medicine,
South Valley University, Qena, Egypt

1993 –1996 **High school,**
Osirate High School, Farshout, Qena, Egypt.

Abstracts during my Ph.D. study

Morad SAF, Schmid M, Büchele B, Simmet Th (2008) Antiproliferative effect of a novel semisynthethic compound, 3-cinnamoyl-11-keto-β-boswellic acid, in prostate cancer cells. 49th Annual Meeting of the Deutsche Gesellschaft für Experimentelle und Klinische Pharmakologie und Toxikologie, Mainz, March 11-13. Naunyn-Schmiedeberg's Arch Pharmacol 377 (Suppl 1):301

Morad SAF, Schmid M, Büchele B, Pitterle K, Lunov O, Syrovets T, Simmet Th (2009) Inhibition of Akt induces cell cycle arrest and triggers apoptosis in chemoresistant human prostate cancer cells. 50th Annual Meeting of the Deutsche Gesellschaft für Experimentelle und Klinische Pharmakologie und Toxikologie, Mainz, March 10-12. Naunyn-Schmiedeberg's Arch Pharmacol 379 (Suppl 1):202

Pitterle K, **Morad SAF**, Büchele B, Syrovets T, Simmet Th (2009) Antiproliferative effect of the sesquiterpene lactone arglabin on androgen-independent prostate cancer cells. 50th Annual Meeting of the Deutsche Gesellschaft für Experimentelle und Klinische Pharmakologie und Toxikologie, Mainz, March 10-12. Naunyn-Schmiedeberg's Arch Pharmacol 379 (Suppl 1):205

Morad SAF, Schmid M, Büchele B, Pitterle K, Syrovets T, Simmet Th (2010) A novel semi-synthetic mTOR pathway inhibitor with antitumor properties. 51st Annual Meeting of the Deutsche Gesellschaft für experimentelle und klinische Pharmakologie und Toxikologie, Mainz, Germany, March 23-25. Naunyn-Schmiedeberg's Arch Pharmacol 381 (Suppl 1): 180

Morad SAF, Büchele B, Schneider B, Syrovets T, Hussein A, Simmet Th (2010) Dihydroxy-polypoda-13E,17E,21-triene induces cell cycle arrest and triggers apoptosis in human prostate cancer cells. 51st Annual Meeting of the Deutsche Gesellschaft für experimentelle und klinische Pharmakologie und Toxikologie, Mainz, Germany, March 23-25. Naunyn-Schmiedeberg's Arch Pharmacol 381 (Suppl 1): 187

Papers

Estrada AC, Syrovets T, Pitterle K, Lunov O, Büchele B, Schimana-Pfeifer J, Schmidt T, **Morad SAF,** Simmet Th (2010) Tirucallic acids are novel pleckstrin homology domain-dependent Akt inhibitors inducing apoptosis in prostate cancer cells. Mol Pharmacol 77:378-387

Morad SAF, Schmid M, Syrovets T, Pitterle K, Büchele B, Simmet Th (2010) A novel semi-synthetic triterpenoid inhibits mTOR signaling and induces apoptosis in chemoresistant prostate cancer cells. (submitted)

POSITIONS OF RESPONSIBILITY:

2006 – 2010	- Ph.D. Student (Institute of Pharmacology of Natural Products and Clinical Phamacology, Ulm University, Ulm, Germany)
2005 – 2006	- Assistant lecturer (Department of Pharmacology, South Valley University, Qena, Egypt)
2001 – 2005	- Demonstrator (Department of Pharmacology, South Valley University, Qena, Egypt)